FUNCTIONAL CHARACTERIZATION OF THE MACROPHAGE RECEPTOR MARCO

IDENTIFICATION AND FUNCTIONAL CHARACTERIZATION OF CONSERVED RESIDUES AND DOMAINS IN THE MACROPHAGE SCAVENGER RECEPTOR MARCO

By

KYLE E. NOVAKOWSKI, BSc.

A Thesis

Submitted to the School of Graduate Studies

in Partial Fulfillment of the Requirements

for the Degree

Doctor of Philosophy

McMaster University

Descriptive Note

McMaster University DOCTOR OF PHILOSOPHY (2017) Hamilton, Ontario (Medical Sciences)

TITLE: Identification and Functional Characterization of Conserved Residues and Domains in the Macrophage Scavenger Receptor MARCO

AUTHOR: Kyle E. Novakowski, BSc (University of Waterloo, ON)

SUPERVISOR: Dr. Dawn M. E. Bowdish

NUMBER OF PAGES: cciv, 204

Lay Abstract

Some of the most ancient mechanisms of host defense rely on invariant recognition of pathogens through the use of pattern recognition receptors, such as the macrophage receptor with collagenous structure (MARCO). MARCO plays an integral role to allow for specialized subsets of white blood cells to bind pathogens, activate signalling complexes and to bring pathogens inside the white blood cell for destruction. Current literature suggests the C-terminal Scavenger Receptor Cysteine Rich (SRCR) domain of MARCO is required for these processes. This remains under scrutiny, as other closely-related receptors have been shown to operate independently of the SRCR domain. Herein, we utilized a variant of MARCO which lacks the SRCR domain and patterns of evolution to confirm both that the SRCR domain is critical for receptor function and to discover novel sites within the human MARCO protein that play indirect, but important roles in receptor function.

Abstract

Host defense against pathogenic organisms represents one of the most important and highly-conserved biological processes across the evolutionary timescale. The ability to detect, engulf and destroy particulates for either nutrition or host defense is conserved from single-celled protists to complex multicellular organisms. A central component of host defense is the recognition of invariant, conserved patterns on pathogenic organisms through the use of pattern recognition receptors (PRRs), such as macrophage receptor with collagenous structure (MARCO). MARCO modulates binding and phagocytosis of unopsonized microorganisms and particulates, tethers ligands to signalling complexes and enhances cellular adhesion. Current literature suggests these functions are mediated via the C-terminal scavenger receptor cysteine rich (SRCR) domain. The relative importance of this domain remains unclear, as other, closely-related scavenger receptors function independently of the SRCR domain via a shared lysine-rich motif.

In chapter 3.1, we discovered and cloned a naturally-occurring transcript variant of MARCO which lacks the SRCR domain, termed MARCOII. We demonstrated that the SRCR domain is required for ligand binding and internalization and that MARCOII can form heteromeric complexes with MARCO and reduce receptor function. Furthermore, the SRCR domain enhanced TLR2/CD14-mediated pro-inflammatory responses to *Streptococcus pneumoniae*. Finally, it was demonstrated that the SRCR domain modulates MARCO-mediated cellular adhesion.

In chapter 3.2, we used comparative phylogenetics to identify human specific mutations and residues undergoing positive selection in human MARCO. We demonstrated that humans possess a unique phenylalanine residue at position 282 that is polymorphic, with some humans encoding an ancestral serine residue. We also demonstrated that glutamine at position 452 is found in Denisovans, Neanderthals, and extant humans, but all other non-primate, terrestrial, and aquatic mammals possess an aspartic acid residue. We cloned the ancestral residues and loss-of-function mutations and demonstrated that these residues enhance ligand association and phagocytosis of *Escherichia coli*.

Acknowledgements

Graduate school has been a whirlwind of exciting discoveries, frustrating endeavors, emotional and mental challenges and personal growth. Throughout my graduate career, I have matured as a scientist, a boyfriend/fiancée/husband, a son, a brother and a friend. I owe everything to my supervisor, Dr. Dawn Bowdish for giving me the opportunity to pursue my love of scientific discovery within her research programme. Dawn afforded me the opportunity to join her lab as a MSc. student and encouraged me to continue in pursuit of a PhD. She has been a supervisor of many faces; she has been my cheerleader when even the simplest of experiments failed, my boss when I needed to be reminded of the importance of reading scientific literature, my mentor when it came time to writing manuscripts or scholarship applications, and my friend when I needed an ear to listen. Dawn's constant pursuit of becoming a better leader and manager speaks volumes of her character and of the leadership and training I received.

I have been extremely lucky to be surrounded by a fantastic group of professors, mentors and scientific leaders. Dr. Mark McDermott was integral in providing me with a crash course in immunology and scientific writing. He provided valuable guidance that spanned across multiple facets of my academic career, including career planning, organizing scientific conferences and managing lab personnel. Most importantly, Mark was always willing to share a dram or two of single-malt scotch.

My years of post-secondary education might have been very different if my love for science and discovery had not been fostered throughout my adolescent years. My eighth grade science teacher, Joe Abraham, greatly helped to curate my love for science through exciting and challenging projects. This mentorship continued throughout my secondary school education thanks to some very quirky and talented teachers. Thank you to Mrs. Dunne-Samsworth, Mrs. Round, Mr. Litzgus, Mr. Picone and Mr. McCarthy.

My gateway to graduate education came through the lab of Dr. Mungo Marsden at the University of Waterloo. Mungo afforded me the opportunity to pursue a 4th year thesis project in his lab and provided a sneak peek into the world of scientific research. Graduate students Dr. Catherine Studholme and Bhanu Pilli provided valuable training that eventually became my bread and butter of daily graduate school work.

My supervisory committee has also provided valuable guidance over the years of my graduate education. Dr. Karen Mossman frequently challenged me to think deeper, and to always assess whether my experiments properly addressed my hypotheses. Additional members of my committee, including Dr. Tim Gilberger, Dr. Brian Lichty and Dr. Martin Stämpfli all provided unique and insightful advice to many aspects of my project. The assistance of my contributing authors and peripheral advisors, Dr. G. Brian Golding, Dr. Kaori Sakamoto, Dr. Bryan Heit and Dr. Alba Guarné was also exceptionally useful in helping guide and shape my projects. I was also fortunate to experience detailed and patient training in many techniques in my graduate career.

This includes April Scott in the McMaster central animal facility, Hong Liang in the MIRC flow cytometry facility and Dr. Susan Collins in the Mossman lab.

Completing a PhD would have been infinitely more difficult if I wasn't surrounded by the best colleagues and friends throughout my tenure in the Bowdish lab. Dr. Chris Verschoor provided a vast amount of time and energy helping design experiments, troubleshooting cloning and acting as a sounding board when experiments weren't going as planned. Chris also provided me with the opportunity to be involved in his own work and my very first contributing authorship on a scientific publication.

I was exceptionally lucky to be surrounded by some of the brightest, most dependable and honest graduate students, who I can now call some of my best friends. Dr. Michael Dorrington, future Drs. Dessi Loukov, Pat Schenck, Avee Naidoo, and Nicholas Yap all provided me with the advice of top-notch scientists and the support of the best of friends. I wouldn't have survived the rigours of graduate education if I wasn't surrounded by this support network.

The Bowdish lab was also home to many bright undergraduate students who were a delight to train and collaborate with on a daily basis. Charles Yin, James Han, Jason Fan and Mohammad Malik were helpful additions to "team scavenger receptor".

I would not be anywhere in life had it not been for the constant love and support of my family. From my early years of building science projects in grade school, to proof-reading lab reports in high school and providing much needed hot coffee, cold beer and tuition funding during undergraduate and graduate studies, my Mother, Leanna

and Father, Eugene have always supported me. Even during my grumpiest, lowest, most miserable-of-times, my parents always made sure I was fed, had a roof over my head and a working vehicle to get to Waterloo or McMaster. My parents worked selflessly for years to save for my education, often putting aside their own personal wants and needs. I hope to be as good of a parent as you both, one day. I love you both.

My brother, Justin has also served as a much needed source of laugher and ventilation during the stresses of graduate school. I'm lucky to have shared so many concerts, rounds of golf and bottles of beer with my only brother. Thanks for always having my back.

My extended family, including the Novakowski and Toker families on Stoneybrook Trail, have served as constant oases of mental health reprieve. All of you constantly checked in on how my studies were progressing and made sure I was taking care of myself.

Last, but certainly not least, I owe every ounce of thanks to my wife and partner in life, Christina. You have been through hell and high water with me since the very beginning. You've shown me nothing but love and support through nearly a decade of post-secondary education, all while dealing with your own stresses of academia, career juggling and beyond. Even in my weakest moments, including when you dealt with a first year biology report are spewing out of my printer at 3AM, you always made sure I was prepared to succeed. No matter how badly I felt I would fail an

assignment, exam, or presentation, you were a source of constant encouragement. If only I had the faith in myself that you have in me. I love you and I hope that one day, all this hard work will make our lives brighter.

This thesis is dedicated to the memory of my grandmother, Lorraine M. Sweet. You loved me like a parent, supported me like a best friend and always made life bright as could be, just like the laundry. I know you would be proud. I love you.

Table of Contents

List of Figures and Tables

List of Abbreviations

AKT	Protein kinase B
APC	Antigen presenting cell
BCA	Bicinchoninic Acid
BDB	Bisdiazonium-benzidine
bp	Base Pairs
BSA	Bovine Serum Albumin
cA-SR	Class A Scavenger Receptor
CPZ	Chlorpromazine
DAMP	Damage-associated molecular pattern
DMEM	Dulbecco’s modified Eagle's medium
ECM	Extracellular matrix
FBS	Fetal Bovine Serum
FCA	Freud’s Complete Adjuvant
FcR	Fragment (crystallisable region) receptor
GAPDH	Glyceraldehyde 3-phosphate dehydrogenase

GM-CSF	Granulocyte-Macrophage Colony-Stimulating Factor
GTPase	Guanosine-triphosphatase
HBSS	Hank's Balanced Salt Solution
HEK	Human Embryonic Kidney
HKLD	Heat-Killed, Lysozyme Digested
hM 293T	Human Embryonic Kidney cells stably expressing human MARCO
hMII 293T	Human Embryonic Kidney cells stably expressing human MARCOII
IFN	Interferon
IFN-γ	Interferon gamma
IgG	Immunoglobulin G
IL-	Interleukin-
I-TASSER	Iterative threading assembly refinement
kDa	Kilodalton
KLH	Keyhole Limpet Hemocyanin
LAMP	Lyososme-associated molecular protein

LB	Lysogeny Broth
LD	Linkage Disequilibrium
LPS	Lipopolysaccharide
LRR	Leucine-rich repeat
LTA	Lipoteichoic acid
MAFFT	Multiple Alignment by Fast Fourier Transform
Mal-BSA	Maleylated Bovine Serum Albumin
MARCO	Macrophage Receptor with Collagenous Structure
MBL	Mannose binding lectin
MOI	Multiplicity of Infection
MyD88	Myeloid differentiation primary response gene 88
NCBI	National Center for Biotechnology Information
NF-κB	Nuclear Factor Kappa-light-chain-enhancer of activated B cells
NHP	Non-human primate
NRF2	Nuclear factor (erythroid-derived 2)-like 2
NZW	New Zealand White

PAMP	Pathogen-associated molecular pattern
PBMC	Peripheral Blood Mononuclear Cell
PBS	Phosphate Buffered Saline
PCR	Polymerase Chain Reaction
PFA	Paraformaldehyde
PI3K	Phosphatidylinositol-4,5-bisphosphate 3-kinase
PVDF	Polyvinylidene Difluoride
RIPA	Radioimmunoprecipitation Assay
ROS	Reactive oxygen species
RPM	Rotations per Minute
RSV	Respiratory syncytial virus
RT	Room Temperature
S.E.M.	Standard error of the mean
SAS	Solvent Available Surface area
SCARA3	Scavenger Receptor class A3
SCARA4	Scavenger Receptor class A4

SCARA5	Scavenger Receptor class A5
SDS	Sodium Dodecyl Sulfate
SEAP	Secreted Embryonic Alkaline Phosphatase
SNP	Single Nucleotide Polymorphism
SR	Scavenger Receptor
SR-AI	Scavenger Receptor class A I
SR-AII	Scavenger Receptor class A II
SR-AIII	Scavenger Receptor class A III
Src	Proto-oncogene tyrosine-protein kinase Src
SRCR	Scavenger Receptor Cysteine Rich
Syk	Spleen tyrosine kinase
TBST	Tris-buffered Saline with 0.1% Tween-20
TDM	Trehalose 6,6’-dimycolate

TFEB	Transcription factor EB
TIR	Toll/IL-1 receptor
TLR	Toll-like Receptor
TRIF	TIR-domain-containing adapter-inducing interferon-β
TRIS	Tris(hydroxymethyl)aminomethane
TSA	Tryptic Soy Agar
V-ATPase	Vacuolar adenosine-triphosphatase
WT	Wildtype

Declaration of Academic Achievement

This thesis contains the data from two studies prepared for publication in peer reviewed journals. In both publications, I am listed as the primary author. The study outlined in chapter 3.1 is already published and the study in chapter 3.2 is currently in revision, pending acceptance into the journal *Molecular Biology and Evolution*. Scientific discovery often requires collaboration, teamwork and alternating roles being a leader and being a protégé. While I was the primary contributor to the design, execution, documentation and manuscript preparation, others have provided valuable contributions to my work.

The published manuscript in chapter 3.1 (*Immunology and Cell Biology* 94:(7), 646-655 Feb, 2016. Copyright 2016. The Australasian Society for Immunology, Inc.) is a study that I designed with the assistance of Dr. Dawn Bowdish. I was responsible for performing the majority of the experiments, interpreting the results and preparing the manuscript. Dr. Dawn Bowdish initially discovered the MARCOII transcript variant. Charles Yin designed the recombinant SRCR construct experiment and Angela Hyunh created and purified the construct under the supervision of Dr. Alba Guarné. The flow cytometry for this experiment was performed by Dr. Michael Dorrington. Under my guidance, James Han performed the NF-κB reporter assays. Zhongyuan Tu previously performed the inhibitor studies to validate the microsphere binding and internalization assays, which was included in the supplemental figures at a reviewer's request[1]. Dr. Chris Verschoor performed the flow cytometry in figure 9J.

The manuscript in chapter 3.2 is a study that I designed with the assistance of Dr. Dawn Bowdish, Dr. G. Brian Golding and Nicholas Yap. At the time of thesis submission, the manuscript is being revised for acceptance in *Molecular Biology and Evolution*. I was responsible for performing the majority of the experiments, interpreting the results and preparing the manuscript. Nicholas Yap previously identified residues Q452 and F282 as sites of interest under the supervision of Dr. G. Brian Golding[2,3]. Dr. G. Brian Golding performed additional tests for positive selection on site F282 at a reviewer's request . I collaborated with Charles Yin, under the supervision of Dr. Bryan Heit, to optimize the transfection of RAW 264.7 cells with our MARCO constructs and to perform the phagocytosis assays. Once the assay was optimized, Charles Yin was ultimately responsible for the generation and interpretation of the bacterial phagocytosis data.

CHAPTER I: INTRODUCTION

1.1. A Brief History of Disease & Immunity

The earliest concepts of white blood cells and their importance in the responses to infection and injury were discovered nearly two millennia ago, when the ancient Greek physician Galen of Pergammum described pus in gladiators' wounds as *"pus bonum et laudabile"* ["good and commendable pus"][4]. While the inference that pus was a necessary stage in wound healing represented one of the earliest stepping stones towards a modern understanding of immunity, it took nearly 1700 years before it was understood that pus represented a response to substantial infections. It wasn't until the late 1800s that our understanding of the relationships between microbes, infectious disease and cellular components of innate immunity began to catalyze. Indeed, the discoveries and expansions upon early theories by monumental figures such as Edward Jenner, Robert Koch, John Snow and Louis Pasteur rapidly expanded our knowledge of disease.

While the initial focus of host-pathogen interactions largely revolved around bacteriology and the causative agents of disease, some of the earliest and most pivotal advances in understanding host cells were made soon after. The most primitive of such discoveries involved the earliest descriptions of phagocytosis, 'to devour'; the process of a cell ingesting a solid particle. These are often credited to Ernst Haeckel, a German marine biologist who demonstrated the ability of mollusk leukocytes to ingest India ink particles in 1862, and Elie Metchnikoff, a Russian

zoologist who demonstrated the ability of ‘phagocytes’ to surround and kill pathogens in starfish larvae in 1882[5]. An important, but often forgotten contributor to the discovery of phagocytosis is the Canadian physician William Osler, who demonstrated the uptake of coal dust particles in human alveolar cells from an autopsy specimen of a coal miner in 1876[6]. Despite the chronological anomalies in the discoveries surrounding the concepts of phagocytosis, Metchnikoff is generally cited as the first to coin the term ‘phagocyte’, the first to characterize the cells as ‘macrophages’ or ‘microphages’ (later to be named granulocytes) and as the founder of the concept of cellular immunity[5].

Since then, our understanding of phagocytes, phagocytosis and innate immunity has expanded immensely. Macrophages have been identified in virtually every tissue of the human body and have been shown to be exceptionally heterogeneous in their origins and functions[7]. While macrophages perform a broad array of functions via phagocytosis, ranging from direct recognition and killing of pathogens to tissue homeostasis and wound healing, the mechanisms that govern such processes are less well understood. It is understood that phagocytosis is a receptor-mediated process involving an exceptionally broad repertoire of ligands and ligand types[8]. Therefore, the current understanding of how phagocytic receptors function across multiple roles in innate immunity remains incomplete. The focus of this thesis is to identify and characterize domains and motifs of the phagocytic receptor macrophage receptor with collagenous structure (MARCO) that are necessary for receptor function.

1.2 The Macrophage: Origins and Functions

Macrophages are commonly thought to function as sentinel cells of the innate immune system that detect, phagocytose and destroy endogenous and exogenous materials that bear certain molecular signatures such as damage- or pathogen-associated molecular patterns (DAMPs/PAMPs). While this conceptual framework is valid, it also is vastly oversimplified. Macrophages are multi-functional cells that play a variety of roles in health and disease. It is now understood that macrophages are involved in systemic metabolism, cold adaptation, tissue homeostasis, wound repair and embryonic development[9].

Macrophage-like cells have been shown to exist in many different organisms ranging from mammals, to simple vertebrates to invertebrates and arthropods, where they exist as hemocytes[9]. It has even been suggested that macrophages and single-celled protists such as *Acanthamoeba* may be evolutionarily related due to a number of shared morphological, biochemical and host-defense properties[10]. While the evolutionary origins of mammalian macrophages may remain unclear, it is evident that mononuclear phagocytes represent a critical population of cells across the evolutionary timescale.

The framework of macrophage origins within humans has rapidly evolved in the 21st century. The previous 'mononuclear phagocyte system' model suggested that tissue-resident macrophages arise solely from bone marrow-derived monocytes[11]. Monocytes are a heterogeneous population of mononuclear phagocytes that arise from hematopoetic stem cells (HSCs) in the bone marrow and are constantly seeded

into the blood. Monocytes exist in the blood for 1 to 7 days, depending on their subset, and can extravasate to sites of inflammation[12]. Here, depending on their phenotype and the local stimuli, monocytes contribute to both inflammatory and anti-inflammatory processes. Certain populations of monocytes can differentiate into macrophages and serve to replenish peripheral populations. For example, the postnatal intestine is *primarily* populated by macrophages which differentiate from bone marrow-derived monocytes whereas other tissue-specific macrophages can be derived from three progenitor cell lineages in a series of temporal waves during embryonic development[9,13–15].The first wave of progenitors, erythro-myeloid progenitors (EMPs), emerge from the yolk sac and give rise to the brain microglia[13,15].The second wave of progenitors is driven by hematopoetic stem cells (HSCs), a lineage of cells that is distinct from EMPs that seeds the fetal liver prior to hematopoeisis and gives rise to populations such as Kupffer cells of the liver[13]. The final wave involves HSCs forming the bone marrow (BM), which will ultimately produce monocytes, which serve as a source of macrophage replenishment in peripheral tissues that undergo 'homeostatic inflammation', such as the intestine and mammary gland[15]. Importantly, it appears that macrophages of fetal origin, such as Kupffer cells, Langerhans cells, microglia, alveolar macrophages, peritoneal macrophages and splenic macrophages are all self-maintaining populations via local proliferation[13].

The roles of these localized populations of macrophages can significantly vary. For example, alveolar, intestinal and splenic macrophages are involved in immune

surveillance while cardiac, bone (osteoclast) and eye macrophages serve in organ remodeling whereas macrophages in the testis and ovaries influence steroid hormone production[16]. Many of these populations are programmed both intrinsically and by the local microenvironment to have suppressed responses to damaged-host and microbiota-derived stimuli[17]. This localized suppression serves to prevent the development of massive localized or systemic inflammation and the development of autoimmunity, which can ultimately result in further damage or death to the host.

Macrophages are diverse in both their origins and functions and can be found in virtually all tissues of the human body. Thus, the role(s) of macrophage receptors, such as MARCO, as well as their expression profile across macrophage subsets can vary greatly. MARCO has been shown to be constitutively expressed on only a small subset of 'specialized' macrophages and is difficult to induce expression of the receptor in non-expressing subsets. This will be discussed in detail in chapter 1.4.1.

1.2.1. Macrophage Activation and Classification

Macrophages are subjected to an incredibly complex mixture of environmental cues that dictate their phagocytic capacity, cytokine and chemokine production, motility and more. The resulting phenotypes are highly diverse, yet have historically been classified under an archaic nomenclature that was originally derived to define subsets of T cells[18]. Macrophages were classified into two subsets; 'classically activated' or 'M1' and 'alternatively activated' or 'M2'. This classification was proposed by Charles Mills, who observed differences in macrophage arginine metabolism in mice which had skewed lymphocyte responses towards either a Th1

or Th2 profile after stimulation with the mitogen Concanavalin A[19]. It was demonstrated that Th1 cells, which produced high levels of interferon gamma (IFN-γ), induced the production of toxic nitric oxide (NO) in macrophages; a phenotype associated with killing intracellular pathogens. This was contrasted with a Th2 response, which generated high levels of interleukin 4 (IL-4) and transforming growth factor-beta (TGF-β) and resulted in the production of ornithine; a phenotype associated with wound repair and proliferation[18,19]. The M2 classification of macrophages was later expanded by others to include M2a, M2b, M2c and M2d phenotypes, which can be induced by a variety of cytokines and macromolecules, such as glucocorticoids, immunoglobulins and immune complexes[18,20,21]. The M1 classification of macrophages has not been expanded, despite the fact that a number of stimuli have been shown to support the development of this phenotype. These include bacterial products such as lipopolysaccharide (LPS) and lipoteichoic acid (LTA), viruses and growth factors such as granulocyte-macrophage colony stimulating factor (GM-CSF). Furthermore, M1 macrophages appear to evoke overlapping molecular pathways in responding to these stimuli, such as interferon regulatory factors (IRFs), nuclear factor kappa-light-chain-enhancer of activated B cells (NF-κB) and signal transducer and activators of transcription (STATs)[18,22].

The M1/M2 paradigm of macrophage classification has fallen in favor of a spectral macrophage classification system, defined by a combination of surface receptor expression, cytokine and chemokine production, phagocytic capacity and metabolic properties of macrophages. Indeed, a number of examples, such as alveolar

macrophages and tumor-associated macrophages do not conform to the M1/M2 classification system and appear to have pleiotropic molecular signatures[7]. It is likely that this system will only become more complicated, as more unique macrophage populations, such as macrophages that express T-cell receptors, are discovered and characterized[23,24]. Adding to this incongruity in the context of this thesis, it is currently unclear what phenotypes of macrophages express MARCO and what stimuli are required to induce its expression. This topic will be further discussed in chapter 1.4.1.

1.2.2. Phagocytosis and Phagosomes

Phagocytosis is a central component of a large number of macrophage functions ranging from host defense to removal of apoptotic cells and tissue remodelling. The current definition of phagocytosis is the ingestion of particles greater than 0.5 µm in diameter[8]. The process of phagocytosis is closely related to endocytosis and pinocytosis, whereby a non-particulate ligand, such as soluble proteins or lipids are internalized[25]. Phagocytosis is a receptor-mediated process that can be performed by a variety of cell types, which are generally divided into two subclasses; “professional” and “non-professional” phagocytes[26]. This division is based on the phagocytic efficiency of various immune and non-immune subsets of cells. Professional phagocytes include neutrophils, monocytes, macrophages, dendritic cells (DCs), osteoclasts and eosinophils[25]. Non-professional phagocytes are cells that do not primarily function to phagocytose, but rather are capable of phagocytosis in a facultative manner, and include epithelial cells, endothelial cells, fibroblasts and

mesenchymal cells[25]. This is mostly due to their expression of a more limited repertoire of phagocytic receptors. Generally, the non-professional phagocytes are responsible for processes such as the clearance of apoptotic cells (efferocytosis), rather than direct recognition and destruction of pathogens.

The process of phagocytosis begins when a phagocytic receptor recognizes its cognate ligand on a target particle, for example, MARCO binding to bacterial ligands on the surface of *Streptococcus pneumoniae*[27]. This is sometimes termed the 'phagocytic synapse', an analogous comparison to the immunologic synapse between an antigen presenting cell (APC) and T-cell[25]. Although phagocytosis is often described in the context of a single ligand-receptor interaction, in a true physiological context, a number of ligands will interact with many different receptors simultaneously. Never-the-less, this 'probing' of the ligand is associated with membrane ruffling and actin polymerization, which enhances the contact between receptor and ligand[27]. If the ligand is coated with complement or immunoglobulin G (IgG), complement receptor 3 or Fcγ receptors will drive the process of 'opsonic phagocytosis', respectively[27]. An example of non-opsonic phagocytosis would be MARCO binding to *Streptococcus pneumoniae*, without the aid of complement or immunoglobulins. Following particle recognition, receptors cluster at the site of ligand binding, the phagocytic 'cup', and early signalling processes occur[27]. It was a long-held belief that phagocytosis and the resulting signalling cascades occur by 'zippering' of receptors that are mostly static on the cell surface, but are progressively engaged as a particle is engulfed[28,29]. This has recently been

challenged, as it has been shown that a number of receptors involved in phagocytosis, such as Fc receptors (FcRs) and CD36, actively diffuse and cluster at sites of ligand recognition within the cell membrane[30,31]. This process can involve a number of cell membrane constituents, such as actin, which can restrict receptor diffusion under some conditions, but become severed to 'free' receptors during activated states[29,32]. Lipid rafts, also called lipid microdomains, have also been shown to play a role in phagocytic receptor responses to ligands[33]. Simultaneous to receptor clustering, early signalling processes begin at the site of phagocytic cup formation. This process can involve a dizzying array of signalling pathways that largely depend on which receptors are involved at the phagocytic cup. Generally speaking, cytosolic tyrosine kinases are the primary signalling constituents responsible for remodeling the actin cytoskeleton and include moieties such as spleen tyrosine kinase (Syk) and proto-oncogene tyrosine-protein kinase Src (Src)[27]. Next, pseudopods are extended by polymerized actin filaments that force the membrane to protrude outward, which allows the cell membrane to wrap around the particle[27]. This process is driven by another diverse set of signalling molecules, such as small GTPases and phosphatidylinositol-4,5-bisphosphate 3-kinase (PI3K)[27]. The final step of phagocytosis is the closure of the phagosome. This occurs when the pseudopods surrounding the particle fuse together to fully enclose the cargo and the phagosome is detached from the membrane[27].

While the signalling and receptor clustering capacities of scavenger receptors has largely been unexplored, some inferences can be made to bridge the gap in

knowledge between MARCO binding a particle and delivery of the particle to the phagosome. Scavenger Receptor class A (SRA), the most well-studied class A scavenger receptor (cA-SR), has been shown to require the PI3K and Src families of non-receptor tyrosine kinases to adhere to surfaces. Cellular adhesion has long been considered a 'frustrated' phagocytic event whereby a cell attempts to phagocytose an infinitely large object[34]. MARCO alone, however, cannot induce the production of cytokines, as demonstrated by serial truncations of the short cytoplasmic domain, which had no effect on pro-inflammatory responses to mycobacterial ligands[35]. While the role of the cytoplasmic domain of MARCO remains unclear, the cytoplasmic domain of cA-SRs, however, may play a critical role in ligand internalization[1,36,37].

The internalized particle is now encased within a nascent phagosome. The phagosome will proceed through a process of maturation in order to degrade the internalized contents. The increasingly hostile environment eventually leads to the destruction of the contents and generation of peptides that can later be presented to cells of the adaptive arm of immunity[27]. The first stage is the formation of the early phagosome and includes fusion of the phagosome with early endosomes via the Rab5 GTPase and a variety of other effector proteins[8]. The early phagosome also begins to acidify and drops in pH from 7.4 to ~6.5 due to the presence of vacuolar ATPases (V-ATPase)[8]. During the transition from an early/intermediate phagosome, the phagosome can acquire a variety of sorting molecules via fusion with multivesicular bodies. This, combined with the acquisition of Rab7, loss of Rab5 and

continuous pumping of protons by V-ATPases results in a distinct new entity, termed the late phagosome, which is now even more acidic at approximately pH ~5.5[8,27]. The late phagosome also acquires lysosome-associated membrane proteins (LAMPs) and dyneins, which serve to guide the complex along microtubules towards a central location that allows for the late endosome to fuse with lysosomes[8,27]. This results in the formation of a phagolysosome. The phagolysosome is not only highly acidic (pH = ~4.5), but it is also rich in a variety of proteases and bacterial membrane-permeabilizing peptides, such as cathepsins, reactive oxygen species (ROS) as well as nucleases and lipases[27].

Despite this arsenal of antimicrobial properties within the phagolysosome, human pathogens have evolved a variety of mechanisms to avoid destruction. Examples include *Mycobacterium tuberculosis*, which arrests the maturation and acidification of the phagosome, and *Listeria monocytogenes*, which secretes a pore-forming toxin to destroy the phagosomal membrane[8]. Other bacteria, such as *Streptococcus gordonii* and *Streptococcus mutans,* encode proteins such as peptidyl-prolyl isomerises (PpiA), that actively suppress phagocytosis by blocking phagocytic receptors, such as MARCO[38,39].

1.3. Pattern Recognition Receptors

Pattern recognition receptors (PRRs) are a collection of sensory receptors that are responsible for the recognition of invariant molecular patterns. These patterns were initially described by Charles Janeway and were termed PAMPs, found on microbial pathogens, and DAMPs, altered host components resulting from cell damage or

death. Bruno Le Maître and Jules Hoffman were the first to identify a PRR, when they discovered that flies lacking the *Toll* gene were more susceptible to *Aspergillus fumigates* infection, suggesting its involvement in host defense[40]. One year after this discovery, Ruslan Medzhitov and Charles Janeway identified a homologous 'toll-like' receptor in humans and demonstrated that activation of this receptor induced signalling pathways and cytokine production associated with both innate and adaptive immunity. Indeed, these represent the two key constituents of PRR activation; to signal danger such that adequate innate immune responses can initiate early host defense and to induce APCs to present antigens to cells of the adaptive arm of immunity[41]. Since then, an astounding number of PRRs have been identified and characterized. Furthermore, this is one of the earliest examples of the evolutionary conservation of receptors involved in innate immunity.

PRRs are located in both the cell membrane and cytoplasm in leukocytes and non-immune cells. In humans, the membrane-bound PRRs consist of the Toll-like receptors (TLRs); the most well studied PRRs, C-type lectin receptors (CLRs) and the Scavenger Receptors (SRs). It is important to note that some TLRs exist within endosomes, such as TLR3 and TLR7. The cytosolic PRRs include the nucleotide oligomerization domain-like receptors (NOD) and retinoic acid-inducible gene-I-like receptors (RLR). An additional family of intracellular PRRs, termed the absent in melanoma-2-like receptors (ALRs) have been proposed as an expansion to this family[42]. All of these families of receptors have multiple subtypes of receptors that recognize distinct ligands and activate specific, but often overlapping signalling

pathways. Generally, PRR activation leads to a multitude of transcriptional changes that result in the production of cytokines and interferons (IFNs) to initiate an immune response. Other non-transcriptional changes include the up-regulation of phagocytosis, autophagy, apoptotic and cytokine processing pathways[42]. The vast majority of descriptions of PRR activation in the literature describe a single ligand-receptor activation event. It is important to be cognizant that numerous PRRs are activated both simultaneously, and sequentially, as ligands are recognized and internalized.

The TLR family of receptors consists of both membrane bound and cytoplasmic receptors that recognize bacterial, viral and fungal ligands. 10 TLR receptors are encoded in the human germline, and an non-functioning pseudogene for TLR11[43]. The TLRs are generally classified into two groups based on their location within the cell. TLRs 1,2,4,5,6 and 10 are expressed at the cell surface and TLRs 3,7,8 and 9 are located intracellularly. In general, cell surface TLRs are thought to be responsible for detecting bacterial PAMPs, such as LPS (TLR4), LTA (TLR2/1 or TLR2/6), and flagellin (TLR5). Many of these receptor-ligand interactions, especially lipid-based ligands, require the presence of co-receptors. For example, TLR2/1 requires CD14 to fully elicit an inflammatory response to triacylated lipopetides[44]. Intracellular TLRs are implicated in sensing viral PAMPs, such as single- (TLR7) and double-stranded RNA (TLR3), and unmethylated CpG DNA (TLR9). These functions are not exclusive, as bacterial PAMPs can activate intracellular TLRs upon phagocytosis (such as CpG DNA and TLR9) and viral envelope glycoproteins can

activate extracellular TLRs upon binding (such as respiratory syncytial virus (RSV) and TLR4)[45,46].

All TLRs share two common domains that are critical for receptor function. First, a leucine-rich repeat (LRR) domain serves to recognize ligands and second, a Toll/IL-1 receptor (TIR) domain functions as a signalling domain and molecular 'dock' for multiple adapter proteins. When TLRs bind a ligand, the receptors form homo- or heterodimers and initiate signalling pathways. This signalling cascade is initiated by adapter molecules docking to the TIR domain, such as myeloid differentiation primary response gene 88 (MyD88) or, in the case of TLR3, TIR-domain-containing adapter-inducing interferon-β (TRIF)[41]. A series of subsequent TLR adaptors ultimately result in the activation of two major inflammatory pathways; NF-κB-mediated cytokine production or IRF-mediated type I IFN production. In general, TLRs on the cell membrane are thought to signal via the NF-κB pathway and intracellular TLRs are thought to signal via the IRF pathway. Yet again, there are examples of TLRs that can signal in both the NF-κB pathway and IRF pathway, such as TLR2 which induces type I IFN production in response to bacterial and viral infections once the receptor has been internalized[47,48].

Our understanding of TLR biology is incomplete. For example, it is known that other PRRs can enhance TLR activation in response to ligands, however the mechanisms that govern this 'molecular tethering' are not known[35,48,49].

The CLRs are comprised of a very large family of receptors that are subdivided into 17 groups based on their structure[42]. CLRs exist as soluble opsonins (for example, mannose binding lectin, MBL) and membrane-bound receptors. A C-type lectin domain is shared by all members of the family of receptors and is responsible for the recognition of carbohydrates[50]. Generally, the ligands recognized by CLRs are fungal or bacterial, such as β-glucans, which are recognized by the prototypical CLR, Dectin-1[42]. The best-characterized group of CLRs are the collectins, which contain a collagen-like domain and contain soluble and membrane-bound receptors such as MBL and collectin-placenta 1/scavenger receptor class A4 (CL-P1/SCARA4), respectively. Interestingly, SCARA4 represents a CLR that is also classified as an SR[51]. This cross-categorization is a small example of the difficulties that have been encountered when trying to classify PRRs into respective families and groups.

NOD receptors are cytosolic PRRs that are divided into four subfamilies based on their amino-terminal effector domains[41]. NOD1 and NOD2 are the best-characterized NLRs and are primarily responsible for the recognition of bacterial ligands, such as muramyl dipeptide (MDP) and the subsequent activation of NF-κB[41]. In addition to prototypical ‘danger sensing’, NLRs play a central role in the formation of a large multimeric complex of inflammatory proteins termed an ‘inflammasome’. The best characterized inflammasome assembly is driven by the NLR NALP3 and involves the activation of caspase-1 and subsequent cleavage and activation of cytokines such as IL-1β[52]. This inflammatory pathway can ultimately result in pyroptosis, a form of

apoptosis that is associated with inflammation[41]. Similar to the cytosolic TLRs, NLRs often require the delivery of ligands to the NLR by other phagocytic or endocytic PRRs, such as SRs[48,49,53].

Finally, RLRs are a small family of 3 receptors that sense viral double stranded RNA. Retinoic acid inducible gene I (RIG-I) has been shown to preferentially recognize shorter RNA molecules with 5' triphosphorylated ends, whereas melanoma differentiation-associated protein 5 (MDA5) recognizes longer RNA molecules[41].

Scavenger receptors will be discussed *ad libitum* in the following chapter.

1.3.1. Scavenger Receptors

The SRs are a diverse group of PRRs that were originally described in 1979 by Michael Brown and Joseph Goldstein based on their ability to bind modified lipoproteins such as oxidized and acetylated LDL (oxLDL, acLDL), maleylated albumin and sulfated polysaccharides such as fucoidin and dextran sulfate[54]. Throughout the 1980s, many aspects of SR biology remained poorly understood, including structure-function relationships, role(s) in host defense and/or homeostasis and tissue expression of the receptors. The prevailing understanding of SRs focused on their roles to modulate lipid uptake in models of atherosclerosis[55]. In the 1990s, a number of discoveries helped to characterize many aspects of SR biology that were previously unknown. The majority of these discoveries were made in the laboratory of Monty Kreiger and include the first description of the "Type I Scavenger Receptor", currently known as Scavenger Receptor class A I (SR-AI)[56]. These

studies of SR-A uncovered the protein domain structure of the receptor and identified splice variants, including SR-AII[57–59]. Additional cloning and sequencing experiments also identified ancient and highly conserved protein domains within SR-AI, including the presence of a Scavenger Receptor Cysteine Rich (SRCR) domain at the C-terminus of the receptor[59]. This identification of an SRCR domain within the class A SRs would later result in highly contentious findings surrounding the role(s), or lack thereof-, of such protein domains.

In addition to better understandings of the domain architecture of SR-AI/II, it was found that the receptor exists as a large (>200kDa) homotrimeric glycoprotein[58,60]. Perhaps the most pivotal advance in SR biology was the discovery that bacterial cell wall constituents, including endotoxin (LPS) and teichoic acids (LTA) are SR ligands, leading to the first suggestion that SRs may have a role in host defense against pathogens[61,62]. In the late 1990s and into the 21st century, multiple novel SRs were discovered, including macrophage receptor with collagenous structure (MARCO), cellular stress response 1/scavenger receptor class A3 (CSR1/SCARA3), scavenger receptor with C-type lectin/scavenger receptor class A4 (SRCL/SCARA4) and scavenger receptor class A5 (SCARA5)[51,63–65]. The discovery of additional, closely-related members of the SR family highlighted that while there are many similarities within the family of receptors, such as domain structure, their functions are highly heterologous. Eventually, this led to the proposal to classify SRs into distinct families based on their sequence homology[66]. As more SRs were discovered the number of distinct classes quickly expanded to eight; A through H, despite inconsistencies in

nomenclature[67]. This expansion also resulted in more detailed analyses of the phylogenetic relationships between members of the same family[68]. While these phylogenetic analyses did not suggest the addition-to or removal of members of the class A SRs, the study provided insights into the ancient evolutionary origins of these receptors and their respective domains. Recently, the nomenclature and classification of SRs has been challenged[69]. This has led to the expansion of SR classes from eight to twelve and the standardization of SR nomenclature across all classes[67].

Regardless of nomenclature, the primary function of SRs was initially thought to be a combination of host defense and homeostatic scavenging of macromolecular debris, such as oxidized lipids. It is now understood that SRs have a much broader repertoire of functions, such as altering cellular adhesion, influencing macrophage polarization and in the maintenance of the micro architecture of lymphoid organs[36,70,71]. The current consensus definition of a scavenger receptor is “a cell surface receptor that typically binds multiple ligands and promotes the removal of non-self or altered-self targets. They often function by mechanisms that include endocytosis, phagocytosis, adhesion, and signalling that ultimately leads to the elimination of degraded or harmful substances”[67]. The majority of research published in the last decade has focused on three classes of SRs; A, B and I. Class A SR research has primarily examined the roles of SR-AI and MARCO in innate immunity and diseases with inflammatory elements. The smaller family of class B SRs are heavily implicated in cardiovascular disease and atherosclerosis due to their

affinities for modified lipids and lipoproteins. Class I SR research has primarily focused on the roles of CD163 in homeostasis. Specifically, CD163 functions as a SR for hemoglobin-haptoglobin complexes and is associated with alternative macrophage activation and anti-inflammatory responses during tissue repair[72]. Similar to other SRs, CD163 appears to have diverse functions, and has been shown to bind gram positive and negative bacteria and in erythropoiesis[73].

1.3.1.1. Class A Scavenger Receptors

The cA-SRs are a group of five multi-functional "ligand promiscuous" receptors that enhance anti-bacterial immunity, cellular adhesion, motility, and immune homeostasis[71,74]. The current members of the cA-SRs are SR-AI/II/III, MARCO, SCARA3, SCARA4 and SCARA5. Constitutive expression of this family of receptors was initially thought to be restricted to myeloid cells, such as dendritic cells (DCs) and specialized subsets of macrophages, such as alveolar, resident peritoneal and within the marginal zone of the spleen. While SRA and MARCO expression appear to follow this restricted pattern of expression, SCARA3, 4 and 5 have been shown to be expressed in non-immune cells in the lung, heart, placenta, intestine and epithelial cells[51,75].

cA-SRs all share similar structural homology, but also contain unique domains and motifs that differentiate their respective functions. All cA-SRs possess a short N-terminal cytoplasmic domain that has been shown to have signalling capacities in some, but not all cA-SRs[35–37]. This is followed by a transmembrane domain that serves to anchor the receptor into the cell membrane and a spacer domain that has

been suggested to help stabilize the receptor and may directly bind ligands[56,57]. This is followed by a collagenous domain that is required for receptor trimerization and varies in length; from <100 residues in SCARA5 to >250 residues in MARCO[60,68]. cA-SRs share a conserved lysine-rich motif within the collagenous domain that was shown to bind ligands by SR-AI/II, SCARA3 and SCARA5, yet this motif has been suggested to be dispensable for ligand binding by MARCO[76–78]. Thus, the collagenous domain has been a nucleating site for controversy with respect to the identification of domains that are required for ligand binding by cA-SRs. The C-terminus is where cA-SRs are most heterologous; SR-AI, MARCO and SCARA5 share a SRCR domain, SCARA3 terminates in the collagenous domain and SCARA4 contains a C-type lectin domain[71].

Interestingly, cA-SRs can undergo alternative splicing, which gives rise to different isoforms of the same receptor. SR-A has been shown to exist as multiple splice variants; full-length (SR-AI), lacking the SRCR domain (SR-AII), and a dominant negative isoform trapped in the endoplasmic reticulum (SR-AIII)[79]. While the expression of SRA splice variants is differentially regulated, SR-AI/II have been shown to bind ligands with similar specificity and affinity, providing evidence that the SRCR domain is not required for ligand binding[60,80]. Multiple splice variants of MARCO have been deposited to public databases, but have never been functionally characterized. These splice variants represent a potential wealth of untapped knowledge with respect to the structure-function relationship of MARCO domains and motifs.

1.3.2. Nomenclature

Similar to other PRRs, the nomenclature used to describe SRs has been disorderly and confusing; as receptors have historically been named based on the tissue(s) they are expressed in or the protein domains that are encoded within the receptor. This system of nomenclature has given rise to numerous, lengthy names shared by the same receptor. For example, scavenger receptor class A4 (SCARA4), collectin-like placenta 1 (CL-P1) and scavenger receptor with C-type lectin domain (SRCL) all define the same receptor. To address this issue, an assembly of SR experts formulated a universal nomenclature system to classify the receptors between 2014 and 2017[67,69]. It was determined that SR nomenclature would follow a system of SR-XY.Z, where X represents the class, Y represents the order in the class and .Z represents an alternatively spliced form of the respective receptor[67]. For example, SR-AII would become SR-A1.1 and MARCO would become SR-A6. This new system of nomenclature, while greatly improved in clarity, also contains anomalies, such as naming MARCO SR-A6, as opposed to the more logical SR-A2, which more closely matches the formalized gene name *MARCO*/*SCARA2*. This was a designation that was agreed upon by the assembled panel to avoid confusion between the truncated isoform of SR-A (SR-AII) and what would have been the current nomenclature for MARCO[67]. Despite these best efforts, literature continues to be published using the old style of nomenclature, suggesting that adoption of the new system of nomenclature may take time. For the purposes of clarity, this thesis has been prepared using the same nomenclature that was utilized in original

manuscript publications, however it is important to be cognizant that future research may adapt the new system of nomenclature.

1.4. MARCO

MARCO is a homotrimeric type II transmembrane glycoprotein that is approximately 210 kDa in size[64]. The five-domain structure of MARCO consists of a 50 amino acid (aa) cytoplasmic domain, a 25 aa transmembrane domain, a 75 aa spacer domain, a 270 aa collagenous domain and a 100 aa SRCR domain. Unlike the cytoplasmic domain of SRA, which appears to have intrinsic signalling capabilities, the cytoplasmic domain of MARCO is not likely to be involved in signalling[35–37]. The function of cytoplasmic domain of MARCO has remained largely enigmatic, partly due to a low degree of homology between cytoplasmic domains of the class A SRs. As in all class A SRs, the transmembrane domain serves to anchor MARCO into the cell membrane and the spacer domain separates the receptor from the cell membrane and may stabilize the receptor. Apart from receptor trimerization, the function of the collagenous domain of MARCO has remained enigmatic. This is in part due to the shared lysine-rich motif found in all cA-SRs that has been shown to play a critical role in ligand binding in SR-AI/II, SCARA3 and SCARA5[57,68,81]. This is also due to the scrutiny placed on findings that suggest the SRCR domain is the primary ligand binding site of MARCO[77].The reason for this scrutiny is bipartite; first, the artificial truncations and site-directed mutants used to study MARCO function showed highly different expression patterns, a phenomenon that was not normalized in this study. Second, the SRCR domain is dispensable for function in both SR-AI/II

and SCARA5[57,68,81]. Despite this, the SRCR domain of MARCO has been proposed as the primary ligand binding site due to via two highly conserved arginine residues, termed the RxR or RGRAEVYY motif[68,77]. Given the dichotomy of the evolutionarily conserved domains and motifs but differences in ligand binding sites; the role of the SRCR domain of MARCO in ligand binding has remained contentious.

1.4.1. Expression

MARCO was initially thought to only be constitutively expressed on specific subsets of macrophages; such as in the marginal zone of the spleen and in the lymph nodes[82]. Interestingly, MARCO-expressing macrophages have been shown to play a critical role in the maintenance of the spleen microarchitecture and are required for B cell retention[70]. It was later shown that MARCO is also constitutively expressed in peritoneal and alveolar macrophages[74,83,84]. MARCO expression is not limited to macrophages, as DCs have been shown to up-regulate MARCO in response to various PAMPs and DAMPs, such as LPS, CpG DNA and tumor cell lysates[85–87].

Currently, there is no consensus on what cytokines, chemokines, growth and transcription factors or PAMPS/DAMPS are required to up-regulate MARCO expression. This is due to the fact that some findings suggest that M2-like macrophages up-regulate MARCO expression whereas other findings suggest M1-like macrophages up-regulate MARCO expression[80,88]. It is certainly feasible that these findings are not mutually exclusive, and that these findings are not conflicting, but rather highlight the archaic and outdated system of classifying macrophages using the M1/M2 system. Never-the-less, the largest body of evidence currently

supports IL-10 as a moderate inducer of MARCO expression in peripheral blood mononuclear cell (PBMC) -derived macrophages[78,88–90].

It has recently been demonstrated that the levels of IFN-γ in the lung are negatively correlated with MARCO expression in a model of influenza infection[91]. Interestingly, during the homeostatic reduction of IFN-γ after the viral infection was resolved, MARCO expression increased[91]. Transcriptome profiling and chemical activation and inhibition suggested that protein kinase B (AKT) and the transcription factors nuclear factor (erythroid-derived 2)-like 2 (NRF2) and transcription factor EB (TFEB) are master regulators of MARCO expression. To date, this is the most detailed study of MARCO expression regulation and serves to highlight the most convincing methods for induction of MARCO. Our incomplete understanding of MARCO expression and regulation has posed as a major hurdle to studying the physiological and biochemical properties of the receptor.

1.4.2. Structure

MARCO has been hypothesized to exist as an elongated, flexible homotrimer that may be capable of forming large oligomeric clusters that are capable of domain swapping[92]. In doing so, large MARCO oligomers would form a large, charged surface that acts as a ‘molecular catcher’s mitt’ that is capable of binding large ligands such as bacteria and apoptotic cells. The crystal structure of a homotrimeric MARCO molecule has never been resolved due to a number of common difficulties that are encountered in the study of transmembrane proteins. First, expression of a receptor in a recombinant prokaryotic system that allows for proper membrane

targeting and post translational modifications is required[93]. This is important, given that MARCO has been shown to contain sites of glycosylation[74]. Furthermore, the collagenous domains of cA-SRs have been described as 'flexible', a property which poses difficulty during crystallization[93,94]. Other hurdles to proper study of transmembrane proteins via X-ray crystallography include solubilisation, purification and signal-to-noise ratios during data collection[93]. Despite these challenges, Marko Sankala *et al.* demonstrated that MARCO is a matchstick-shaped receptor with a globular SRCR domain 'head'[95]. This was done by replacing the cytoplasmic and transmembrane domains of a MARCO monomer with the secretory signal sequence of an immunoglobulin gene.

Unsurprisingly, the SRCR domain of MARCO is the most well-studied domain of the receptor. SRCR domains exist as two types; group A domains, which contain six cysteine residues and group B domains, which contain eight[96].The formation of disulfide bonds plays a major role in the proper formation of a compact, globular structure of the group A SRCR domain of MARCO[96]. Juha Ojala *et al.* solved the structure of monomeric and dimeric murine SRCR domains and demonstrated the presence of acidic and basic clusters; the latter of which is required for ligand binding[77,92]. Furthermore, it was demonstrated that unlike SR-A, ligand binding by MARCO requires divalent cations, possibly due to a partial 'quenching' of the acidic cluster of the SRCR domain[92].

1.4.3. Evolution and Conservation

Sequences of MARCO have been shown to exist in animals that predate the origin of jawed vertebrates, such as *Petromyzon marinus* (sea lamprey). The exact origin of the cA-SRs remains unknown, however it was previously demonstrated that the five modern cA-SRs likely arose from ancient precursor proteins via 4 unique gene duplication events, followed by domain fusions, internal repeats, and deletions[68]. This diversification of the cA-SRs likely led to their specialization of function. For example, SR-AI has been implicated as a homeostatic regulator of lipid and protein clearance, SCARA3 has been shown to be involved in cellular responses to oxidative stress, whereas MARCO has been primary associated with host defense[63,97].

MARCO contains numerous conserved motifs, many of which have never been functionally characterized. The best-described motifs include the lysine-rich motif and the RxR or RGRAEVYY motif. The lysine-rich motif is a conserved cluster of 4 lysine residues that act synergistically to mediate ligand binding. Doi *et al.* demonstrated that deletion of more than 2 lysine residues abrogates ligand binding by SR-A[76]. SCARA4 and SCARA5 have also been shown to bind ligands via their collagenous domains and SCARA3 has been hypothesized to behave similarly[63,65,81]. Interestingly, it has been demonstrated that partial truncation of the distal collagenous domain of MARCO, which contains the lysine-rich motif, has only a modest negative effect on ligand binding[77].

Unlike the lysine-rich motif, the RxR or RGRAEVYY motif is not found in all five members of the cA-SRs, but rather is unique to MARCO. The cluster of positive charge created by the presence of these arginine residues has been demonstrated to be the central mediator of polyanionic ligand by MARCO[77]. This finding is contentious, since MARCO also contains a lysine-rich motif. This interpretation is complicated by the fact that truncation and site directed mutagenesis of MARCO can considerably affect receptor expression[77].

Recently, a number of additional conserved motifs and residues have been identified. Yap *et al*. identified the WGTVCDD motif and three additional residues that are under positive selection[2]. Surprisingly, the RxR motif was not identified as undergoing positive selection. This may be due to either technical limitations of this phylogenetic approach or, more likely, due to the lack of diversity of organisms from which genomes have been sequenced and published. The study identified one particular site, position 452, which may play a role in receptor function. Interestingly, humans encode a glutamine (Q) residue, non-human primates vary and all other terrestrial and aquatic mammals encode an aspartic acid (D) residue[2]. MARCO has been shown to play a critical role in the innate immune response to human-specific pathogens such as *S. pneumoniae*[48,78] and *M. tuberculosis*[35,98,99], thus it is possible these pathogens placed selective pressure on MARCO during the transition from apes to humans. Furthermore, *how* a residue *outside* the RxR motif can alter ligand binding and/or internalization is unknown.

For example, using phylogenetic analysis, we have identified additional motifs, such as the PKPRRN motif in the cytoplasmic domain, that are highly conserved *within* MARCO but are not conserved *between* the five members of the cA-SRs. Therefore it is difficult to infer role(s) in receptor function without performing a direct analysis via site-directed mutagenesis or truncation. Bowdish *et al*. have demonstrated that MARCO constructs which lack the cytoplasmic domain show no abrogation of ligand binding and signalling pathway induction[35]. This suggests that MARCO does not possess any intrinsic signalling abilities.

1.4.3.1. The SRCR domain and cA-SR Phylogeny

While 60% of the cA-SRs contain an SRCR domain, this protein domain predates the cA-SRs by many millions of years. The SRCR domain is evolutionarily ancient and is found in soluble and membrane-bound receptors in mammals, birds, reptiles, fish, and invertebrates, such as insects, sponges, and echinoderms[96]. Although the ancestral function of the SRCR domain is unclear, it has been hypothesized that the SRCR domain-containing proteins of the purple sea urchin may be required for processes such as cell-cell adhesion, rather than host defense[100]. Generally, SRCR domains are 90-110 amino acids and are classified into two categories; type A, which are encoded by two or more exons and contain six cysteine residues or type B, which are encoded by a single exon and contain eight cysteine residues[96]. SRCR domains can exist as single domains (e.g. xyzA or xyzB) or as tandem repeats (e.g. xyzAAAA or xyzBBBB) within the same receptor, but never as both types of SRCR within the same receptor[96]. This is likely the result of intron/exon duplication events.

The SRCR domain-containing transmembrane proteins involved in host defense began to arise in early fish, such as *Petromyzon marinus* (sea lamprey) and *Callorhinchus milii* (ghost shark)[101]. The first phylogenetic analysis of the Class A SRs suggested that while SR-AI, MARCO and SCARA5 all contain SRCR domains, MARCO is more evolutionarily related to the non-SRCR domain containing cA-SRs SCARA3 and SCARA4[68]. This relationship was met with some criticism, as MARCO shares a much higher percent sequence identity with SR-AI and SCARA5. Indeed, more recent phylogenetic analyses utilized more stringent out-group proteins and included additional genomic analyses from ancient fish for improved resolution. These findings led to the suggestion that MARCO shares a more recent common ancestor with SR-AI and SCARA5[2]. Given this molecular relationship and the confounding evidence supporting both the lysine-rich and RxR motifs as probable ligand binding sites in MARCO, further investigation of the receptor is warranted.

1.4.4. Functions in Innate Immunity

MARCO plays an integral role in many facets of innate immunity. This includes host defense against a variety of bacterial pathogens in the lung and upper airways, homeostatic removal of particulates, maintenance of the architecture of lymphoid organs and anti-tumor activity[48,70,83,84,87,102]. The development of a homozygous MARCO knockout mouse in the lab of Dr. Karl Tryggvason provided an essential tool that led to many important discoveries in host-pathogen interactions and innate immunology.

The most well-explored facet of receptor function is the role of MARCO in host defense against bacterial pathogens in the airways. The lungs and nasopharynx are home to resident macrophages that mediate the removal of pathogenic bacteria independently of opsonins[48,84,103]. Alveolar macrophages have been shown to constitutively express MARCO, whereas nasopharyngeal macrophages have not been examined[84]. *Streptococcus pneumoniae* is perhaps the most well-studied pathogen in the context of MARCO function[48,83]. MARCO-expressing macrophages are vital for early detection of the bacterium, which drives an enhanced cytokine and chemokine response and ultimately results in the recruitment of effector cells that mediate clearance[48,83]. Additional *ex vivo* studies using human alveolar macrophages treated with MARCO blocking antibodies suggest that MARCO is required for binding *Escherichia coli,* and *Staphylococcus aureus*[84]. *Neisseria meningitidis* and *Cryptococcus neoformans* have also been identified as pathogens that are contained by MARCO-expressing alveolar macrophages and recruited monocyte-derived phagocytes[104,105]. In addition to pathogenic microorganisms, MARCO-expressing macrophages modulate the clearance of inert inorganic particles from the lung, such as titanium dioxide and silica[83,84,106].

1.4.5. Polymorphisms and Disease

Single Nucleotide Polymorphisms (SNPs) are variations at specific genomic locations that can be found in all segments of a gene, including in promoters, untranslated regions and within the open reading frame. It is estimated that 1 in every 1000 bases is polymorphic in the human genome[107]. To be classified as a

SNP, a nucleotide variant must occur in at least 1% of a population. SNPs are found at varying rates, or allele frequencies, *within* and *between* human populations. Genetic differentiation between populations, such as allele frequencies, can be influenced by evolutionary forces such as genetic drift and natural selection as well as environmental factors, such as migration and population expansion.

Genome-wide association studies (GWAS) are a method to link human polymorphisms to phenotypes, such as diseases, by determining if the allele(s) are more or less commonly found in samples with a specific trait. GWAS are correlational studies that are limited to providing an estimate of risk of developing a specific phenotype, rather than a cause-and-effect relationship. This is because while GWAS can identify genetic loci that may be *associated* with a phenotype, not all SNPs in a haplotype may ultimately influence the phenotype. Therefore, SNPs can represent a wealth of untapped knowledge, but interpretation of the impact of a given SNP on a specific phenotype can be difficult. Many published studies examining linkages between SNPs and phenotypes lack a mechanistic approach to understand *how* a SNP may drive a phenotype. For example close to 4000 SNPs in MARCO have been entered into public databases. While only a very small fraction of these polymorphisms may play *any* role in human health or influence disease phenotypes, it is certainly plausible that non-synonymous mutations and mutations affecting gene expression could affect a host's innate immune responses.

A number of candidate gene studies have linked MARCO polymorphisms to susceptibility or resistance to lung pathogens such as *Mycobacterium tuberculosis*

(*Mtb*)[99,108–110]. These studies focus on allelic variation and biological impacts within predetermined genes. Patients were grouped in a case-control fashion; healthy controls and those who tested positive for pulmonary tuberculosis. After genotyping, the authors calculated genotype-specific odds ratios for pulmonary tuberculosis risk and thus, were able to apply the data to a 95% confidence interval and calculate *p* values, therefore associating specific SNPs with changes to pulmonary tuberculosis risk. The first study to directly examine MARCO polymorphisms in association with human disease was performed by Ma *et al.* in 2011. The authors identified 1 SNP and 2 haplotypes (comprised of 2 and 4 SNPs, respectively) associated with an increased risk of pulmonary tuberculosis[99]. Bowdish *et al.* identified four additional SNPS associated with altered susceptibility to *Mtb* in a Gambian population. Interestingly, whereas three SNPs were found to be associated with susceptibility to pulmonary tuberculosis, one was associated with *resistance* to pulmonary tuberculosis. These and other candidate gene approaches have identified SNPs located in either introns or the promoter region. While no biological mechanism has been proposed to explain *how* any of these specific polymorphisms could affect disease susceptibility (likely due to many of these SNPs being in linkage disequilibrium), it is possible that altered gene regulation or transcript splicing explains this phenomenon.

Other studies have linked MARCO polymorphisms to sepsis in patients with chronic obstructive pulmonary disease (COPD) [111]. Thomsen *et al*. demonstrated that a non-synonymous mutation in the spacer domain of MARCO was associated with

increased risk of sepsis in COPD patients. Although the biological mechanism for this phenomenon is unknown, changes in structure in this domain could alter expression or MARCO-mediated phagocytosis or inflammatory signalling. For example, High *et al*. demonstrated that a MARCO polymorphism associated with worsened disease severity in respiratory syncytial virus (RSV) infection was located in an antioxidant reporter element for Nrf2 within the promoter region. This SNP completely abrogated receptor expression[112]. Severity of symptoms in COPD patients has also been linked to decreased Nrf2 expression and expression of- and phagocytosis by- MARCO[113]. This is unsurprising, given that Wu *et al.* recently demonstrated that Nrf2 is one of the 'master regulators' of MARCO expression[91]. There appears to be a link between SNPs in the promoter region of MARCO, Nrf2 signalling, decreased phagocytosis and disease, but the interplay between these potential mechanisms remains unclear.

Interestingly, many of the phenotypes associated with MARCO polymorphisms involve altered susceptibility or resistance to *human-adapted* pathogens, such as *Mtb* and RSV[114–116]. It is possible that airway pathogens, such as *Mtb*, have placed selective pressure on *MARCO*. Barreiro *et al.* demonstrated that positive and negative selection can influence genetic differentiation between populations, and thus disease-related phenotypic differences in distinct populations[117]. Therefore, we employed a two-pronged approach to study the relationship between MARCO function and genetic differences *within* the human population and *between* different species.

1.5. Central Paradigm

MARCO has been well documented to play a central role in innate immunity, however the mechanisms that govern receptor functions in ligand binding, activation of pro-inflammatory signalling and cellular adhesion remain contentious. It has been proposed that the SRCR domain is critical for ligand binding, despite MARCO containing a lysine-rich motif within the collagenous domain which is required for ligand binding by other cA-SRs. Additional data has suggested that mutation of regions outside of the RxR motif can also reduce receptor function, however which site(s) and *how* these mutations can affect receptor function have not been addressed. To address this, we present the following specific hypotheses.

1.6. Specific Hypotheses

1. We hypothesize that the SRCR domain of MARCO is integral to ligand binding and internalization, enhances pro-inflammatory signalling by other PRRs and enhances cellular adhesion.

2. We hypothesize that human-specific residues and sites undergoing positive selection within MARCO will enhance ligand binding and internalization.

CHAPTER II: MATERIALS AND METHODS

2.1. Cell Lines and Culturing

HEK 293T (ATCC #CRL-3216) cells were maintained in complete Dulbecco's modified Eagle's medium (DMEM) supplemented with 10% heat inactivated fetal bovine serum (FBS), 2 mM L-glutamine, 100 U/mL penicillin and 100 mg/mL streptomycin at 37°C and 5% CO_2. Cells were replenished from frozen aliquots before the passage number surpassed 30. RAW 264.7 cells (ATCC #TIB-71) were propagated under the same conditions without the presence of penicillin and streptomycin. Immunoprecipitation experiments were performed using HEK 293T cells stably expressing human MARCO (hM 293T). This cell line was created by Zhongyuan Tu by linearizing a pcDNA3.1$^{(+)}$/Hygro plasmid (Invitrogen, Carlsbad, CA, USA) containing the human MARCO gene via FspI digestion (NEB, Ipswitch, MA), transfection of HEK 293T with GeneJuice (Novagen, Madison, WI) at a 3:1 reagent to DNA ratio and selection at 48 h post-transfection using 350 µg/mL hygromycin B (Thermofisher, Carlsbad, CA)[1]. HEK 293T cells stably expressing human MARCOII (hMII 293T) were created following the same protocol. hM 293T and hMII 293T were cultured with 350 µg/mL hygromycin B to maintain selective pressure for cells that integrated the MARCO or MARCOII plasmid into their genome. All cell lines were regularly tested for mycoplasma contamination.

2.2. Plasmids

Human MARCO plasmids were provided by Timo Pikkarainen. Human MARCOII cDNA (clone CS0DM004YJ08) was subcloned from pCMVSPORT 6 plasmid

provided by Wu-Bo Li (GenBank accession number CR603381) into pcDNA 3.1/Hygro$^{(+)}$. Briefly, hMARCOII cDNA was excised using HindIII and XbaI restriction enzymes (Fementas, Carlsbad, CA) and purified using a QIAquick gel extraction kit (Qiagen, Hilden, Germany) following manufacturers recommended protocol. pcDNA3.1$^{(+)}$/Hygro was linearized and purified using the same methods. Insert and vector were ligated using T4 DNA ligase (New England Biolabs) overnight at RT. A 3:1 insert to vector ratio was used for a total reaction size of 100 ng in 20 µL. 2 µL of the reaction was transformed into subcloning efficiency *Escherichia coli* DH5-α cells following manufacturers recommended protocol. *E. coli* was then plated on lysogeny broth (LB) agar containing 100 µg/mL ampicillin to select for transformants. Colonies picked and grown in 5 mL LB broth containing 100 µg/mL ampicillin overnight at 37°C with shaking at 225 rotations per minute (rpm). Plasmids were isolated and purified using an EZ-10 spin column miniprep kit (Biobasic, Markham, ON) following manufacturers recommended protocol. Plasmids were sequenced at the McMaster MOBIX facility using T7 and BGH forward and reverse primers, respectively. Sequences were analyzed using Seqscanner 2.0 software (ABI Biosystems, Foster City, CA) and aligned using Clustal Omega.

Human TLR2 and CD14 plasmids were provided by Dr Cynthia Leifer (Cornell University, Ithaca, NY, USA). NF-κB secreted embryonic alkaline phosphatase (SEAP) reporter plasmid was purchased from InvivoGen (San Diego, CA, USA). All plasmids were amplified by subcloning efficiency *Escherichia coli* DH5-α cells (Invitrogen) and purified using a HiPure Plasmid Filter Midiprep Kit (Invitrogen).

Addition of C-terminal myc tags to MARCO and MARCOII was performed by PCR amplification with primers that contained the myc sequence and restriction enzyme sites to facilitate cloning (Table 2). Briefly, PCR was performed using KOD hot start DNA polymerase (EMD Millipore, Billerica, MA) on hMARCO and hMARCOII constructs in pcDNA3.1$^{(+)}$/Hygro. Cycling conditions followed the manufacturers recommended protocol, with annealing temperatures reduced to account for the myc, restriction enzyme and stop codons not annealing to the template. PCR products were run on a 1% agarose gel and purified using a QIAquick gel extraction kit (Qiagen). Products and pcDNA3.1$^{(+)}$/Hygro were then digested with HindIII and XbaI restriction enzymes (Fermentas) and ligated, transformed, selected, miniprepped and sequenced as previously described.

Q452A, Q452D and F282S constructs were generated by performing site-directed mutagenesis on the Myc-MARCO pcDNA3.1$^{(+)}$/Hygro plasmid. Mutagenic primers were designed using NEBaseChanger and PCR was performed using a Q5 site-directed mutagenesis kit (New England Biolabs) following manufacturers recommended protocol. All plasmids were transformed, amplified, purified, and sequenced as previously described. All plasmid maps have been deposited into the Bowdish lab server for future reference.

2.2.1. Transfection

1-2x10^5 HEK 293T cells were seeded into 6-well plates in complete DMEM supplemented with 10% FBS, 2 mM L-glutamine, 100 U/mL penicillin and 100 mg/mL streptomycin at 37°C and 5% CO_2. Cells were allowed to adhere overnight.

For each well, cells were transfected by mixing 2 µg of plasmid DNA with 12 µL of 1 mg/mL polyethyleneimine (Sigma Aldrich, Oakville, ON) in 100 µL incomplete DMEM in a 15 mL polystyrene tube. The solution was vortexed and allowed to incubate at room temperature (RT) for 15-20 min. 600 µL complete DMEM was then added to the tube and mixed by pipetting. Media was removed from the plated cells and carefully replaced with the transfection mixture for 2-3 h before an additional 1.5 mL of complete DMEM was added. The transfection reaction was scaled accordingly for transfection of multiple wells. Cells were incubated with transfection complexes for 48 h.

$1x10^5$ RAW 264.7 cells were seeded onto glass cover slips in 1 mL complete DMEM in a 12-well plate overnight. Transfection complexes were generated by vortexing 1 µg of plasmid DNA with 3.3 µL FuGene HD (Active Motif Inc, Carlsbad, CA) in 100 µL incomplete DMEM for 15 min at RT, per well. Transfection complexes were directly added to each well, dropwise. At 48 h post-transfection, cells were washed once with phosphate buffered saline (PBS) and resuspended in fresh DMEM.

2.3. Antibodies

Primary antibodies that were used in flow cytometry, Western blotting and Co-IP experiments included; monoclonal mouse anti-beta actin (Sigma Aldrich) used at 0.2 µg/mL, monoclonal mouse anti-Myc (9E10) at 10 µg/mL, rabbit polyclonal anti-hMARCO (1:500 dilution), rabbit polyclonal anti-hMARCOII (1:500 dilution) and a rabbit polyclonal anti-hMARCO cytoplasmic domain (1:500 dilution), as in Elomaa *et al*[82]. Primary antibodies for immunofluorescence microscopy and flow cytometry

included Alexa Fluor-647 conjugated anti-myc 9B11 (Cell Signaling Technology) used at 1:250 dilution.

MARCO (SRCR)-specific rabbit polyclonal immunoglobulin G (IgG) was previously produced by Zhongyuan Tu by immunizing two New Zealand White (NZW) rabbits each with a hapten consisting of the 17-18 C-terminal amino acids of MARCO (KYGHHDCSHEEDAGVECSV)[1]. The same protocol was followed for the generation of MARCOII-specific antibodies (KYGQFSVSGHGEYPVELHQE)[78]. Lysine (K) was added to allow for later purification via gel-coupling. Tyrosine (Y) was added to allow for coupling to the KLH carrier. Briefly, the peptide was solubilised in sterile water and cross-linked to keyhole limpet hemocyanin (KLH) (Sigma Aldrich) by mixing 5 mg of the peptide to 450 µL sodium borate buffer (0.2 M sodium borate, 0.15 M NaCl, pH = 9) and adding 4 mg of KLH (in sodium borate buffer). The pH was then re-adjusted between 8 and 9 using NaOH. 100 µL of Bisdiazonium-benzidine (BDB) was added to initiate coupling. The tube was quickly inverted and allowed to mix for 2 h at 4°C with gentle rocking. The solution was then split into 400 µg aliquots and stored at -80°C. BDB was generously provided by Dr. Peter Whyte. Synthesis of BDB was performed by dissolving 115 mg of benzidine HCl in 22.5 mL 0.2N HCl. 87.5 mg sodium nitrate was dissolved in 2.5 mL H_2O. The two liquids were combined and mixed at 4°C for 1 h.

For each rabbit to be immunized, one 400 µg aliquot was thawed and mixed with 450 µL PBS. 500 µL Freud's Complete Adjuvant (FCA) (Sigma Aldrich) was drawn from a sterilized bottle using a 20G needle and a 3 mL syringe. The peptide-PBS

mixture was then drawn into the syringe and the needle was carefully removed. A sterile emulsifying connector was attached to the syringe and an additional 3 mL syringe was connected to the other end. The syringes were alternately plunged back and forth approximately 15 to 20 times to create a homogenous solution. The solution was allowed to sit for 5 minutes to ensure separation of phases did not occur. Rabbits were then sedated via acepromazine injection and each given four 0.25 mL subcutaneous injections for a total of 1 mL per animal. Injection sites were monitored for 1 week post-injection for signs of infection or abcess. The immunization was repeated once every three weeks following the same protocol, except using Freud's incomplete adjuvant for a total of 3 boosts.

A peptide affinity purification column was prepared by creating a 50% slurry of Affigel-10 (Bio-Rad, Mississauga, ON) in 70% ethanol. 8 mL of the slurry was centrifuged at 4,000 x *g* for 2 min at 4°C. The gel was washed 3 times in 20 mM HEPES buffer (pH = 7), suspended in 8 mL HEPES buffer with 5 mg of unconjugated MARCO or MARCOII peptide and incubated at 4°C for 2 h with gentle mixing. The gel was then washed 3 times with HEPES buffer, resuspended in 1 M ethanolamine (pH = 8) and incubated for 1 h at 4°C with gentle mixing. The gel was washed 3 times with HEPES buffer and resuspended in PBS with 0.01% sodium azide. A resin column was cleaned with 70% ethanol, followed by sterile water. The gel suspension was then transferred to the column, allowed to settle and stored at 4°C.

Ten days after the third boost immunization, 10 mL of blood was collected from each rabbit in a non-heparinized tube. The blood was placed at 37°C for 30 min to allow for clotting before being transferred to 4°C for an additional 30 min. The blood was then centrifuged at 4,000 x *g* for 10 min at 4°C and serum was removed. The serum was then diluted 1:1 in PBS. The appropriate peptide affinity column was then washed twice with PBS and loaded with the diluted serum and allowed run through the column into a clean collection tube twice. The eluent was stored at -80°C for future purifications. The column was then washed three times with PBS. Peptide-specific antibodies were eluted into twelve fractions by adding 1 mL 100 mM glycine (pH = 2.7) in twelve steps. The eluent was captured in 1 mL tubes containing a pre-determined volume of 1 M tris(hydroxymethyl)aminomethane (TRIS) buffer that was sufficient to neutralize 1 mL glycine (pH 2.7) to a final pH of approximately 7. The fractions were quickly vortexed and the amount of eluted peptide-specific IgG was quantified using a Nanovue spectrophotometer (GE Healthcare). The 3-5 aliquots with the highest concentration of IgG were pooled into Slide-A-Lyzer dialysis cassettes with a 10,000 molecular weight cut off (Thermofisher) and dialyzed overnight in 4 L PBS with gentle stirring at 4°C.

Antibody specificity was tested by Western blotting against lysates from HEK 293T cells transfected with either pcDNA3.1$^{(+)}$/Hygro or human MARCO. The presence of a single dark band at approximately 50 kDa in the electrophoretic lane containing MARCO sample and little-to-no non-specific bands in the vector-control lane indicated the successful generation of MARCO-specific antibodies. Rabbits were

euthanized by exsanguination and blood was processed as above. All procedures were performed in accordance with the McMaster Animal Research Ethics Board guidelines and Institutional Animal Care.

Secondary antibodies included Alexa Fluor-633 or Alexa Fluor-647 goat anti-mouse IgG (Invitrogen) for flow cytometry and horseradish peroxidase-conjugated goat anti-mouse (1:5,000) or goat anti-rabbit IgG (1:10,000) for Western Blotting and Immunoprecipitation (Genway, San Diego, CA, USA). Donkey anti-rabbit conjugated to Cy3 was used in *E. coli* phagocytosis experiments examined via confocal microscopy (Jackson ImmunoResearch, Westgrove, USA).

2.4. Primers

The following primers were used for semi-quantitative PCR experiments and cloning.

Table 1: Primers used in semi-quantitative PCR experiments

Primer Name	Sequence (5'→3')
hMARCO (Forward)	AGGTGTGAAGGGAGAACAGG
hMARCO (Reverse)	GTGCAGCTCCACAGGGTACT
hGAPDH (Forward)	GAGTCAACGGATTTGGTCGT
hGAPDH (Reverse)	TTGATTTTGGAGGGATCTCG

Table 2: Primers used in cloning experiments

Primer Name	Sequence (5'→3')
Myc-MARCO I/II (Forward)	AAGCTTACCATGAGAAATAA
Myc-MARCO (Reverse)	ACTGTTTCTAGACTACAGATCTTCTTCAGA AATAAGTTTTTGTTCGACGCTGCACTCCA CGCCTGCGTCCT
Myc-MARCOII (Reverse)	ACTGTTTCTAGACTACAGATCTTCTTCAGA AATAAGTTTTTGTTCTTCTTGGTGCAGCTC CACAGGGTACT
Myc-MARCO Q452A (Forward)	TGACGAGTGGGCAAATTCTGATGCC
Myc-MARCO Q452A (Reverse)	TCGCAAATTGTCCCCCAG
Myc-MARCO Q452D (Forward)	TGACGAGTGGGACAATTCTGATGC
Myc-MARCO Q452D (Reverse)	TCGCAAATTGTCCCCCAG
Myc-MARCO F282S (Forward)	AAAGGTGACTCCGGGAGGCCAG
Myc-MARCO F282S (Reverse)	ACTCCCCTGGGCTCCAGG

2.5. Human Macrophage Generation and Culture

Peripheral blood mononuclear cells (PBMCs) were collected from donors who provided informed written consent. All studies were approved by the Hamilton Integrated Research Ethics Board. PBMCs were isolated from buffy-coat preparations by Ficoll density gradient centrifugation. Briefly, 15 mL of whole blood was mixed at a 1:1 ratio with PBS, loaded in a LeucoSep tube (VWR, Radnor, PA) and centrifuged at 500 x *g* for 10 min at RT with no brake. The buffy coat was isolated by careful aspiration of the upper PBS layer, resuspension of the buffy coat in fresh PBS and centrifugation at 400 x *g* for 10 min at RT with brake in a new 50 mL conical tube. Cells were plated on non-tissue culture treated polystyrene dishes and differentiated for 7 days in X-VIVO 10 culture media (Lonza, Basel, Switzerland) supplemented with 5% human AB serum (Lonza) and 20 ng/mL granulocyte-macrophage colony-stimulating factor (GM-CSF). PBMCs were stimulated for 48 h

with either PBS, lipopolysaccharide (100 ng/mL), interleukin-10 (20 ng/mL) or interferon-γ (20 ng/mL).

2.6. Semi-Quantitative PCR

Cells were lysed and RNA was isolated using a GENEzol TriRNA Pure Kit (Froggabio, North York, ON) following the manufacturer's protocol. cDNA was synthesized from 2 µg PBMC RNA using Moloney murine leukemia virus reverse transcriptase (New England Biolabs) following the manufacturer's protocol. Semi-quantitative PCR was then performed using Taq polymerase (Invitrogen) for 30 cycles using primers surrounding exons 14/17 of the human MARCO mRNA transcript or GAPDH as a housekeeping control transcript. Cycling parameters followed manufacturer’s protocol. PCR products were run on a 2% agarose gel, stained with ethidium bromide and imaged on an AlphaImager Imaging System (Alpha Innotech, San Leandro, CA). To confirm each transcript identity, bands were excised and purified using a GenElute Gel extraction kit (Sigma Aldrich) following the manufacturer’s protocol. Sequencing was performed at the McMaster University MOBIX facility.

2.7. Production of a Recombinant Soluble SRCR Domain

The SRCR region of MARCO (residues 400–520) was subcloned into a modified pET15b bacterial expression plasmid including a 6x His tag followed by a tobacco etch virus protease cleavage site. The integrity of the resulting HIS6-SRCR construct was confirmed by DNA sequencing (MOBIX, McMaster University). *Escherichia coli* Rosetta-Gami2 cells (Novagen, San Diego, CA, USA) were transformed and grown

in Luria–Bertani media to an OD_{600} of approximately 0.7. Protein production was induced with isopropyl β-D-1-thiogalactopyranoside to a final concentration of 0.5 mM and the culture was incubated at 37°C for 3 h with orbital agitation. Cells were harvested by centrifugation at 3500 x *g* for 15 min. Cell pellets were resuspended in lysis buffer (20mM Tris pH = 8, 500 mM NaCl, 2.8 mM β-mercaptoethanol, 5% v/v glycerol) supplemented with protease inhibitors (phenylmethanesulfonyl fluoride, leupeptin, benzamidine and pepstatin A) and lysed by sonication. As the SRCR domain was found in the insoluble fraction of the lysate, pellets were washed twice with lysis buffer and resuspended in denaturing buffer (20mM TRIS pH = 8, 500 mM NaCl, 2.8mM β-mercaptoethanol, 6 M urea and 5% v/v glycerol). The solution was then centrifuged at 40,000 x *g* for 40 min to remove insoluble cell debris. Unfolded SRCR was then loaded onto a HiTrap Ni-chelating column (GE Healthcare, Mississauga, Ontario, Canada) equilibrated with denaturing buffer and eluted with a step gradient (0.3 M imidazole). Denatured SRCR was concentrated to 5.0 mg/mL and refolded by massive dilution in refolding buffer (50 mM TRIS pH = 8, 800 mM L-arginine and 10 mM β-mercaptoethanol). Refolded SRCR was concentrated to 0.5 mg/mL, dialyzed in storage buffer (50 mM TRIS pH = 8, 200 mM NaCl, 400 mM L-arginine, 10 mM β-mercaptoethanol and 5% v/v glycerol) and fractionated by size exclusion chromatography using a Superdex200 10/300 GL column (GE Healthcare). The fractions containing the SRCR trimer were pooled and concentrated to 1 mg/mL in storage buffer. Monodispersity of the refolded SRCR

trimer was confirmed by dynamic light scattering on a Zetasizer NanoS (Malvern, Malvern, UK).

2.8. Generation of Ligand-Coated Microspheres

Bovine Serum Albumin (BSA) was added to 0.2 M sodium carbonate buffer (pH = 8.5) to a final concentration of 10 mg/mL in a total volume of 10 mL. Maleic anhydride was added to a final concentration of 0.1 M and the pH was adjusted above 7.5 using 0.5 M NaOH. The reaction was gently mixed for 1 h at RT. 0.5 mL of a 2.5% suspension of 0.5 µm polystyrene yellow-green fluorescent microspheres was centrifuged at 12,000 x *g* for 10 min at RT and washed twice in 0.1 M sodium borate buffer (pH = 8.5) (Polysciences, Warrington, PA). The microsphere pellet was resuspended in 1 mL sodium borate buffer and 500 µL Mal-BSA was added and incubated overnight at RT with gentle mixing. Microspheres were then centrifuged at 12,000 x *g* for 10 min at RT and the supernatant was saved for quantification of adsorbed protein. The microsphere pellet was resuspended in sodium borate buffer and incubated for 30 min at RT, followed by two additional washes before being resuspended in 1 mL PBS.

The amount of protein adsorbed to the microspheres was determined by comparing the total amount of protein in the supernatant after coating the microspheres overnight to the initial 10 mg/mL protein solution used to coat the microspheres. The protein concentrations were compared using a Nanovue spectrophotometer. Adsorbed protein ranged from 350-600 µg per tube.

2.9. Microsphere Binding, Association and Internalization Assays

At 48 h post transfection, HEK 293T cells were lifted by forceful pipetting, pooled and centrifuged at 400 x *g* for 10 min. Media was removed and cells were resuspended in Opti-Mem (Invitrogen). Cell numbers were normalized in 1 mL aliquots of each transfectant and aliquotted into replicates with conditions of ± microspheres and 4 °C or 37 °C. Cell numbers ranged from $3.5x10^5$ /mL to $1x10^6$ /mL. Mal-BSA microspheres were added to the cells at approximately 320 microspheres per cell. The tubes were then incubated with gentle agitation at 4 °C and 37 °C for 1.5 h. Following incubation, the cells were centrifuged for 10min at 500 x *g* at 4°C or RT, respectively. The media was removed from each tube and cells were washed twice with 1 mL PBS to remove all unbound microspheres. Following washes, the cells were centrifuged at 500 x *g* for 10 min at room temperature and resuspended in 200 µL PBS. Samples were added to a black 96-well plate and fluorescence was measured on a Spectramax M3 spectrophotometer (Molecular Devices, Sunnyvale, CA) at Ex441nm/Em486nm. Given that ligand binding, but not phagocytosis occurs at 4°C, microsphere internalization was calculated by subtracting the relative fluorescence of cells incubated at 4 °C (bound microspheres) from cells incubated at 37°C (total microsphere association; bound and internalized microspheres).

2.9.1. Knockdown or Rescue of Function Assays

Knockdown assays were performed using hM 293T cells. Cells were transiently transfected with either 2 µg pcDNA3.1$^{(+)}$/Hygro or 0.5 µg MARCOII and 1.5 µg

pcDNA3.1$^{(+)}$/Hygro. Rescue of function assays were performed using hMII 293T cells. Cells were transiently transfected with either 2 µg pcDNA3.1$^{(+)}$/Hygro or 0.5 µg MARCO and 1.5 µg pcDNA3.1$^{(+)}$/Hygro. Microsphere binding, association and internalization assays were performed as in chapter 2.9.

2.10. *S. pneumoniae* culture and heat killing

S. pneumoniae serotype 23 F, clinical isolate P1121 was grown in tryptic soy broth at 37°C and 5% CO_2 until cultures reached mid-log phase, OD_{600} = 0.5. Bacteria were then centrifuged at 10,000 x *g* for 2 min and resuspended in 1 mL Hanks Balanced Salt Solution (HBSS). Bacteria were titrated by serial dilution and plating 10 µL droplets on tryptic soy agar (TSA) supplemented with 5 % defibrinated sheeps blood and 10 µg/mL neomycin. Bacteria were then heat killed by incubation at 65°C for 10 min. Bacteria were treated by addition of 5-10 grains of recombinant human lysozyme to the solution and incubated at RT overnight with gentle agitation. The resulting heat-killed, lysozyme digested (HKLD) bacteria were stored at 4°C.

2.11. NF-κB Reporter Assays

HEK 293T cells were transfected with combinations of plasmids outlined in Table 3.

Table 3: Plasmids Used in NF-κB Reporter Assay

Plasmid	Transfection Amount
NF-κB SEAP	60 ng
hCD14/hTLR2 (pDUO)	60 ng
eGFP-N1	200 ng
hMARCO or hMARCOII	600 ng
pcDNA3.1$^{(+)}$/Hygro	To 2 µg

HEK 293T cells were stimulated with HKLD *S. pneumoniae*, prepared as above, for 48 h post transfection using HEK Blue detection media (InvivoGen) supplemented with 1 µg/mL of TLR2 agonist Pam3Csk4 (InvivoGen) as a positive control, or HKLD *S. pneumoniae* at a multiplicity of infection (MOI) of 50:1. NF-κB activation was measured for Pam_3Csk_4-stimulated cultures after 24 h and *S. pneumoniae*-stimulated cultures after 48 h. Cultures were first analyzed on a Typhoon Trio variable mode imager and quantified using ImageQuant software (ImageMaster, Ann Arbor, MI, USA) to determine green fluorescent protein expression. The cultures were then read on a SpectraMax 384 Plus spectrophotometer (Molecular Devices) at 655 nm absorbance to determine SEAP expression (NF-κB activity). NF-κB activity (Abs630nm) was normalized by dividing secreted embryonic alkaline phosphatase activity by green fluorescent protein expression.

2.12. Cellular Adhesion Assays

HEK 293T cells were seeded in complete DMEM at $1x10^5$ cells per well into six-well plates and transfected with plasmids expressing MARCO, MARCOII or with an empty vector control. At 48 h post transfection, a confluent monolayer was observed. In order to measure the strength of adhesion, cells were treated with 1 mL Accutase cell detachment enzyme (BD Biosciences, Mississauga, Ontario, Canada), an enzymatic cocktail containing EDTA, which eliminates integrin-mediated, but not MARCO-mediated adhesion. After 0, 15, 30 and 45 min of Accutase treatment, cells were washed and adherent cells were quantitated. Each well was stained with 1 mL crystal violet solution for 2 min and washed three times with water to remove excess

dye. Plates were dried overnight at room temperature. Following drying, 1 mL 0.2% sodium dodecyl sulfate (SDS) solution was added to each well to solubilise the crystal violet. Relative amount of cell adhesion was quantitated by measuring the Abs550nm on a Nanovue spectrophotometer (GE Healthcare).

2.13. Immunofluorescence Microscopy (Surface Expression of MARCO)

Immunofluorescence microscopy to evaluate surface expression was performed using transfected HEK 293T cells adherent on poly L-lysine-coated 24-well glass cover slips. Samples were fixed in 2% paraformaldehyde (pH 7.4) at 37 °C for 10min followed by three washes with PBS for 10min. Slides were blocked with 5% BSA for 1 h at room temperature and stained overnight with mouse anti-Myc at 4 °C. Samples were then washed three times with PBS, and stained with Alexa-Fluor 488 or 633 goat anti-mouse IgG (Invitrogen) or Texas Red Phalloidin (Invitrogen) for 30 min at room temperature. Alternatively, some samples were stained with mouse anti-myc (9B11)-Alexa Fluor-647 (Cell Signaling Technologies). Samples were washed a final three times with PBS for 10 min. Slides were mounted with ProLong Gold (Invitrogen) and were imaged on a Leica DM IRE2 inverted fluorescence microscope (Leica, Wetzlar) and adjusted for brightness and contrast using OpenLab 5.5.0 and ImageJ (NIH, Bethesda, MD). All adjustments were applied equally to all images.

2.13.1 Immunofluorescence Microscopy (Microsphere Binding)

Immunofluorescence microscopy to evaluate microsphere binding was performed using transfected HEK 293T cells adherent on poly L-lysine-coated 24-well glass

cover slips. Microspheres binding was performed as in chapter 2.9. Fixation, staining and imaging was performed as in chapter 2.13.

2.14. Scanning Electron Microscopy

Scanning electron microscopy was performed using transfected HEK 293T cells adherent on poly L-lysine-coated 24-well glass cover slips. Samples were immersed in 2% glutaraldehyde in 0.1 M sodium cacodylate buffer (pH 7.4) overnight. The samples were rinsed twice in buffer solution and post-fixed for 1 h in 1% osmium tetroxide in 0.1 M sodium cacodylate buffer. After the second fixation step, the samples were dehydrated through a graded ethanol series (50, 70, 70, 95, 95, 100, 100 and 100%) and then dried in a critical point dryer. After drying, the samples were mounted onto scanning electron microscopy stubs. The stubs were sputter coated with gold and viewed with a Tescan Vega II LSU scanning electron microscope (Tescan, Brno, Czech Republic).

2.15. Flow Cytometry to Quantify MARCO Expression

To evaluate surface expression of MARCO constructs, transfected HEK 293T cells were stained with either 9E10 mouse anti-myc antibody at 10 µg/mL, or rabbit polyclonal anti MARCO or MARCOII in 5% BSA for 1 h at RT followed by two washes with PBS. Secondary staining was performed using Alexa Fluor 633 goat anti-mouse IgG (Invitrogen) antibodies in 5% BSA for 30 min at room temperature in the dark. Following staining, cells were washed twice with PBS, filtered and assayed with a BD FacsCanto II flow cytometer (BD Biosciences) and analyzed using FlowJo version 7.6.2 software (TreeStar, Ashland, OR, USA).

2.15.1. Flow Cytometry to Quantify SRCR Construct Binding

S. pneumoniae serotype 23 F, clinical isolate P1121 was prepared as in chapter 2.10. $5x10^7$ bacteria or BSA/Mal-BSA-coated microspheres were incubated with 40 µg SRCR construct in folding buffer at room temperature for 2 h. Bacteria or microspheres were washed with PBS and stained as in chapter 2.15 using a rabbit polyclonal anti-SRCR antibody. Bacteria or microspheres were washed again with PBS and secondary staining was performed as above using Alexa Fluor 633 goat anti-rabbit IgG (Invitrogen) antibodies. Antibody specificity was validated using isotype controls. Data were gathered using FACSDiva software (BD Biosciences) and analyzed using FlowJo version 7.6.2 software (TreeStar, Ashland, OR, USA).

2.16. Western Blotting and Co-Immunoprecipitation

Western blotting was performed on lysates collected from transiently transfect HEK 293T cells at 48 h post-transfection. Briefly, adherent cells were washed once with PBS and lysed with 250 µL radioimmunoprecipitation assay buffer (RIPA) and stored on ice. Lysates were sonicated twice at 7 output control and 25% duty cycle for 12 s using a Sonifer cell disruptor (Branson Sonic Power Co, Danbury, CT). The sonicator probe was cleaned with 70% ethanol and distilled water between samples. Protein concentration was quantified using a Pierce bicinchoninic acid (BCA) protein assay, following manufacturer's recommended microplate protocol (Thermofisher). Protein concentrations were normalized by mixing samples with 5X Laemmli sample buffer and brought to equal volumes with distilled water. Samples were then boiled for 10 min and cooled for 5 min on ice. Equal volumes of sample were loaded into a

1.5 mm thick 12% polyacrylamide gel containing SDS. Kaleidoscope protein ladder (Bio-Rad) was used as a size marker. Separation was performed in Tris-Glycine running buffer with a constant voltage of approximately 120 V applied for 1.5 h or until appropriate size separation was observed. Gels were transferred to polyvinylidene difluoride (PVDF) membranes in transfer buffer (25 mM Tris, 192 mM glycine, pH = 8.3) containing 10% methanol at a constant current of 400-500 mA for approximately 75 min in a 4°C room, packed in ice. Membranes were then washed once with Tris-buffered Saline with 0.1% Tween-20 (TBST) and incubated in 5% skim milk powder in TBST at RT for 1 h. Primary antibodies were added at concentrations in chapter 2.3 and membranes were incubated at 4°C overnight with gentle rocking. Membranes were then washed three times with TBST and incubated with secondary antibodies in 5% skim milk powder in TBST for 1 h at RT. The membrane was then washed three times with TBST and incubated with Amersham Enhanced Chemiluminescence (ECL) reagent (GE Life Sciences) for 1 min at RT with gentle agitation. Membranes were transferred to an X-ray cassette and exposed to Biomax XAR autoradiography film (Kodak) for 2 min and developed using a Konica Minolta SRX 101-A X-ray developer, in the dark. Exposure time was adjusted up or down, depending on the band intensity of the 2 min exposure.

Immunoprecipitation was performed using lysates from HEK 293T cells stably expressing MARCO that were transiently transfected to express myc-MARCOII or with an empty vector control. MARCO (SRCR)-specific rabbit polyclonal IgG was

used for immunoprecipitation, and western blotting for myc-MARCOII was performed with monoclonal mouse anti-Myc (9E10), as above.

2.17. Phylogenetic and SNP Analyses of MARCO

Amino acid sequences of MARCO were acquired using the National Center for Biotechnology Information (NCBI) and ENSEMBL databases, and aligned using multiple alignment by fast fourier transform (MAFFT)[2]. Residue 282 was identified as a site of interest by comparing human, Neanderthal, Denisova and ape MARCO sequences and identifying human-specific residues. To determine if residue 282 was polymorphic, human SNP data was examined for the entire chromosomal region of MARCO from the 1000 Genomes Project and the Great Apes Genome Project using PERL scripts[118,119]. SNPs from the Neanderthal and Denisovan genomes were accessed from the Max Planck Institute for Evolutionary Anthropology[120,121]. SNPs present within exons of MARCO were characterized as being non-synonymous or synonymous substitutions using NCBI's dbSNP database. SNP data from the Great Apes Genome Project included: *Pan troglodytes*, *Pan paniscus*, *Pongo pygmaeus*, and *Gorilla gorilla*. Residue 282, within the collagenous domain, was identified as polymorphic, as humans who possess the rs6761637 SNP have a non-synonymous phenylalanine to serine substitution. Estimates of the amount of genetic diversity, θ, were calculated by $\theta = 4N_e\mu$, where N_e is the population size and μ is the mutation rate per locus using the methods of Watterson, Tajima, and Fay and Wu. Tests for selection were done using the methods of Tajima's D statistic and Fay and Wu's H statistic[122–125].

All linkage disequilibrium analyses were performed using LDLink with European, Gambian, and Chinese Han populations from the 1000 Genomes project[126]. Published MARCO polymorphisms that are associated with disease susceptibility or resistance were compared against the rs6761637 polymorphism within the respective population for which the polymorphisms were originally identified in. Alleles were determined to be in linkage disequilibrium if $R^2 > 0.1$ and $p < 0.05$. SNP frequencies were generated using the 1000 Genomes Project Version 3.1 build 144 (October 2015).

Residues Q452 and F282 was previously identified as being under positive selection by Yap *et al*[2,3]. These residues were originally identified using a branch-site model with free variation of ratios of non-synonymous to synonymous substitutions. Results were confirmed with a likelihood ratio test at 95% significance interval. All sequences were visualized in WebLogo 3[127].

2.18. Murine Peritoneal Macrophage Isolation

C57Bl/6 mice were given an intraperitoneal injection of 1 mL 2% (w/v) BioGel P100 45-90 µm-diameter microbeads in PBS (Bio-Rad). At 4-5 d post-injection, peritoneal lavages were performed with 10 mL cold PBS. Cells were centrifuged at 400 x *g* for 10 min at 4°C and resuspended in warm Roswell Park Memorial Institute (RPMI)-1640 media supplemented with 10% heat inactivated FBS, 2 mM L-glutamine, 100 U/mL penicillin and 100 mg/mL streptomycin at 37°C and 5% CO_2. Cells were allowed to adhere for 2-3 h and then washed with warm media to remove non-adherent cells. Adherent cells were incubated overnight. All procedures were

performed in accordance with the McMaster Animal Research Ethics Board guidelines and institutional animal care.

2.19. Bacterial Association Assays

S. pneumoniae serotype 23 F, clinical isolate P1121, was prepared as previously described. Briefly, $5x10^7$ bacteria were incubated with either folding buffer alone, 40 µg BSA or 40 µg recombinant soluble SRCR construct in folding buffer at 4°C for 2 h. Cells were then washed twice in HBSS.

BioGel elicited macrophages were lifted using Accutase cell detachment enzyme (BD Biosciences), centrifuged at 400 x *g* for 10 min at RT and resuspended in Opti-MEM (Invitrogen). Approximately $2.5x10^5$ macrophages were infected with an MOI of 25 *S. pneumoniae* that was pre-treated with folding buffer, BSA or SRCR construct, as above. Macrophages were incubated at 37°C for 30 min with gentle agitation. Macrophages were then washed once with PBS to remove non-associated bacteria followed by lysis in sterile water. Serial dilutions were performed in water and plated on TSA supplemented with 5 % defibrinated sheeps blood and 10 µg/mL neomycin. Colonies were counted after overnight incubation at 37°C. Bacterial association was normalized to buffer-alone treated bacteria.

2.20. Bacterial Phagocytosis Assays

Escherichia coli strain ML35 was grown to stationary phase in LB at 37°C with shaking at 200 RPM overnight. CFUs were calculated by serial dilution and plating on LB agar. Bacteria were centrifuged for 1 min at 6,000 x *g,* resuspended in PBS,

heat killed at 70°C for 10 min, and then washed twice with PBS. Bacteria were then resuspended in 500 µL PBS (pH = 8) and co-incubated with 0.2mg EZ-link NHS-LC-biotin (Thermofisher) for 20 min at RT with gentle agitation. Unreacted NHS-LC-biotin was quenched with 500 µL LB broth for 10 min at RT and washed twice with PBS. Cells were subsequently resuspended once again in 500 µL PBS and fluorescently labelled with 0.5 µL CellTrace Far-Red (ThermoFisher) for 20 min at RT with gentle agitation. Unreacted CellTrace was quenched with 500 µL LB broth for 10 min at RT and bacteria were washed twice with PBS.

RAW 264.7 cells were transfected as in chapter 2.2.1. Labelled bacteria were added at a MOI of 100 and samples were centrifuged for 1 min at 500 x *g*. Samples were incubated at 37°C for 30 min to allow phagocytosis to occur. Cells were then washed twice with PBS and stained with Alexa Fluor 488-conjugated streptavidin (BD Biosciences) at a dilution of 1:500 for 20 min at RT. Subsequently, cells were washed three times with PBS and fixed by addition of 4% paraformaldehyde (PFA) for 20 min at RT in the dark. Cells were washed three times with PBS and blocked for 30 min at RT in the dark with 5% BSA and 10% donkey serum in PBS. Cells were stained with anti-c-Myc tag polyclonal antibody (ThermoFisher) at a dilution of 1:400 in 5% BSA in PBS for 30 min at RT in the dark, washed three times with PBS and then stained with donkey anti-rabbit conjugated to Cy3 (Jackson ImmunoResearch). Cells were washed 3 times for 5 min each time, and mounted onto glass slides with PermaFluor mounting medium (ThermoFisher). Slides were imaged on a Leica DSM 6000 upright wide-field fluorescence microscope (Leica). Thirty randomly-selected

MARCO-expressing cells per construct were analyzed for bacterial binding and phagocytosis. To differentiate between bacterial binding versus internalization, bacteria that were dual-positively stained with CellTrace Far Red and Alexa Fluor-488 were considered bound, but not internalized. Bacteria that only stained positive for CellTrace Far Red were considered internalized. The phagocytic index was calculated as number of internalized bacteria divided by the number of RAW 264.7 macrophages counted. To determine whether our constructs were equally expressed in transfected RAW 264.7 macrophages, the membrane of each cell was manually traced and pixel intensity was quantified using ImageJ (NIH). Additional image processing was performed in ImageJ (NIH).

2.21. Molecular Modelling and Structural Analysis

All structural and molecular analyses were performed using the iterative threading assembly refinement (I-TASSER) version 5.0[128]. Sequences of wildtype (WT), Q452A and Q452D SRCR domains were inputted into the I-TASSER server (NSVSVRIVGSSNRGRAEVYYSGTWGTICDDEW**[Q/A/D]**NSDAIVFCRMLGYSKGRALYKVGAGTGQIWLDNVQCRGTESTLWSCTKNSWGHHDCSHEEDAGVECSV). Models with the highest confidence score (C-score) were used for analysis. Visualization was performed using UCSF Chimera 1.1[129]. Coulombic surface charge analyses were performed using DelPhi Web Server and visualized in UCSF Chimera 1.1[130].

2.22. Statistical Analysis

Statistical analyses were performed using GraphPad Prism 5.01 or GraphPad Prism 7.0 (Graphpad Software, San Diego, CA, USA). Data are expressed as mean ± standard error of the mean. Results were considered statistically significant if $p < 0.05$.

CHAPTER III: RESULTS

3.1. A naturally-occurring transcript variant of MARCO reveals the SRCR domain is critical for function

Although the SRCR domain of MARCO is critical for ligand binding in one study, this was met with some controversy, as most cA-SRs use the collagenous domain for ligand binding[77,131]. Additionally, the authors demonstrated varying levels of surface expression of different truncated and mutated MARCO constructs[77]. Thus, the importance of the SRCR domain in MARCO function is unclear. We hypothesized that the SRCR domain of MARCO is integral to ligand binding and internalization, enhances pro-inflammatory signalling by other PRRs and enhances cellular adhesion. The findings presented in chapter 3.1 (Published in *Immunology and Cell Biology*) confirmed that the SRCR domain of MARCO is required for binding and internalization of ligands, enhancing pro-inflammatory signalling in response to *S. pneumoniae* and enhancing cellular adhesion. This study utilized a novel approach to study the role of the SRCR domain, whereby a naturally-occurring variant of MARCO lacking the domain was utilized to study function, rather than artificial truncations. Importantly, this addressed two major discrepancies. MARCO shares a conserved lysine-rich motif with all five cA-SRs that has been shown to play a central role in ligand binding by other cA-SRs. Studies of MARCO function using artificial truncation or site-directed mutagenesis of the SRCR domain showed wide variation in surface expression of different constructs, adding difficulty to the interpretation of results. Additional data that was not included in the manuscript has been added.

3.1.1. Identification and characterization of a MARCO splice variant

In order to characterize the functional importance of the SRCR domain of MARCO, we cloned a transcript variant lacking the SRCR domain using the Aceview human 2010 transcript database (GenBank accession number CR603381), which we call MARCOII. The domain structure of MARCO consists of a N-terminal cytoplasmic domain (aa 1–50) followed by a transmembrane domain (aa 51–74), spacer domain (aa 75–149), collagenous domain (aa 150–419) and SRCR domain (aa 420- 520). In comparison, the predicted structure of MARCOII was identical to full-length MARCO for the first four domains, but was considerably different in the SRCR domain. The SRCR domain of MARCOII contained only the first 8 residues followed by an out-of-frame region of 19 residues (Figures 1A,B). To validate the presence of MARCO transcript variants in primary human leukocytes, we used PCR to amplify exons 16 and 17 (surrounding the putative SRCR domain) in human peripheral blood mononuclear cells (PBMCs) followed by gel electrophoresis analysis. As indicated by the presence of a small band (approximately 200 bp) in addition to a large band (approximately 400 bp) (Figure 1C), we confirmed the presence of MARCO transcript variant (MARCOII) with a truncation of the putative SRCR domain.

3.1.2. MARCOII is not expressed in all individuals and is not induced by the same stimuli as MARCO

To determine if expression of the MARCOII transcript could be induced, PBMCs were stimulated for 48 h with either phosphate- buffered saline (PBS) (unstimulated, US), lipopolysaccharide, interleukin-10 or interferon-γ. Following RNA isolation,

cDNA preparation and semi-quantitative PCR, transcripts were analyzed by semi-quantitative PCR using primers surrounding exons 14/17. Although MARCO transcript was detected in all samples, the MARCOII transcript was not expressed in 2/4 donors (Figure 2A). Primer specificity was confirmed by using HEK 293T cells transiently transfected with either MARCO or MARCOII. The identity of the transcripts from primary human samples was confirmed by excising the bands and sequencing the gel-purified products.

3.1.3. MARCOII can be transiently expressed at the same level as MARCO

To better understand the functional properties of MARCOII as well as the importance of the SRCR domain, the MARCOII cDNA was subcloned into pcDNA3.1/Hygro(+). Expression of MARCOII was assessed in transiently transfected HEK 293T cells first by western blot analysis using antibodies targeting the cytoplasmic domain and out-of-frame ‘SRCR region’ of MARCOII. MARCOII was shown to have comparable expression to full-length MARCO (Figure 3A). Next, we added a C-terminal myc tag to better compare surface expression of MARCO and MARCOII by immunofluorescence microscopy and flow cytometry. In our transient transfection system, myc-MARCOII was shown to be expressed at the cell surface (Figures 3C-J) and at similar levels as full-length MARCO (Figure 3B). Myc-tagged constructs were used for subsequent immunofluorescence microscopy experiments.

3.1.4. The SRCR domain is required for ligand binding and internalization

We compared the ability of MARCO and MARCOII to bind 500 nm polystyrene microspheres, which were passively coated with maleylated bovine serum albumin

(Mal-BSA; a previously confirmed MARCO ligand). Transiently transfected HEK 293T cells expressing MARCO showed a 300% increase in binding Mal-BSA-coated microspheres when compared with MARCOII-expressing cells (Figures 4A-H, I). Similarly, MARCO-transfected cells showed a 230% increase in internalization of Mal-BSA-coated microspheres when compared with MARCOII-expressing cells or empty vector control cells (Figure 4J). The same trend was observed for myc-tagged constructs, suggesting that the addition of a C-terminal myc tag does not interfere with ligand binding (Figure 4K). In order to confirm these quantitative data were due to microsphere binding to MARCO-expressing cells, we performed immunofluorescence microscopy, (Figure 4A-D). This phenomenon was not observed in myc-MARCOII-expressing cells (Figure 4 E-H), further indicating that microsphere binding was dependent on the SRCR domain of MARCO. Additionally, MARCO-transfected HEK 293T cells showed increased microsphere binding to the unaided eye, relative to vector- or MARCOII-transfected cells (Figure 4L). Finally, we performed chemical inhibition of clathrin, and thus phagocytosis, via chlorpromazine (CPZ) treatment to validate that microsphere internalization, not simply increased binding, occurred at 37°C relative to 4°C (Figure 4M-N)[1].

3.1.5. MARCO and MARCOII can form a heteromeric complex

Given that MARCO and MARCOII share identical collagenous domains which are required for receptor trimerization, we sought to determine if MARCO and MARCOII can form heteromeric complexes. We performed a co-immunoprecipitation and

showed that MARCO and MARCOII indeed can form heterotrimeric complexes in transiently transfected HEK 293T cells (Figure 5A).

3.1.6. Receptor function can be rescued or knocked down by co-expressing MARCO and MARCOII

To determine if expression of MARCOII can affect endogenous MARCO function, we transiently transfected a HEK 293T cell line stably expressing MARCO with MARCOII and performed ligand-coated microsphere binding and uptake assays as above. This resulted in a reduction in ligand binding to 72% and a reduction in ligand internalization to 61%, relative to the sample transfected with empty vector alone (Figures 6A,B). We used a similar approach to determine if expression of MARCO could rescue the function of MARCOII-expressing cells. Conversely, we transfected a HEK 293T cell line stably expressing MARCOII with MARCO and performed the above assay. We observed an increase to 172% in ligand binding and an increase to 218% for ligand internalization (Figures 6C,D).

3.1.7. The SRCR domain directly binds *S. pneumoniae* and enhances cell association with *Escherichia coli*

In addition to our microsphere binding assay, we sought to determine whether the SRCR domain could directly bind *Streptococcus pneumoniae*, a pathogenic bacterium that was previously shown to be cleared from the murine nasopharynx in a MARCO-dependent manner[48]. To do so, we created a recombinant, soluble SRCR trimer. Following incubation of the SRCR construct with BSA- or Mal-BSA-coated microspheres, analysis by flow cytometry confirmed the SRCR domain binds Mal-

BSA-coated microspheres. In addition, we confirmed that the SRCR domain binds *S. pneumoniae* (Figure 7A).

To assess whether the soluble SRCR trimer alone could alter endogenous binding and phagocytosis of *S. pneumoniae* by primary murine macrophages, we pre-incubated the bacterium with either folding buffer, BSA or the SRCR construct. It was determined that incubation with the SRCR construct enhanced total cell association by approximately 40% compared with controls, rather than blocking function (Figure 7B).

3.1.8. The SRCR domain is required to enhance TLR2/CD14-mediated NF-κB activation in response to *S. pneumoniae*

Although MARCO has never been shown to directly signal in response to ligand binding, it has been shown to enhance TLR2/CD14 signaling in response to *S. pneumoniae*[48]. We hypothesized that the SRCR domain of MARCO may be required to enhance the activation of other pattern recognition receptors such as TLR2. To test this, we used a NF-κB secreted embryonic alkaline phosphatase reporter assay to assess pro-inflammatory signals in response to HKLD *S. pneumoniae* stimulation. HEK 293T cells transfected with MARCO, TLR2 and CD14 showed a significant increase in NF-κB response when stimulated with HKLD *S. pneumoniae* for 48 h when compared with TLR2 and CD14 alone (Figure 8A). Cells transfected with MARCOII, TLR2 and CD14 showed no significant change in NF-κB activation when compared with cells transfected with TLR2 and CD14 alone (Figure 8A). This

suggests that the SRCR domain of MARCO is critical for enhancing NF-κB activity via TLR2.

3.1.9. The SRCR domain is required to enhance cellular adhesion and alters cell morphology

To determine whether the SRCR domain of MARCO contributed to the altered cell morphology that is observed in MARCO-expressing cells, we visualized HEK 293T cells transfected with myc-MARCO, myc-MARCOII by scanning electron microscopy. MARCO-transfected cells produced a large number of thin (<1 μm), branched, dendritic-like processes (Figures 9A-D). This phenotype was not observed in MARCOII-transfected cells (Figures 9E-H), indicating that the SRCR domain is required for the production of dendritic-like processes. To further understand the role of the SRCR domain in cellular adhesion, we quantified cellular adhesion using transiently transfected HEK 293T cells. HEK 293T are weakly adherent to tissue culture-treated plastic but were observed to increase in adherence when transfected with MARCO. First, murine resident peritoneal macrophages were treated with either PBS or Accutase to confirm that the enzyme does not cleave MARCO. Receptor expression did not decrease with Accutase treatment, as measured by flow cytometry (Figure 9I). When adherence was directly quantified by an adhesion assay, MARCO-transfected cells showed a 300% increase in adherence when compared with MARCOII-transfected cells after 45 min of Accutase treatment (Figure 9J). This indicates that MARCO can enhance cellular adhesion via the SRCR domain.

3.1.10. Summary of Results

In chapter 3.1, we have demonstrated that the SRCR domain is essential for several receptor functions, including binding and internalizing ligands, enhancing TLR2/CD14-mediated NF-κB responses and enhancing MARCO-mediated cellular adhesion. By cloning and expressing a naturally-occurring transcript variant lacking the SRCR domain, we employed a novel approach to study the role of the SRCR domain. While some human donors expressed both MARCO and MARCOII transcripts, we did not observe donors that only expressed MARCOII. Co-expression of MARCO and MARCOII in a transiently transfected cell line demonstrated that MARCO and MARCOII can form heteromeric complexes. Furthermore, expression of MARCOII reduced ligand binding and internalization by a MARCO-expressing cell line and *vice versa*.

3.2. Human-specific mutations and positively-selected sites in MARCO confer functional changes

In chapter 3.1, we demonstrated that the SRCR domain of MARCO is critical for multiple functions, however we sought to identify specific residues that can enhance or are required for function. Yap *et al*. highlighted three residues within the SRCR domain of MARCO undergoing positive selection which presumably contribute to receptor function[2]. We also identified other residues outside of the RxR motif and even outside the SRCR domain that were under positive selection and that may contribute to ligand binding and internalization. The findings presented in chapter 3.2 (Submitted to *Molecular Biology and Evolution*) describe the identification of two

residues within the human MARCO protein that are undergoing positive selection and are human specific, respectively. Specifically, we identified residue 282 in the collagenous domain and residue 452 in the SRCR domain as sites of potential function. Residue Q452 in the SRCR domain was identified as undergoing positive selection and was identified as unique to humans[2]. Residue F282 in the collagenous domain was also identified as both unique to-, and is polymorphic in- humans. Individuals that possess the rs6761637 SNP encode for the ancestral residue at position 282, serine. We also show that this polymorphism is in linkage disequilibrium with other MARCO SNPs that were previously associated with disease susceptibility or resistance.

To determine whether Q452 and/or F282 were required for MARCO function, we performed site directed mutagenesis on WT human MARCO and cloned three variants; Q452A, Q452D and F282S. To determine if mutation of these residues altered protein structure, we performed molecular modelling of the SRCR and collagenous domains. We showed that the residue at position 452 dictates the exposure, or solvent available surface area (SAS), of the first arginine residue in the RGRAEVYY motif. Due to the highly repetitive nature and lack of a crystal structure, we were unable to utilize protein modelling software to examine how the residue at position 282 influences the structure of the collagenous domain.

To determine if these residues were important for receptor function, we performed microsphere association assays and bacterial phagocytosis assays. We showed that while the ancestral D452 residue did not differ in function from the modern Q452

residue, mutation to alanine (A452) reduced receptor function. The ancestral S282 residue also reduced the receptor function. Together, these findings identified two novel residues within MARCO that play important roles in receptor function.

These findings are important, given that many studies of MARCO function have focused solely on investigating the ligand-binding sites. Here, we show that other residues that are either human-specific and/or under positive selective pressure can play important, indirect roles in enhancing receptor function. Second, we showed that phylogenetic analysis and SNP data can provide excellent starting points for the investigation of structure-function relationships in receptor biology.

3.2.1. Phenylalanine 282 is a human-specific residue in the collagenous domain of MARCO

To identify residues that are unique to humans, we searched for differences in the MARCO sequences between apes and hominins using sequence data from the 1000 Genomes Project, Great Apes Genome Project, and Neanderthal and Denisova sequences[118–121]. We identified SNPs within *Pan troglodytes*, *Pan paniscus*, *Pongo pygmaeus*, and *Gorilla gorilla* that mapped to the human MARCO gene. All of the ape species possessed a serine residue at position 282, whereas humans possess a phenylalanine residue (Figure 10A, Table 6). We also found that both Neanderthals and Denisova, the closest phylogenetic relatives to humans, also possess the ancestral serine residue, suggesting that F282 is uniquely human.

3.2.2. F282 is undergoing positive selection and is polymorphic in humans

Residue 282 was found to be polymorphic in modern humans (Figure 11A)[99]. Interestingly, the ancestral serine residue is found within humans that possess the rs6761637 SNP. This polymorphism was determined to have a global minor allele frequency (MAF) of 16.8%. Analysis of the 1000 Genomes Project identified the rs6761637 SNP to have a frequency of 34.5%, 12.3%, and 18.6% in African, East Asian and South Asian populations, respectively (Figure 11A). Smaller frequencies of 4.8% and 3.6% were noted for North American and European populations. rs6761637 was previously shown to be a member of a haplotype linked to rs17009726 and associated with increased susceptibility to pulmonary tuberculosis [99]. Therefore, we examined whether rs6761637 was in linkage disequilibrium (LD) with other polymorphisms in MARCO that have been associated with human disease. We identified five SNPS, rs2278589, rs6751745, rs17009726, rs12998782 and rs13389814, all in linkage disequilibrium with rs6761637 (Figure 11B-D, Table 4). All five polymorphisms in LD with rs6761637 were located in introns.

In order to visualize the frequency of mutation within MARCO, a site frequency spectrum for each of the primate species was created (Figure 12A). Although the samples are not randomly chosen and sometimes include different subspecies (e.g. the samples contain sequences from *P. t. troglodytes*, from *P. t. schweinfurthiii*, etc.), these data suggest that the amount of variation within the gene is small. The largest number of derived alleles in humans is at residue 282, with 1915 derived alleles and

269 ancestral alleles. This implies that either a change in population size or selection acted on the population, and thus warranted further investigation.

To determine if the mutation rate (θ) at residue 282 is indicative of positive selection, we calculated estimates of θ. Using chimpanzees as the outgroup, we used the human spectra and calculated estimates of theta ($\theta = 4N\mu$), four times the effective population size multiplied by the mutation rate, using Watterson's method (θ_W) , Tajima's method (θ_π) and Fay and Wu's (θ_H) method [122–124]. These give estimates of theta as $\theta_W = 3.15$, $\theta_\pi = 0.418$ and $\theta_H = 1.54$, respectively. Watterson's estimate is based on the number of segregating sites; Tajima's estimate is based on the number of pairwise differences, while Fay and Wu's estimate of theta is weighted by the homozygosity of derived alleles. Each estimate responds differently to population parameters. To test for the presence of selection, Tajima's D statistic and Fay and Wu's H statistic were calculated. Tajima's D statistic is -2.01 indicating a significant negative deviation and rejecting neutrality at this locus. Fay and Wu's H statistic is -1.12. A significant negative Fay and Wu's H indicates an excess of high-frequency derived SNPs suggesting that selection has acted to alter the protein in comparison to the chimpanzee outgroup; however these results must be interpreted judiciously as we were not able to generate random populations of any of the species due to the relatively modest number of available genomes. Fay and Wu suggest that following a selective hitchhiking event both their estimate and Watterson's estimate of θ should be larger than Tajima's. These data are consistent with positive selection at site 282 since the large negative value of Fay and Wu's H statistic is largely driven

by the high frequency of the derived non-synonymous allele at residue 282 (Figure 12). However these results must be interpreted cautiously as human populations do not match the assumptions that these tests are built upon (i.e. random mating, and constant population size).

3.2.3. Residue 452 in the SRCR domain is undergoing positive selection

Position 452 was previously identified as one of several positions in the SRCR domain of MARCO having potentially been subject to positive selection[2]. Using sequences from various groups of mammals, we generated an alignment of the SRCR domain of MARCO. Here we show that position 452 encodes an aspartic acid residue in aquatic and land mammals, exclusive of primates and hominins. Primates, including *Macca mulatta* (rhesus macaque), *Pan troglodytes* (chimpanzee), and *Pongo abelii* (Sumatran orangutan) all possess a histidine residue and *Nomascus leucogenys* (northern white-cheeked gibbon) possesses a glutamine residue. Neanderthal, Densiovan, and human sequences also have a glutamine at position 452 (Figure 13A, Table 5, 6). Taken together, the evidence supporting positive selection at residue 452 and the divergence in amino acid structure and charge across the evolutionary timescale, including recent divergence between NHPs and hominins, suggested a potential role in receptor function.

3.2.4. Mutation of residue 452 alters the surface availability an arginine residue that is critical for ligand binding

To assess the roles of residues 452 and 282 in receptor structure, we performed protein structure modelling and analyzed domain structure (Figure 14A), surface

charge and surface availability of the RxR motif. We observed minor changes in SRCR domain structure (Figure 14B) and surface charge (Figure 14D), but did observe changes in the surface availability of the RGRAEVYY motif (Figure 14C), suggesting that mutation of residue 452 may alter ligand binding and/or internalization by partially reducing the accessibility the RGRAEVYY motif to ligands. We calculated solvent available surface area (SAS) and found that the Q452A mutation reduced the surface availability of the first arginine residue within the RGRAEVYY motif from 114.73 Å² to 71.90 Å² (Figure 14E). Due to the highly repetitive nature of the collagenous domain, we were unable to generate accurate structural models of the collagenous domain using currently available software.

3.2.5. Mutation of residues 452 and 282 do not affect expression of MARCO

In order to determine if residue 452 is required for MARCO function, we generated human MARCO constructs using site-directed mutagenesis. We generated a Q452D construct to assess if the ancestral aspartic acid residue affects receptor function relative to the human glutamine residue. We also generated a Q452A construct to replace the larger, charged residue with a smaller, neutral one to create a 'functional knockout'. We also cloned the ancestral F282S substitution to assess if a serine substitution at position 282 affected receptor function.

To ensure that all MARCO constructs are equally expressed in transiently-transfected HEK 293T cells, we performed Western blotting on lysates of HEK 293T cells at 48 h post-transfection using antibodies targeting the C-terminal myc tag. We observed a similar level of total protein expression in all constructs (Figure 15A). To

compare surface expression, we performed flow cytometry and observed equal surface expression of all constructs relative to MARCO (Figure 15B).

We also analyzed surface expression of MARCO in a model of bacterial phagocytosis. We used FuGene (Active Motif) to transiently-transfect our MARCO constructs into RAW 264.7 cells. We observed equal expression of myc (MARCO) in all of our constructs (Figure 15C).

3.2.6. Residues at positions 452 and 282 influence ligand association

We compared the functional importance of residues Q452 and F282 in a cell-association assay using 0.5 μm MaI-BSA-coated polystyrene microspheres as ligands. Relative to empty-vector control transfected HEK 293T cells, we observed a 212% increase in microsphere association in MARCO-transfected cells (Figure 16A-B). Similar to our previous findings [78], HEK 293T transfected with a truncated variant of MARCO lacking the SRCR domain, MARCOII, showed no significant difference in microsphere association relative to empty-vector control transfectants. Mutation of glutamine 452 to the ancestral aspartic acid residue (Q452D) resulted in no significant change in microsphere association, but mutation to alanine (Q452A) resulted in a 70% reduction in microsphere association, relative to MARCO (Figure 16A-B). Mutation of phenylalanine 282 to the ancestral serine residue resulted in a 79% reduction in microsphere association (Figure 16A-B).

To determine if the human residues at positions 452 and 282 enhanced binding and phagocytosis of bacteria, we performed binding and phagocytosis assays using

transiently transfected RAW 264.7 murine macrophages and heat-killed *Escherichia coli* as a ligand. Using fluorescent labelling before and after phagocytosis, we quantitated the number of bacteria associated with the surface of the macrophage and bacteria that were internalized. Variants expressing the A452 and S282 residues demonstrated significantly lower bacterial uptake. Relative to human MARCO-transfected cells, the Q452A had an 80% reduction in phagocytosis, and the F282S construct resulted in an 84% reduction in phagocytosis (Figure 16C-D).

3.2.7. Summary of Results

In chapter 3.2, we identified two human-specific residues in the human MARCO protein that are undergoing positive selection and determined whether the 452 and 282 residues were required for MARCO function. Using molecular modelling, we demonstrated that the residue at site 452 can influence the ability of the RxR motif to access ligands. Thus, we cloned the human and ancestral variants of MARCO for functional analysis. While we were unable to demonstrate the structural impact of different residues at position 282, we showed that humans are polymorphic at this site. A high MAF of rs6761637 is found in African and Asian populations and the polymorphism is in linkage disequilibrium with other SNPs linked to pulmonary tuberculosis susceptibility. Given that this SNP encodes a non-synonymous mutation that substantially alters the hydrophobicity and charge at residue 282, we sought to clone this mutation for functional analysis. We demonstrated that the residues at sites 452 and 282 are important for both association with known MARCO ligands and for phagocytosis of bacteria.

CHAPTER IV: DISCUSSION

4.1. Scientific Contribution

The data presented in this thesis supports two fundamental advances in the structure-function relationship in the class A scavenger receptor MARCO. First, the data generated in chapter 3.1 demonstrates the central role of the scavenger receptor cysteine rich domain in ligand binding and internalization, enhancing toll-like receptor 2-mediated pro-inflammatory signalling and cellular adhesion. Second, the data generated in chapter 3.2 identifies two novel residues that indirectly enhance ligand binding and phagocytosis by MARCO.

4.2. Discussion of the experimental approach

The class A family of scavenger receptors contains five members including SR-A, MARCO, SCARA3, SCARA4 and SCARA5. Despite belonging to the same class, the cA-SRs share varying degrees of protein domain homology and, importantly, function[71,77]. The functional heterogeneity of the cA-SRs has made it difficult to assign unifying functions to shared protein domains. This is especially true in the case of the SRCR domain, a domain shared by SR-AI, MARCO and SCARA5. Several MARCO transcript variants have been identified using Aceview human 2010 transcript database (NCBI), yet have never been functionally characterized.[132] We sought to characterize the functional importance of the SRCR domain of MARCO using a naturally-occurring transcript variant.

The MARCOII transcript variant was identified using publically-available transcript variant databases. Current molecular biology technology allows for simple and efficient creation of site directed mutations, gene truncation and editing via PCR and CRISPR/Cas9, thus analysis of naturally-occurring transcript variants is not often pursued. However, the existence of a truncated transcript variant of MARCO in humans is paradoxical. On one hand, SR-A exists as multiple splice variants in all humans; SR-AI/II/III[79]. SR-AI and SR-AII are differentially expressed, but have been demonstrated to function similarly; independently of the SRCR domain[60,80]. On the other, *in vitro* analysis of artificially truncated MARCO variants suggests the SRCR domain is essential for receptor functions, suggesting that transcript variants lacking the SRCR domain would be deleterious to innate immune defense[77]. Several possibilities were investigated to explain the existence of a naturally-occurring transcript variant of MARCO in humans which lacks the SRCR domain. Given that semi-quantitative PCR of human PBMCs using exon-spanning primers surrounding the SRCR domain generates two bands in a fraction of donors, two inferences can be made. First, unlike SR-AI/II, not all humans encode for a MARCO variant lacking the SRCR domain. Second, this would suggest that humans that do encode for this variant are heterozygous carriers of an allele that encodes for alternative splicing of the MARCO transcript. There are numerous MARCO SNPs that have been deposited into human polymorphism databases, such as dbSNP. Currently, there are 29 SNPs deposited that encode for a frameshift and/or gained stop codon. Unfortunately, none of these encode for a transcript that aligns to the sequence

which we observed, specifically the near-entire truncation of the SRCR domain and frameshift mutation of approximately 20 amino acids. It is possible that a SNP which resides within a MARCO intron could alter both the rate and location of transcript splicing. Alternative splicing as a result of intronic polymorphisms have been observed in numerous genes and can result from point-mutations, such as SNPs, at- or proximal to- splice donor or acceptor sites[133–135]. Indeed, thousands of intronic MARCO SNPs have been deposited to dbSNP. Therefore, it is reasonable to postulate that intronic polymorphism(s) could be the origin of the MARCOII transcript. Furthermore, a MARCO polymorphism located in the 16th intron was previously demonstrated to be associated with an increase in susceptibility to pulmonary tuberculosis[98]. Rs13389814 is a polymorphism which encodes an [A/G] substitution gives rise to the sequence NNN[A/G]T, which once the G allele variant is transcribed, will resemble the splice donor site GU. However, given that rs13389814 is in linkage disequilibrium with numerous other SNPs, it is difficult to definitively conclude that rs13389814 is the causative agent of MARCO truncation and increased susceptibility to disease.

The MARCOII transcript was not observed in all donors, and those which did express the transcript expressed both MARCO and MARCOII transcripts, suggesting heterozygosity. This was later confirmed by excision of bands from semi-quantitative PCR experiments and sequencing. We pursued an investigation of whether the MARCOII transcript was differentially regulated relative to MARCO, possibly as a negative regulator. To do so, we stimulated PBMCs with known positive and

negative regulators of MARCO expression and quantified transcript levels. To our disappointment, numerous attempts at quantitative measurement of MARCO and MARCOII transcripts were fruitless due to a lack of specificity of several primer and primer/probe sets. To overcome this and to semi-quantitatively visualize differences in regulation, we performed semi-quantitative PCR. Our data suggested that MARCO and MARCOII are differentially regulated and expressed (Figure 2A). The levels of MARCO transcript followed others' observed patterns of induction; an increase in expression when stimulated with IL-10 and a modest reduction when stimulated with IFN-γ[78,88–90].

Unfortunately, all donors who expressed the MARCOII transcript also expressed MARCO transcript. Given this, and that the MARCOII transcript was disparately regulated, we pursued functional analyses of the role of the SRCR domain by cloning the MARCO and MARCOII cDNA into mammalian expression vectors. A central concern that we aimed to address was the disparate expression of artificial truncations and mutations in MARCO that were observed in the published works of others[77]. To do so, we generated polyclonal antibodies specific to the SRCR domain of MARCO and the out-of-frame 'stump' of MARCOII to validate protein-level expression of each receptor irrespective of the other. We concurrently generated myc-tagged MARCO and MARCOII constructs to directly compare expression of our constructs in HEK 293T cells. HEK 293T cells were selected for their high transfection efficiency, their low endogenous phagocytic capacity and because they do not express SR-AI/II or MARCO[136].

Initially, we generated HEK 293T polyclonal cell lines that stably expressed MARCO and MARCOII, however due to highly unequal expression of MARCO and MARCOII between the two respective cell lines; we pursued transient transfection as a method for equal, but heterogeneous expression. Equal total expression would allow for accurate conclusions to be drawn from functional assays. Therefore we quantified MARCO and MARCOII expression via Western blot, immunofluorescence microscopy and flow cytometry to be certain that our constructs were evenly expressed. We observed comparable expression by qualitative methods and equal expression by quantitative methods, suggesting that any possible future observations of functional differences would not be due to unequal expression.

We performed ligand binding and internalization assays using maleylated bovine serum albumin-coated polystyrene microspheres as a ligand. While HEK 293T cells do not express Fc receptors, we performed all ligand binding and internalization assays in a serum-free environment, as anecdotal evidence has suggested that MARCO can bind to antibodies. Furthermore, to maximize the availability of the receptors to interact with ligands, we performed our assays using cells that were in suspension. In addition to this, cA-SRs have been shown to modulate cellular adhesion, thus by using cells in suspension, receptor engagement of Mal-BSA microspheres would not be limited by adhesion to tissue-culture treated polystyrene[36,87,131,137,138].

Another drawback to the aforementioned studies of MARCO function by truncations and mutations was the semi-quantitative assessment of ligand binding via

immunofluorescence microscopy. While this method demonstrated ligand association mostly with cells that were successfully transfected, it remains a low throughput and non-quantitative methodology. To address this, we performed ligand binding and internalization assays both via microscopy and spectroscopy. Spectroscopic analysis was performed on samples that were normalized for CFU/mL prior to the addition of ligand. To differentiate between ligand binding and internalization, we performed the assay at 4°C, a temperature at which the cellular processes required for phagocytosis, such as actin polymerization, cannot occur, and 37°C, where both binding phagocytosis can occur. We observed a significant decrease in ligand binding in MARCOII-transfected cells, relative to MARCO-transfected cells. We also determined that ligand internalization is greatly reduced in MARCOII-transfected cells, by subtracting the relative fluorescence of our 4°C samples, which represents the bound fraction of microspheres from the 37°C samples, which represents both bound and internalized microspheres. It was previously demonstrated that MARCO-mediated phagocytosis is dependent on clathrin. Given that chemical inhibition of clathrin via CPZ treatment abolished ligand internalization at 37°C, but not binding at 4°C, we were confident that our cells were internalizing microspheres at 37°C.

To confirm that MARCO-expressing cells were predominantly responsible for binding and internalizing the ligand-coated microspheres, we performed this assay on cells transfected with myc-MARCO/MARCOII that were adherent to cover slips. Myc-tagged MARCO constructs were selected in order to perform staining using primary

anti-myc antibodies, which result in much lower non-specific binding relative to the MARCO and MARCOII rabbit polyclonal antibodies. Furthermore, this allowed more accurate comparisons of expression between samples. To ensure that addition of a C-terminal myc tag did not interfere with ligand binding or internalization, we performed assays as above and observed no changes in our trend. The data acquired by IF microscopy was consistent with the spectroscopic data. Additionally, a small degree of non-specific binding by untransfected cells and residual microspheres on the cover slip were observed. This explains why the empty-vector and MARCOII-transfected samples were observed to have an increased relative fluorescence value relative to samples that did not contain microspheres. Regardless, our data is in agreement with previously published findings that suggest the SRCR domain is the central mediator of ligand binding[77].

Taken together, this data hinted that the endogenous 'function' of MARCOII may be to act as a dominant negative mutation. Dominant negative mutations can be defined as altered gene products that can antagonize the function of a wildtype product. The most common example of dominant negative mutations occurs in oligomeric proteins, such as MARCO, that are disrupted by an altered gene product, such as MARCOII, that forms a heteromeric complex. While SR-AI/II heteromers have never been reported, nor does SR-AII reduce the function of SR-AI due to the shared reliance on the collagenous domain, a dominant negative isoform of SR-A, SR-AIII has been characterized[79]. The alternatively-spliced SR-AIII molecule was

demonstrated to negatively modulate AcLDL internalization due to the receptor becoming trapped in the endoplasmic reticulum[79].

Given that we observed expression of MARCO and MARCOII transcripts in humans, we hypothesized that induced expression of MARCO concurrently with MARCOII would rescue ligand binding and internalization. Conversely, we hypothesized that induced expression of MARCOII would reduce the endogenous functions of MARCO. To test this hypothesis, we co-expressed MARCO and MARCOII to determine if the presence of one receptor affected the other. We observed a 172% increase in ligand binding and 218% increase in internalization in our rescue of function assay and a 72% reduction in ligand binding and 61% reduction in ligand internalization in our knock down assay.

Next, we investigated the possible mechanism by which MARCOII can knock-down endogenous functions of MARCO. Given that the collagenous domain of cA-SRs are required for trimerization and that MARCO and MARCOII share identical collagenous domains, we hypothesized MARCO and MARCOII may form heteromeric complexes[60]. To test this, we performed a Co-IP of myc-MARCOII from lysates generated from the hM 293T cell line transfected with either an empty vector as a negative control or myc-MARCOII. The lack of bands in our negative controls; vector-transfected lysate and immunoprecipitation with normal IgG, combined with the presence of identical bands at the expected size in our positive control lane, 10% of total protein, and our myc-IP sample, supports our hypothesis.

MARCO has been shown to have a vital role in the recognition and clearance of bacterial infections in low-opsonic environments, as well as tethering bacterial ligands to other complexes to initiate an inflammatory response[35,48]. This tethering interaction between MARCO and other pattern recognition receptors (such as TLR2) is likely a critical step in initiating an innate immune response, as MARCO has never been shown to signal directly. On one hand, this is surprising, given that other cA-SRs have been demonstrated to either signal directly from the cytoplasmic domain or to interact with adapter proteins[36,139,140]. On the other, truncation of the cytoplasmic domain of MARCO has not been shown to affect inflammatory signalling in response to bacterial ligands[35]. Furthermore, the degree of conservation between cA-SR cytoplasmic domains is low. Therefore, we sought to determine whether the SRCR domain is required to enhance the pro-inflammatory response to *S. pneumoniae* via TLR2/CD14.

We have previously shown that MARCO is important in the pathway leading to Nod2 and TLR2-dependent NF-κB activation in response to *S. pneumoniae*[48]. We first sought to determine if the SRCR domain of MARCO is required to directly bind *S. pneumoniae* irrespective of the collagenous domain. To test this, we created a recombinant, soluble SRCR trimer and performed binding assays using BSA and Mal-BSA-coated microspheres and *S. pneumoniae* as ligands. We ensured that our soluble SRCR constructs were trimerized by size exclusion chromatography, as it has been demonstrated that soluble monomeric SRCR domains are unable to

significantly bind bacteria[95]. We showed by flow cytometry that in addition to Mal-BSA-coated microspheres, the SRCR construct bound *S. pneumoniae* directly.

Given these results, we hypothesized that pre-treatment of bacteria with a soluble SRCR construct would block endogenous functions of MARCO. We generated a soluble SRCR construct containing 20 residues of the collagenous domain for trimerization. Initial attempts to perform bacterial association assays with transiently HEK 293T and CHO-K1 cell lines were unsuccessful, as samples were observed to have no differences in some experiments and varying trends in repeats of the same experiment. Given that others have utilized soluble SRCR constructs in similar assays using murine macrophages, we performed our assay with biogel-elicited murine peritoneal macrophages[88]. To our initial surprise, we observed an increase in bacterial association when *S. pneumoniae* was pretreated with recombinant SRCR construct, relative to BSA-treated or untreated controls. Our findings are in agreement with previous studies that treatment of *Haemophilus ducreyi* with a recombinant SRCR trimer *enhanced* phagocytosis of the bacterium by bone marrow-derived macrophages[88]. Given that recombinant, soluble MARCO proteins have been demonstrated to form star-shaped oligomeric complexes, it is possible that treatment of bacteria induces the clustering of multiple bacteria[95]. Therefore, receptor engagement of a ‘single’ bacterium by a macrophage may in fact result in the cell associating with multiple bacteria. Further analysis by immunofluorescence microscopy would help to prove or disprove this proposed mechanism.

Ligand binding is a critical step not only in phagocytosis, but also for the receptor interactions that are required to signal in response to pathogens. MARCO has been shown to have a vital role in enhancing the NF-κB pro-inflammatory response to *Mycobacterium tuberculosis* by tethering the cell wall glycolipid trehalose 6,6-dimycolate to TLR2/CD14[35]. Additionally, MARCO has been demonstrated to enhance NOD2- and TLR2-mediated responses to unidentified pneumococcal ligands[48]. It has been proposed that MARCO mediates this response by 'tethering' ligands to signalling receptors on the cell membrane, such as TLRs. We therefore hypothesized that the SRCR domain is required to enhance TLR2-dependent NF-κB activity.

To test this, we performed an NF-κB reporter assay using cells expressing MARCO or MARCOII. We observed a significant increase in NF-κB activity in response to stimulation with HKLD *S. pneumoniae* in MARCO-transfected cells, relative to those transfected with TLR and CD14 alone. Cells transfected with MARCOII showed no significant change in NF- κB response to *S. pneumoniae* stimulation when compared with cells transfected with TLR2 and CD14 alone. These data indicate that the SRCR domain of MARCO is essential to indirectly enhance NF-κB activity via TLR2/CD14.

Recent advances in single molecule tracking and quantification of receptor diffusion would greatly aid in our understanding of the mechanisms that govern MARCO interactions with other signalling PRRs such as TLR2 and NOD2. For example, activation of TLRs can enhance the diffusion and clustering of B cell receptors and

enhances phagocytosis by class B SRs, such as CD36[141,142]. The current 'picket fence' model of phagocytic receptor diffusion suggests that receptors are confined to specific regions within the cell membrane and are restricted in their movement by actin filaments[29,32]. Receptor activation, such as TLRs binding bacterial products, can activate actin-severing enzymes to 'free' the diffusion of receptors bound within spatially confined regions and enhance receptor association with lipid microdomains[141,143]. Thus, tracking MARCO and TLR receptor diffusion and interaction by single particle tracking and/or Förster resonance energy transfer (FRET) in the context of ligand stimulation could provide valuable insights into the interactions of MARCO and other PRRs.

Apart from enhanced ligand binding, uptake and downstream inflammatory responses, expression of MARCO has also been shown to drastically alter cellular morphology and adhesion[144]. Given the similarities between the receptors required for- and cellular processes utilized in phagocytosis, cellular adhesion is often contextualized as 'frustrated' phagocytosis of an infinitely large particle[145]. Generally, cellular adhesion is defined as an extension or connection of the actin cytoskeleton to a neighboring cell or an extracellular matrix, such as collagen. This involves a complex network of adhesion molecules, such as integrins, adapter proteins and dynamic actin remodelling. Presumably, this remodelling of the actin cytoskeleton, can influence cell morphology.

MARCO expression has been shown to alter actin remodelling and cell morphology during adhesion and phagocytosis[87,144,146]. Pikkarainen *et al.* suggested that

MARCO-mediated cellular adhesion is likely modulated by a proximal region (in later publications, identified as the RxR motif) of the SRCR domain. In contrast, SRA-mediated adhesion has been shown to be dependent on the collagenous domain[131,147]. Thus, we sought to characterize the role of the SRCR domain of MARCO in both SR-induced morphological changes and cellular adhesion.

During our investigation of the role of SRCR domain in ligand binding and internalization, we noted that MARCO-transfected cells were morphologically distinct, compared to vector- or MARCOII-transfected cells. Closer analysis of MARCO-transfected cells by scanning electron microscopy showed that MARCO-transfected cells formed numerous thin (<1 μm), highly branched, dendritic-like processes, similar to what was reported by Pikkarainen *et al*[144]. This morphology was not observed in MARCOII-transfected or vector control cells, which adhered by large, unbranched processes. Interestingly, the MARCO-transfected cells exhibited this phenotype in both early adherence prior to cell spreading and late adherence, when cell spreading resulted in the formation of flattened shapes.

Given that cA-SR-mediated adhesion has been proposed to alter cellular retention at sites of injury, infection and tumor growth, we sought to determine if MARCO-mediated cellular adhesion is enhanced by the SRCR domain[148,149]. Preliminary evidence for the role of the SRCR domain in cellular adhesion was observed during passaging of stable MARCO- or MARCOII-expressing HEK 293T cells. MARCO-expressing cells required significantly more force and repetitions when using forceful pipetting of media as a lifting method, which suggested a possible role of the SRCR

domain in cellular adhesion. To test this, we performed an adhesion assay whereby vector, MARCO or MARCOII-transfected cells were treated with a cell detachment enzyme, accutase, across a time course. The remaining adherent cells were stained with crystal violet, which was later solubilised and optically quantified by a spectrophotometer. Across a 45-minute time course, MARCO-transfected cells remained more adherent compared to vector- or MARCOII-transfected cells. Our observations supported our hypothesis. This work would benefit from closer examination of the distribution of MARCO receptors on cells that are adhering to surfaces. Our preliminary data suggested that MARCO was highly expressed along the membrane protrusions, however this preliminary data must be interpreted cautiously, as abnormally high laser power and gain was required to visualize these processes by confocal microscopy.

Together, our results demonstrate the central role of the SRCR domain in multiple functions of MARCO. Yet, the evolutionary conservation of residues *outside* of the SRCR domain of MARCO convolutes these findings. While conservation of residues and motifs is an imperfect metric to imply biological function, it can provide clues to be further examined. The SRCR domain of MARCO is indeed highly conserved across chordates and it is now abundantly clear that the SRCR domain of MARCO is vital for receptor function. In organisms that predate vertebrates, however, the functions of this domain were not necessarily for host defense. It has been hypothesized that early receptors containing SRCR domains were involved in cell-cell adhesion[100]. The most ancient organism from which a class A SR (i.e. plasma

membrane-expressed, with one SRCR domain) has been sequenced is *Petromyzon marinus* (sea lamprey), suggesting that that the earliest precursors to the modern class A SRs likely arose at least 500 million years ago. Whelan *et al*. previously demonstrated that diversification of the class A SRs likely resulted from a single common ancestor protein that underwent gene duplication, domain fusions and deletions[68]. This protein likely contained an SRCR domain, as 3 of the 5 modern class A SRs contain a SRCR domain[68]. This genetic diversification of the class A SRs likely would have allowed for diversification of receptor function, allowing for binding and phagocytosing of a wider variety of ligands, including pathogens and clearance of foreign or endogenous cellular debris. It is conceivable that this specialization of the SRs was the result of positive selective pressure for domains and motifs that enhanced the host defense properties and homeostatic functions of the respective receptors. Ultimately, the resulting five members of the modern cA-SRs in humans are diverse in both receptor structure and function. A large number of motifs and residues of the modern class A SRs are highly conserved and/or under positive selective pressure, but which of these may play a role in the intrinsic function of the receptor remains unknown[2].

Of the five modern class A SRs, MARCO appears to be unique in that its primary function is in host defense, while other members have been shown to regulate processes such as clearance of lipids and proteins and cells undergoing oxidative stress and apoptosis [63,97,150]. We sought to identify both conserved and/or positively selected sites within the MARCO gene followed by characterizing their role in

receptor function. We began by comparing the MARCO gene of non-human primates (NHPs), Denisovans and Neanderthals to extant humans. Yap *et al*. previously identified a site within the SRCR domain, glutamine 452, that is undergoing positive selection[2]. These branch-site analyses were restricted to the SRCR domain due to both the central role of the SRCR domain in MARCO function and the lack of quality sequences available for other domains in MARCO. We re-ran the analysis and included recently published Neanderthal and Denisovan genomes, which did not differ from the original findings[120,121]. Interestingly, all currently available MARCO sequences from aquatic and terrestrial mammals, and *some* NHPs, possess aspartic acid, a negatively-charged residue, whereas *Homo denisovan, H. neanderthalensis* and *H. sapiens* possess a polar, uncharged glutamine residue. Furthermore, this residue is situated near the ligand-binding, RGRAEVYY motif. Given that large changes in residue charge and hydrophobicity can affect receptor structure, we sought to further investigate a potential role for residue 452.

We identified a second site within the collagenous domain, phenylalanine 282 (F282), which we show as being unique to humans, with most ancestral organisms possessing a serine residue (S282). Given that the branch-site model utilizes codon changes to predict sites of positive selection, it is unsurprising that residue 282 was not identified during this initial analysis. While this residue was not identified as undergoing positive selection using the branch-site model, we were perplexed by the

sharp change in residue size and polarity in humans alone. Thus, at first we restricted our analysis of this site to the human population.

In humans, MARCO is an important component of host defense against airway pathogens such as *Mycobacterium tuberculosis (Mtb)*, *Streptococcus pneumoniae,* and *Klebsiella pneumoniae*[35,48,151]. It is therefore unsurprising that studies of MARCO by candidate gene approach have identified SNPs that are associated with susceptibility or resistance to infection[98,99,109]. To our surprise, the rs6761637 polymorphism that was previously linked to increased susceptibility to pulmonary tuberculosis by Ma *et al.* (2011) encodes for the ancestral S282 residue. We further analyzed this polymorphism and found that approximately 17% of humans possess the SNP encoding the ancestral serine residue at position 282. We discovered that the rs6761637 polymorphism is found at high allele frequencies in the South and East Asian populations, as well as in the African population. Haplotype analysis revealed that rs6761637 is in linkage disequilibrium with other polymorphisms associated with increased susceptibility to *Mtb.* Together, this suggested that F282 may also play a role in pathogen-receptor interactions.

Thus, we investigated whether residue 282 was undergoing positive selection by generating estimates of θ, genetic diversity of a population, and applying and comparing statistical analyses. There are multiple methods to calculate θ, however not all datasets are suitable for each method. Each method is sensitive to different sources of error. For example, Tajima's D statistic suggests that a negative value infers that neutral or random mutation is occurring; however this may be due to

population contraction or expansion. Thus, interpreting this statistic in the context of other statistics, such as Fay and Wu's H, provides additional confidence and clarification to interpret the results. Using Watterson's estimate of θ, Tajima's D statistic and Fay and Wu's H statistic, we determined whether patterns of diversity across human and NHP aligned with a model of selective sweep, and thus provides evidence for positive selection. Our data are consistent with positive selection at site 282, however this must be interpreted cautiously. First, our NHP outgroup contains genomes from highly inbred populations and thus our sampling is not random. Second, human populations were modelled under demographic assumptions such as random mating, constant population size and no forms of genetic recombination, such as during meiosis and genetic repair. Third, Fay and Wu's H statistic was not statistically significant in *all* populations examined, however given the frequency of the derived allele in the human populations we analyzed (1915 derived alleles, 269 ancestral alleles), we consider these tests to be consistent with positive selection and thus, warranted further analysis of the functional importance of this residue.

Given that the RGRAVEVYY motif has been suggested as the primary ligand binding site, we sought to determine how mutations *outside* this motif could alter receptor function[77]. To examine if mutation of residue Q452 to the ancestral aspartic acid or a loss-of-function mutation to alanine affected receptor structure, we modelled structural changes in the SRCR domain. The best reference structures for the SRCR domain are the monomeric and dimeric SRCR domains of human MARCO[92]. While mutation of residue 452 did not significantly alter the SRCR

domain structure or coulombic charge distribution, we observed that mutation of residue 452 to alanine partially 'hid' the RGRAEVYY motif of a SRCR monomer. This was further investigated by determining the SAS of each arginine residue. While mutation of Q452 to the ancestral D452 did not significantly alter the SAS of either residue (+14% SAS), mutation to alanine reduced the SAS of the first arginine residue (-37%). This suggested that residue 452 may not be directly involved in ligand binding, but rather may play an important role in the structure of the SRCR domain, such that the ligand-binding RGRAEVYY motif is not fully exposed to ligands. In addition, we attempted to model the structural changes induced by a F282S substitution, but were precluded from obtaining meaningful results due to the lack of a collagen domain reference crystal structure. The collagenous domain of MARCO contains the classic Gly-Xxx-Yyy amino acid signature and likely has similar functions to collagen, such as providing additional stability and flexibility to the receptor. However, similar to collagen, the repetitive structure, relatively low solubility and complex, large size of collagen impedes the ability to model its structure[152]. Given that collagen-like structures heavily rely on steric effects and a delicate balance of hydrophobic and hydrophilic interactions, we hypothesize that the hydrophobicity of the residue at position 282 may alter its location within the collagenous domain. The ancestral serine residue is slightly hydrophilic, and could reside inside or outside of the structure. In contrast, phenylalanine is highly hydrophobic and might localize internally within the domain[153]. The collagenous domain of human MARCO contains two phenylalanine residues, F282 and F293.

F293 is not well conserved across the species we examined, however it is found in some land mammals and NHPs. Phenylalanine residues can interact to provide additional free energy to stabilize secondary structures[154]. Given the proximity of F282 and F293, it is possible that these residues behave in a similar manner. Furthermore, F293 seems to have appeared some time during the 'late'; land mammals, such as domestic dogs and elephants and is conserved in NHPs. Since the collagenous domain is important for receptor trimerization, it is possible that this mutation to F282 in humans favors a more stable conformation of the collagenous domain that may facilitate bacterial binding or uptake[77,147]. Interestingly, human SR-A contains 17 phenylalanine residues, the majority of which are found in spacer domain and collagenous domain. Many of these residues are within 10 amino acids of each other, which could possibly allow for multiple Phe-Phe interactions. This is in agreement with the proposed function the spacer domain; to provide structural support. Human MARCO only contains 10 phenylalanine residues, 5 of which are located on the apical side of the cell membrane. It is possible that a Phe282-Phe293 interaction in human MARCO is highly important for receptor structure, given the relatively short spacer domain and lack of additional phenylalanine residues.

Next, we analyzed surface expression of our mutant constructs to ensure equal expression and showed that our mutations did not alter expression of our constructs relative to human MARCO. We also concluded that the mutations we induced did not abrogate surface expression of the receptor. We then sought to determine if functional differences would be observed between ancestral and modern human

residues of sites 452 and 282. We performed ligand association assays using Mal-BSA-coated polystyrene microspheres, as before[78,79]. We showed that mutation of residue Q452 to the ancestral aspartic acid residue had no effect on ligand association; however mutation to alanine reduced function by 70%. This is in agreement with our molecular modelling data. Taken together, this suggests that residue 452 is important for *indirectly* enhancing ligand association by increasing the SAS of the first arginine residue in the RGRAEVYY motif. Furthermore, we showed that mutation of F282 to the ancestral serine residue reduced ligand association by 79%. This is surprising, given that the SRCR domain has been shown to be the primary ligand binding site for Mal-BSA microspheres[78]. Further investigation into the exact mechanism that F282 contributes to receptor function is highly warranted. It is possible that the human residue results in a more stable receptor conformation and could influence the tertiary and quaternary structures that trimeric and oligomeric MARCO proteins form. Thus, solving the crystal structure would be highly desirable and beneficial.

Next, we demonstrated that residues at sites 452 and 282 played a role in phagocytosis of a physiologically-relevant ligand, *E. coli*. MARCO-mediated phagocytosis of bacteria has been shown to play a central role in the clearance of infection by both phagocytosis and by enhancing inflammatory signalling through TLRs[35,48,151]. MARCO responds to *Mtb* infection by recognizing trehalose 6,6'-dimycolate (TDM), a component of the mycobacterial cell wall [35]. The presence of TDM enhances both MARCO-mediated phagocytosis of the bacterium and

inflammatory signalling through TLR2[35]. Others have demonstrated that phagocytosis of *Mtb* results in additional activation of intracellular, pro-inflammatory receptors such as TLR9 and NOD2[155,156]. Interaction of mycobacterial ligands with TLRs 2/9 and NOD2 represents an early, but important step in activating interferon-gamma and Th-1-type protective immunity against *Mtb*[157]. Therefore, a MARCO allele which enhances the intrinsic phagocytic function of the receptor would likely be advantageous to the host.

We did not observe a difference in binding of *E. coli* in RAW 264.7 cells transfected to express our MARCO constructs, but MARCO-mediated internalization was reduced in specific constructs. We observed an 80% reduction in phagocytosis in the Q452A mutant and an 84% reduction in phagocytosis with our F282S mutant. These findings agree with our microsphere association results. Our data is complimentary to other published ligand binding studies of MARCO, whereby mutation and/or deletion of the varying regions of the either the collagenous or SRCR domain reduced, but did not totally abolish receptor function[77]. While *E. coli* has previously been used to study MARCO function, given the relationship between MARCO and *S. pneumoniae and Mtb,* further optimization of staining these bacteria for use in our phagocytosis assay is highly desirable.

Together, our data suggests that Q452 and F282 are important for ligand association and phagocytosis of bacteria. We show that Q452 and F282 are examples of positively-selected mutations in MARCO, and that both enhance the intrinsic function of the receptor.

4.3. Future Directions

Our findings identified novel residues that enhance the function of MARCO and have also demonstrated the central role of the SRCR domain in MARCO function. While this thesis has presented novel avenues to studying MARCO function, our work has suggested many divergent routes of future study. In chapter 3.1, we examined the connection between a SNP, rs13389814 and the presence of a MARCO splice variant lacking the SRCR domain, MARCOII. While we have proposed that the rs13389814 polymorphism may encode for an alternative splice site upstream of the correct splice site, further investigation could confirm our hypothesis. *In vitro* analysis of pre-mRNA splicing could be achieved using an immortalized human macrophage-like cell line would be desirable, however the closest approximation available is the THP-1 monocyte-like cell line. Unfortunately, pilot studies in our lab have suggested little-to-no detectable MARCO expression in THP-1 cells and others have shown no MARCO transcript present in RAW 264.7 murine 'macrophages'[136]. If we could identify a human macrophage-like cell line that *does* express MARCO, this would present an opportunity to employ CRISPR/Cas9 to perform genome editing and to introduce the rs13389814 SNP to intron 16. In this context, careful attention must be given to proper genotyping of the cell line; as we and others have demonstrated that rs13389814 is in linkage disequilibrium with other SNPs that may affect MARCO expression or splicing[98,99,110].

Our work has demonstrated that the MARCOII transcript is not regulated in a similar fashion that MARCO is. Given that rs13389814 is in LD with other SNPs that are

found in the 5' UTR and first intron, this may suggest that the alternatively spliced transcript is differentially regulated due to differences in the promoter region. Unfortunately there is very little published data to support what transcription factors govern MARCO expression. Unpublished data from our collaborators suggests that ccaat-enhancer binding proteins (C/EBP) are a family of transcription factors that can regulate MARCO expression and that the rs7559955 polymorphism, associated with resistance to pulmonary tuberculosis, increases MARCO expression. This is supported by additional analyses of transcription factor binding sites upstream of *MARCO*[91]. Additional unpublished data has identified multiple NF-κB binding sites in the promoter. While it may not be feasible to dissect the role of every SNP that is in LD with rs13389814, it would be very appealing to examine whether this polymorphism alters transcript expression. It would be of great interest to generate specific primer sets that allow for quantification of each variant when stimulated with known inducers of MARCO expression, such as NRF2 and AKT activators[91].

Given that we generated MARCOII-specific polyclonal antibodies and that Wu *et al.* recently published the first definitive enhancers of MARCO expression, it would be interesting to demonstrate the existence of MARCOII protein in primary human samples. A second MARCO isoform has never been shown to exist at the protein-level. We were precluded from this valuable experiment due to a small cohort size which lacked enough genetic diversity to have many carriers of the MARCOII SNP. In addition to this, it would be of great interest to determine if MARCO and MARCOII can form heteromeric complexes in primary human macrophages. Thus, collecting

PBMCs from donors that carry the rs13389814 polymorphism and analyzing differentiated macrophages by Co-IP with antibodies recognizing MARCO and MARCOII would add to our findings.

We created a soluble SRCR trimer to demonstrate that the SRCR domain can directly bind *S. pneumoniae*. Given that there are currently >90 serotypes described, it is possible that some serotypes are more susceptible to MARCO-mediated phagocytosis than others. Since MARCO-mediated phagocytosis is a central mechanism for clearing pneumococcal colonization, it would be of great interest to determine which serotypes are more or less resistant to MARCO-mediated phagocytosis and what capsular components dictate efficient versus inefficient phagocytosis[48]. It is very likely that the availability of MARCO ligands on the cell capsule, such as LTA, primarily dictate which serotypes are most readily bound by MARCO[158]. However, it is also possible that some serotypes encode anti-phagocytic proteins, such as the members of the lipoprotein family of peptidyl-prolyl cis/trans-isomerases, which have been demonstrated to suppress MARCO-mediated phagocytosis in other streptococci[38,39,159].

Given that the SRCR domain of MARCO interacts with bacterial ligands, a closer elucidation of how MARCO interacts with *other* PRRs, such as TLR2 would help clarify the relationship. CD36 has been shown to associate with TLR2/1 and 2/6 heterodimers within lipids rafts upon stimulation, thus it would be reasonable to hypothesize that MARCO may act similarly[160]. Thus, stimulation of MARCO-expressing cells with various known bacterial ligands, followed by lysis and sucrose

fractionation could help identify the cellular location of MARCO. This study could be bolstered by further analysis by single particle tracking experiments, to better understand how MARCO diffuses in response with soluble and particulate ligand stimulation, as SR diffusion has been shown to influence receptor internalization[31].

In chapter 3.1 we examined whether the SRCR domain can enhance MARCO-mediated cellular adhesion. Our findings suggest that the SRCR domain does enhance cellular adhesion to tissue culture-treated plastic, but would be enhanced by future study using extracellular matrix (ECM) proteins, such as fibronectin, collagen or cell monolayers. These ligands are more physiologically relevant in the context of macrophage adhesion and motility *in vivo*.

Finally, in chapter 3.2, we identified two residues in human MARCO that were later shown to indirectly enhance receptor function. Given that Yap *et al.* demonstrated two additional sites under positive selection, V477 and W442, it is possible that these residues also contribute to receptor function[2]. We selected residue Q452 for further characterization because it had the highest Bayes Empirical Bayes (BEB) score, suggesting that is was the most strongly associated with positive selection. Additionally, we predicted that the change from the ancestral negatively charged SNP to a polar, uncharged glutamine, would affect structure/function relationships. Lastly, the Q452 mutation was in closest proximity to the RxR motif which was known to be required for function and as a consequence, we believed it to be a reasonable choice for our studies. Given that V477 is most distal to the RGRAEVYY motif and is a small, non-polar residue, it would be reasonable tohypothesize that it

is unlikely to be biologically significant. However, given that W442 shares similar size, polarity and hydrophobicity to F282, it is possible that W442 is structurally important for the SRCR domain, and thus, warrants further investigation.

Given the proximity of F282 and F293 and the aforementioned possibility of aromatic-aromatic interactions, the creation of other site directed mutants at these positions for further functional analysis is also highly justified.

4.4. Concluding Remarks

This thesis has contributed to our understanding of how MARCO functions at the molecular level. The work presented in chapter 3.1 demonstrated that the SRCR domain of MARCO is critical for multiple functions of the receptor. Our data supports and builds upon the findings of others. The work presented in chapter 3.2 identified and characterized two novel residues in MARCO that indirectly enhance the intrinsic functions of MARCO. Importantly, we demonstrated roles for residues *outside* of the RGRAEVYY motif and suggested that sites under positive selection may play key roles in enhancing receptor function.

CHAPTER V: REFERENCES

1. Tu, Z. Characterization of MARCO-Mediated Endocytosis. (2012).

2. Yap, N. V. L., Whelan, F. J., Bowdish, D. M. E. & Golding, G. B. The Evolution of the Scavenger Receptor Cysteine-Rich Domain of the Class A Scavenger Receptors. *Front. Immunol.* **6,** 1–9 (2015).

3. Yap, N. Studying Macrophage Receptor Evolution and Function using Bioinformatics. (2016).

4. Gyorki, D. E. *Laudable pus: historic concept revisited*. *ANZ Journal of Surgery* **75,** (2005).

5. Gordon, S. *Phagocytosis: The Host. Advances in cell and molecular biology of membranes and organelles*. (JAI Press, 1999).

6. Ambrose, C. T. The Osler slide , a demonstration of phagocytosis from 1876 Reports of phagocytosis before Metchniko V ' s 1880 paper. *Cell. Immunol.* **240,** 1–4 (2006).

7. Bowdish, D. M. E. Macrophage Activation and Polarization. *Encycl. Immunobiol.* **1,** 289–292 (2016).

8. Flannagan, R. S., Jaumouillé, V. & Grinstein, S. The cell biology of phagocytosis. *Annu. Rev. Pathol.* **7,** 61–98 (2012).

9. Okabe, Y. & Medzhitov, R. Tissue biology perspective on macrophages. *Nat.*

Publ. Gr. **17,** 9–17 (2016).

10. Siddiqui, R. & Ahmed, N. Experimental Parasitology Acanthamoeba is an evolutionary ancestor of macrophages : A myth or reality ? *Exp. Parasitol.* **130,** 95–97 (2012).

11. Ensan, S. *et al.* Self-renewing resident arterial macrophages arise from embryonic CX3CR1 + precursors and circulating monocytes immediately after birth. *Nat. Immunol.* **17,** (2016).

12. Patel, A. A. *et al.* The fate and lifespan of human monocyte subsets in steady state and systemic inflammation. *J. Exp. Med.* (2017). at <http://jem.rupress.org/content/early/2017/06/09/jem.20170355.abstract>

13. Perdiguero, E. G. & Geissmann, F. Development and maintainance of resident macrophages. *Nat. Immunol.* **17,** 2–8 (2016).

14. Epelman, S., Lavine, K. J. & Randolph, G. J. Origin and Functions of Tissue Macrophages. *Immunity* **41,** 21–35 (2014).

15. Varol, C., Mildner, A. & Jung, S. Macrophages : Development and Tissue Specialization. *Annu. Rev. Immunol.* **33,** 643–675 (2015).

16. Pollard, J. W. Trophic macrophages in development and disease. *Nat. Rev. Immunol.* **9,** 259–270 (2009).

17. Murray, P. J. & Wynn, T. A. Protective and pathogenic functions of

macrophage subsets. *Nat. Rev. Immunol.* **11,** 723–737 (2012).

18. Martinez, F. O. & Gordon, S. The M1 and M2 paradigm of macrophage activation : time for reassessment. *F1000 Prime Reports* **13,** 1–13 (2014).

19. Mills, C. D. *et al.* M-1/M-2 Macrophages and the Th1/Th2 Paradigm. *J. Immunol.* **164,** 6166–6173 (2000).

20. Roszer, T. Understanding the Mysterious M2 Macrophage through Activation Markers and Effector Mechanisms. *Mediators Inflamm.* 1–16 (2015).

21. Mantovani, A. *et al.* The chemokine system in diverse forms of macrophage activation and polarization. *Trends Immunol.* **25,** 677–686 (2004).

22. Long, K. B. & Beatty, G. L. Harnessing the antitumor potential of macrophages for cancer immunotherapy. *Oncoimmunology* **2,** 1–9 (2013).

23. Beham, A. W. *et al.* A TNF-Regulated Recombinatorial Macrophage Immune Receptor Implicated in Granuloma Formation in Tuberculosis. *PLoS Pathog.* **7,** (2011).

24. Fuchs, T. *et al.* A combinatorial alpha-beta T cell receptor expressed by macrophages in the tumor microenvironment. *Immunobiology* **222,** 39–44 (2017).

25. Gordon, S. Phagocytosis: An Immunobiologic Process. *Immunity* **44,** 463–475 (2016).

26. Rabinovitch, M. Professional and non-professional phagocytes : an introduction. *Trends Cell Biol.* **5,** 85–87 (1995).

27. Botelho, R. J. & Grinstein, S. Phagocytosis. *Curr. Biol.* **21,** 533–538 (2011).

28. Griffin, B. F. M., Griffin, J. J. A., Leider, J. E. & Silverstein, S. C. STUDIES ON THE MECHANISM OF PHAGOCYTOSIS I . Requirements for Circumferential Attachment of Particle-Bound Ligands to Specific Receptors on the Macrophage Plasma Membrane * Phagocytosis of a variety of inert and metabolically active particulates plays an. *J. Exp. Med.* **142,** 1263–1282 (1975).

29. Jaumouillé, V. & Grinstein, S. Receptor mobility, the cytoskeleton, and particle binding during phagocytosis. *Curr. Opin. Cell Biol.* **23,** 22–29 (2011).

30. Andrews, N. L. *et al.* Actin restricts FcepsilonRI diffusion and facilitates antigen-induced receptor immobilization. *Nat. Cell Biol.* **10,** 955–963 (2008).

31. Jaqaman, K. *et al.* Cytoskeletal control of CD36 diffusion promotes its receptor and signaling function. *Cell* **146,** 593–606 (2011).

32. Freeman, S. A. & Grinstein, S. Phagocytosis: receptors, signal integration, and the cytoskeleton. *Immunol. Rev.* **262,** 193–215 (2014).

33. Vadali, S. & Post, S. R. Lipid rafts couple class A scavenger receptors to phospholipase A 2 activation during macrophage adhesion. *J. Leukoc. Biol.* **96,** 873–881 (2014).

34. Cannon, G. J. & Swanson, J. A. The macrophage capacity for phagocytosis. *J. Cell Sci.* **101,** 907–913 (1992).

35. Bowdish, D. M. E. *et al.* MARCO, TLR2, and CD14 are required for macrophage cytokine responses to mycobacterial trehalose dimycolate and Mycobacterium tuberculosis. *PLoS Pathog.* **5,** e1000474 (2009).

36. Kosswig, N., Rice, S., Daugherty, A. & Post, S. R. Class A scavenger receptor-mediated adhesion and internalization require distinct cytoplasmic domains. *J. Biol. Chem.* **278,** 34219–25 (2003).

37. Fong, L. G. & Le, D. The processing of ligands by the class A scavenger receptor is dependent on signal information located in the cytoplasmic domain. *J. Biol. Chem.* **274,** 36808–16 (1999).

38. Cho, K., Arimoto, T., Igarashi, T. & Yamamoto, M. Involvement of lipoprotein PpiA of Streptococcus gordonii in evasion of phagocytosis by macrophages. *Mol. Oral Microbiol.* **28,** 379–391 (2013).

39. Mukouhara, T., Arimoto, T., Cho, K., Yamamoto, M. & Igarashi, T. Surface lipoprotein PpiA of Streptococcus mutans suppresses scavenger receptor MARCO-dependent phagocytosis by macrophages. *Infect. Immun.* **79,** 4933–40 (2011).

40. Lemaitre, B., Nicolas, E., Michaut, L., Reichhart, J. & Hoffmann, J. A. The Dorsoventral Regulatory Gene Cassette ¨ tzle / Toll / cactus Controls the spa

Potent Antifungal Response in Drosophila Adults. *Cell* **86,** 973–983 (1996).

41. Suresh, R. & Mosser, D. M. Pattern recognition receptors in innate immunity , host defense , and immunopathology. *Adv. Physiol. Educ.* **20742,** 284–291 (2013).

42. Brubaker, S. W., Bonham, K. S., Zanoni, I. & Kagan, J. C. Innate Immune Pattern Recognition : A Cell Biological Perspective. *Annu. Rev. Immunol.* **33,** 257–290 (2015).

43. Yarovinsky, F. Innate immunity to Toxoplasma gondii infection. *Nat. Rev. Immunol.* **14,** 109–121 (2014).

44. Manukyan, M. *et al.* Binding of lipopeptide to CD14 induces physical proximity of CD14 , TLR2 and TLR1. *Eur. J. Immunol.* **35,** 911–921 (2005).

45. Dalpke, A., Frank, J., Peter, M. & Heeg, K. Activation of Toll-Like Receptor 9 by DNA from Different Bacterial Species. *Infect. Immun.* **74,** 940–946 (2006).

46. Kurt-jones, E. A. *et al.* Pattern recognition receptors TLR4 and CD14 mediate response to respiratory syncytial virus. *Nat. Immunol.* **1,** (2000).

47. Stack, J., Doyle, S. L., Connolly, D. J., Reinert, L. S. & Keeffe, K. M. O. TRAM is required for TLR2 endosomal signaling to type I IFN induction. *J. Immunol.* **193,** 6090–6102 (2014).

48. Dorrington, M. G. *et al.* MARCO Is Required for TLR2- and Nod2-Mediated

Responses to Streptococcus pneumoniae and Clearance of Pneumococcal Colonization in the Murine Nasopharynx. *J. Immunol.* **190,** 250–8 (2013).

49. Mukhopadhyay, S. *et al.* SR-A/MARCO-mediated ligand delivery enhances intracellular TLR and NLR function, but ligand scavenging from cell surface limits TLR4 response to pathogens. *Blood* **117,** 1319–28 (2011).

50. Zelensky, A. N. & Gready, J. E. The C-type lectin-like domain superfamily. *FEBS J.* **272,** 6179–6217 (2005).

51. Nakamura, K., Funakoshi, H., Miyamoto, K., Tokunaga, F. & Nakamura, T. Molecular cloning and functional characterization of a human scavenger receptor with C-type lectin (SRCL), a novel member of a scavenger receptor family. *Biochem. Biophys. Res. Commun.* **280,** 1028–35 (2001).

52. Motta, V., Soares, F., Sun, T. & Philpott, D. J. NOD-like receptors: Versatile cytosolic sentinels. *Physiol. Rev.* **95,** 149–178 (2015).

53. Srividya, S., Roy, R. P., Basu, S. K. & Mukhopadhyay, A. Scavenger receptor-mediated delivery of muramyl dipeptide activates antitumor efficacy of macrophages by enhanced secretion of tumor-suppressive cytokines Abstract : We showed that muramyl dipeptide (MDP) conjugated to maleylated bovine serum. *J. Leukoc. Biol.* **67,** (2000).

54. Goldstein, J. L., Ho, Y. K., Basu, S. K. & Brown, M. S. Binding site on macrophages that mediates uptake and degradation of acetylated low density

lipoprotein, producing massive cholesterol deposition. *Proc. Natl. Acad. Sci. U. S. A.* **76,** 333–7 (1979).

55. Steinberg, D., Parthasarathy, S., Carew, T. E., Khoo, J. C. & Witztum, J. L. Beyond Cholesterol: Modifications of Low-Density Lipoprotein That Increase Its Atherogenicity. *New Engl. J.* **320,** 915–924 (1989).

56. Kodama, T. *et al.* Type I macrophage scavenger receptor contains alpha-helical and collagen-like coiled coils. *Nature* **343,** 531–535 (1990).

57. Rohrer, L., Freeman, M., Kodama, T., Penman, M. & Krieger, M. Coiled-coil fibrous domains mediate ligand binding by macrophage scavenger receptor type II. *Nature* **343,** 570–572 (1990).

58. Kodama, T., Reddy, P., Kishimoto, C. & Krieger, M. Purification and characterization of a bovine acetyl low density lipoprotein receptor. *Proc. Natl. Acad. Sci. U. S. A.* **85,** 9238–9242 (1988).

59. Freeman, M. *et al.* An ancient, highly conserved family of cysteine-rich protein domains revealed by cloning type I and type II murine macrophage scavenger receptors. *Proc. Natl. Acad. Sci. U. S. A.* **87,** 8810–4 (1990).

60. Ashkenas, J. *et al.* Structures and high and low affinity ligand binding properties of murine type I and type II macrophage scavenger receptors. *J. Lipid Res.* **34,** 983–1000 (1993).

61. J W Greenberg, W. F. and K. A. J. Influence of lipoteichoic acid structure on

recognition by the macrophage scavenger receptor. *Infect. Immun.* **64,** (1996).

62. Hampton, R. Y., Golenbock, D. T., Penman, M., Krieger, M. & Raetz, C. R. H. Recognition and plasma clearance of endotoxin by scavenger receptors. *Nature* **352,** 342–344 (1991).

63. Han, H. J., Tokino, T. & Nakamura, Y. CSR, a scavenger receptor-like protein with a protective role against cellular damage causedby UV irradiation and oxidative stress. *Hum. Mol. Genet.* **7,** 1039–1046 (1998).

64. Elomaa, O. *et al.* Cloning of a novel bacteria-binding receptor structurally related to scavenger receptors and expressed in a subset of macrophages. *Cell* **80,** 603–9 (1995).

65. Jiang, Y., Oliver, P., Davies, K. E. & Platt, N. Identification and characterization of murine SCARA5, a novel class A scavenger receptor that is expressed by populations of epithelial cells. *J. Biol. Chem.* **281,** 11834–45 (2006).

66. Krieger, M. The other side of scavenger receptors: pattern recognition for host defense. *Current opinion in lipidology* **8,** 275–280 (1997).

67. PrabhuDas, M. R. *et al.* A Consensus Definitive Classification of Scavenger Receptors and Their Roles in Health and Disease. *J. Immunol.* **198,** 3775–3789 (2017).

68. Whelan, F. J., Meehan, C. J., Golding, G. B., McConkey, B. J. & Bowdish, D.

M. E. The evolution of the class a scavenger receptors. *BMC Evol. Biol.* **12,** 227 (2012).

69. Prabhudas, M. *et al.* Standardizing scavenger receptor nomenclature. *J. Immunol.* **192,** 1997–2006 (2014).

70. Chen, Y. *et al.* Defective microarchitecture of the spleen marginal zone and impaired response to a thymus-independent type 2 antigen in mice lacking scavenger receptors MARCO and SR-A. *J. Immunol.* **175,** 8173–8180 (2005).

71. Canton, J., Neculai, D. & Grinstein, S. Scavenger receptors in homeostasis and immunity. *Nat. Rev. Immunol.* **13,** 621–34 (2013).

72. Etzerodt, A. & Moestrup, S. K. CD163 and Inflammation: Biological, Diagnostic, and Therapeutic Aspects. *Antioxid. Redox Signal.* **18,** 2352–2363 (2013).

73. Fabriek, B. O. *et al.* The macrophage scavenger receptor CD163 functions as an innate immune sensor for bacteria. *Blood* **113,** 887–893 (2009).

74. Kraal, G., van der Laan, L. J., Elomaa, O. & Tryggvason, K. The macrophage receptor MARCO. *Microbes Infect.* **2,** 313–6 (2000).

75. Jiang, Y., Oliver, P., Davies, K. E. & Platt, N. Identification and characterization of murine SCARA5, a novel class A scavenger receptor that is expressed by populations of epithelial cells. *J. Biol. Chem.* **281,** 11834–45 (2006).

76. Doi, T. *et al.* Charged collagen structure mediates the recognition of negatively charged macromolecules by macrophage scavenger receptors. *J. Biol. Chem.* **268,** 2126–33 (1993).

77. Brännström, A., Sankala, M., Tryggvason, K. & Pikkarainen, T. Arginine residues in domain V have a central role for bacteria-binding activity of macrophage scavenger receptor MARCO. *Biochem. Biophys. Res. Commun.* **290,** 1462–9 (2002).

78. Novakowski, K. E. *et al.* A Naturally-Occurring Transcript Variant of MARCO Reveals the SRCR Domain is Critical for Function. *Immunol. Cell Biol.* **94,** 646–655 (2016).

79. Gough, P. J., Greaves, D. R. & Gordon, S. A naturally occurring isoform of the human macrophage scavenger receptor (SR-A) gene generated by alternative splicing blocks modified LDL uptake. *J Lipid Res* **39,** 531–543 (1998).

80. Józefowski, S., Arredouani, M., Sulahian, T. & Kobzik, L. Disparate regulation and function of the class A scavenger receptors SR-AI/II and MARCO. *J. Immunol.* **175,** 8032–41 (2005).

81. Mori, K. *et al.* Scavenger receptor CL-P1 mainly utilizes a collagen-like domain to uptake microbes and modified LDL. *Biochim. Biophys. Acta* **1840,** 3345–3356 (2014).

82. Elomaa, O. *et al.* Structure of the human macrophage MARCO receptor and characterization of its bacteria-binding region. *J. Biol. Chem.* **273,** 4530–8 (1998).

83. Arredouani, M. *et al.* The scavenger receptor MARCO is required for lung defense against pneumococcal pneumonia and inhaled particles. *J. Exp. Med.* **200,** 267–72 (2004).

84. Arredouani, M. *et al.* MARCO Is the Major Binding Receptor for Unopsonized Particles and Bacteria on Human Alveolar Macrophages. *J. Immunol.* **175,** 6058–6064 (2005).

85. Kissick, H. T. *et al.* The Scavenger Receptor MARCO Modulates TLR-Induced Responses in Dendritic Cells. *PLoS One* **9,** e104148 (2014).

86. van der Laan, L. J. *et al.* Regulation and functional involvement of macrophage scavenger receptor MARCO in clearance of bacteria in vivo. *J. Immunol.* **162,** 939–47 (1999).

87. Matsushita, N., Komine, H., Grolleau-Julius, A., Pilon-Thomas, S. & Mulé, J. J. Targeting MARCO can lead to enhanced dendritic cell motility and anti-melanoma activity. *Cancer Immunol. Immunother.* **59,** 875–84 (2010).

88. Li, W., Katz, B. P. & Spinola, S. M. Haemophilus ducreyi-induced interleukin-10 promotes a mixed M1 and M2 activation program in human macrophages. *Infect. Immun.* **80,** 4426–34 (2012).

89. Park-min, K., Antoniv, T. T. & Ivashkiv, L. B. Regulation of macrophage phenotype by long-term exposure to IL-10. *Immunobiology* **210,** 77–86 (2005).

90. Jung, M. *et al.* Expression profiling of IL-10-regulated genes in human monocytes and peripheral blood mononuclear cells from psoriatic patients during IL-10 therapy. *Eur. J. Immunol.* **34,** 481–493 (2004).

91. Wu, M. *et al.* Immunomodulators Targeting MARCO Expression Improve Resistance to Post-influenza Bacterial Pneumonia. *Am. J. Physiol. - Lung Cell. Mol. Physiol.* **313,** 138–153 (2017).

92. Ojala, J. R. M., Pikkarainen, T., Tuuttila, A., Sandalova, T. & Tryggvason, K. Crystal structure of the cysteine-rich domain of scavenger receptor MARCO reveals the presence of a basic and an acidic cluster that both contribute to ligand recognition. *J. Biol. Chem.* **282,** 16654–66 (2007).

93. Carpenter, E. P., Beis, K., Cameron, A. D. & Iwata, S. Overcoming the challenges of membrane protein crystallography. *Curr. Opin. Struct. Biol.* **18,** 581–586 (2008).

94. Resnick, J. E., Chatterton, K. S., Schwartz, H. S. & Krieger, M. Structures of Class A Macrophage Scavenger Receptors: Electron microscopic study of flexible, multidomain, fibrous proteins and determination of the disulfide bond pattern of the scavenger receptor cysteine-rich domain. *J. Biol. Chem.* **271,** 26924–26930 (1996).

95. Sankala, M. *et al.* Characterization of recombinant soluble macrophage scavenger receptor MARCO. *J. Biol. Chem.* **277,** 33378–85 (2002).

96. Martínez, V. G., Moestrup, S. K., Holmskov, U., Mollenhauer, J. & Lonzo, F. The conserved scavenger receptor cysteine-rich superfamily in therapy and diagnosis. *Pharmacol. Rev.* **63,** 967–1000 (2011).

97. Pearson, A. M. Scavenger receptors in innate immunity. *Curr. Opin. Immunol.* **8,** 20–8 (1996).

98. Bowdish, D. M. E. *et al.* Genetic variants of MARCO are associated with susceptibility to pulmonary tuberculosis in a Gambian population. *BMC Med. Genet.* **14,** 47 (2013).

99. Ma, M.-J. *et al.* Genetic variants in MARCO are associated with the susceptibility to pulmonary tuberculosis in Chinese Han population. *PLoS One* **6,** e24069 (2011).

100. Bowdish, D. M. E. & Gordon, S. Conserved domains of the class A scavenger receptors: evolution and function. *Immunol. Rev.* **227,** 19–31 (2009).

101. Karlsson, E. K., Kwiatkowski, D. P. & Sabeti, P. C. Natural selection and infectious disease in human populations. *Nat. Rev. Genet.* **15,** 379–393 (2014).

102. Yu, X., Guo, C., Fisher, P. B., Subjeck, J. R. & Wang, X.-Y. *Scavenger Receptors: Emerging Roles in Cancer Biology and Immunology*. *Advances in*

Cancer Research **128,** (Elsevier Inc., 2015).

103. Mccool, T. L. & Weiser, J. N. Limited Role of Antibody in Clearance of Streptococcus pneumoniae in a Murine Model of Colonization Limited Role of Antibody in Clearance of Streptococcus pneumoniae in a Murine Model of Colonization. *Infect. Immun.* **72,** (2004).

104. Mukhopadhyay, S. *et al.* MARCO, an innate activation marker of macrophages, is a class A scavenger receptor for Neisseria meningitidis. *Eur. J. Immunol.* **36,** 940–949 (2006).

105. Olszewski, M. A. *et al.* Containment during Cryptococcal Infection Early Defenses and Contributes to Fungal Scavenger Receptor MARCO Orchestrates Scavenger Receptor MARCO Orchestrates Early Defenses and Contributes to Fungal Containment during Cryptococcal Infection. *J. Immunol.* **198,** 0–0 (2017).

106. Thakur, S. a, Hamilton, R., Pikkarainen, T. & Holian, A. Differential binding of inorganic particles to MARCO. *Toxicol. Sci.* **107,** 238–46 (2009).

107. Syvänen, A. Accessing genetic variation: genotyping single nucleotide polymorphisms. *Nat. Rev. Genet.* **2,** 930–942 (2001).

108. Bowdish, D. M. E. *et al.* Genetic variants of MARCO are associated with susceptibility to pulmonary tuberculosis in a Gambian population. *BMC Med. Genet.* **14,** 47 (2013).

109. Thuong, N. T. T. *et al.* MARCO variants are associated with phagocytosis, pulmonary tuberculosis susceptibility and Beijing lineage. *Genes Immun.* 1–7 (2016). doi:10.1038/gene.2016.43

110. Lao, W. *et al.* Evaluation of the relationship between MARCO and CD36 single-nucleotide polymorphisms and susceptibility to pulmonary tuberculosis in a Chinese Han population. *BMC Infect. Dis.* **17,** 1–9 (2017).

111. Thomsen, M., Nordestgaard, B. G., Kobzik, L. & Dahl, M. Genetic Variation in the Scavenger Receptor MARCO and Its Association with Chronic Obstructive Pulmonary Disease and Lung Infection in 10,604 Individuals. *Respiration* **85,** 1–10 (2012).

112. High, M. *et al.* Determinants of host susceptibility to murine respiratory syncytial virus (RSV) disease identify a role for the innate immunity scavenger receptor MARCO gene in human infants. *EBioMedicine* **11,** 73–84 (2016).

113. Harvey, C. J. *et al.* Targeting Nrf2 Signaling Improves Bacterial Clearance by Alveolar Macrophages in Patients with COPD and in a Mouse Model. *Sci. Transl. Med.* **3,** 1–10 (2011).

114. Hertz, T. *et al.* Mapping the landscape of host-pathogen coevolution: HLA class I binding and its relationship with evolutionary conservation in human and viral proteins. *J. Virol.* **85,** 1310–1321 (2011).

115. Comas, I. *et al.* Out-of-Africa migration and Neolithic coexpansion of

Mycobacterium tuberculosis with modern humans. *Nat. Genet.* **45,** 1176–1182 (2013).

116. Chaguza, C., Cornick, J. E. & Everett, D. B. Mechanisms and impact of genetic recombination in the evolution of Streptococcus pneumoniae. *Comput. Struct. Biotechnol. J.* **13,** 241–247 (2015).

117. Barreiro, L. B., Laval, G., Quach, H., Patin, E. & Quintana-Murci, L. Natural selection has driven population differentiation in modern humans. *Nat. Genet.* **40,** (2008).

118. Durbin, R. M. *et al.* A map of human genome variation from population-scale sequencing. *Nature* **467,** 1061–73 (2010).

119. Prado-Martinez, J. *et al.* Great ape genetic diversity and population history. *Nature* **499,** 471–475 (2014).

120. Noonan, J. P. *et al.* Sequencing and Analysis of Neanderthal Genomic DNA. *Science* **314,** 1113–1118 (2006).

121. Meyer, M. *et al.* A high-coverage genome sequence from an archaic Denisovan individual. *Science* **338,** 222–6 (2012).

122. Watterson, G. A. On the Number of Segregating Sites in Genetical Models without Recombination. *Theor. Popul. Biol.* **7,** 256–276 (1975).

123. Tajima, F. Statistical Method for Testing the Neutral Mutation Hypothesis by

DNA Polymorphism. *Genetics* **123,** 585–595 (1989).

124. Fay, J. C. & Wu, C. I. Hitchhiking under positive Darwinian selection. *Genetics* **155,** 1405–1413 (2000).

125. McDonald, J. H. & Kreitman, M. Adaptive protein evolution at the Adh locus in Drosophila. *Nature* **351,** 652–654 (1991).

126. Machiela, M. J. & Chanock, S. J. LDlink: A web-based application for exploring population-specific haplotype structure and linking correlated alleles of possible functional variants. *Bioinformatics* **31,** 3555–3557 (2014).

127. Crooks, G. E., Hon, G., Chandonia, J. M. & Brenner, S. E. WebLogo: A sequence logo generator. *Genome Res.* **14,** 1188–1190 (2004).

128. Roy, A., Kucukural, A. & Zhang, Y. I-TASSER: a unified platform for automated protein structure and function prediction. *Nat. Protoc.* **5,** 725–738 (2010).

129. Pettersen, E. F. *et al.* UCSF Chimera - A visualization system for exploratory research and analysis. *J. Comput. Chem.* **25,** 1605–1612 (2004).

130. Li, L. *et al.* DelPhi: a comprehensive suite for DelPhi software and associated resources. *BMC Biophys.* **5,** 9 (2012).

131. Gowen, B. B., Borg, T. K., Ghaffar, A. & Mayer, E. P. The collagenous domain of class A scavenger receptors is involved in macrophage adhesion to

collagens. *J Leuk Biol* **69,** 575–582 (2001).

132. Thierry-Mieg, D. & Thierry-Mieg, J. AceView: a comprehensive cDNA-supported gene and transcripts annotation. *Genome Biol.* **7 Suppl 1,** S12.1-14 (2006).

133. Seo, S. *et al.* Functional Analysis of Deep Intronic SNP rs13438494 in Intron 24 of PCLO Gene. *PLoS One* **8,** 6–10 (2013).

134. Kawase, T. *et al.* Alternative splicing due to an intronic SNP in HMSD generates a novel minor histocompatibility antigen. *Transplantation* **110,** 1055–1064 (2017).

135. Wang, G. & Cooper, T. A. Splicing in disease : disruption of the splicing code and the decoding machinery. *Nat. Rev. Genet.* **8,** 749–761 (2007).

136. DeWitte-Orr, S. J., Collins, S. E., Bauer, C. M. T., Bowdish, D. M. & Mossman, K. L. An accessory to the 'Trinity': SR-As are essential pathogen sensors of extracellular dsRNA, mediating entry and leading to subsequent type I IFN responses. *PLoS Pathog.* **6,** (2010).

137. Nikolic, D. M., Cholewa, J., Gass, C., Gong, M. C. & Post, S. R. Class A scavenger receptor-mediated cell adhesion requires the sequential activation of Lyn and PI3-kinase. *Am. J. Physiol. Cell Physiol.* **292,** C1450-8 (2007).

138. Mariliis Kroos, Dawn M.E. Bowdish, S. G. MARCO mediates macrophage adhesion.

139. Jang, S. *et al.* Scavenger receptor CL-P1 mediates endocytosis by associating with AP-2μ2. *Biochim. Biophys. Acta* **1840,** 3226–37 (2014).

140. Chen, Y. *et al.* The di-leucine motif contributes to class A scavenger receptor-mediated internalization of acetylated lipoproteins. *Arterioscler. Thromb. Vasc. Biol.* **26,** 1317–1322 (2006).

141. Freeman, S. a. *et al.* Toll-like receptor ligands sensitize B-cell receptor signalling by reducing actin-dependent spatial confinement of the receptor. *Nat. Commun.* **6,** 6168 (2015).

142. Erdman, L. K. *et al.* CD36 and TLR interactions in inflammation and phagocytosis: implications for malaria. *J. Immunol.* **183,** 6452–6459 (2009).

143. Triantafilou, M., Morath, S., Mackie, A., Hartung, T. & Triantafilou, K. Lateral diffusion of Toll-like receptors reveals that they are transiently confined within lipid rafts on the plasma membrane. *J Cell Sci* **117,** 4007–4014 (2004).

144. Pikkarainen, T., Brannstrom, A., and Tryggvason, K. Expression of Macrophage MARCO Receptor Induces Formation of Dendritic Plasma Membrane Processes. *J. Biol. Chem.* **274,** 10975–10982 (1999).

145. Dupuy, A. G. & Caron, E. Integrin-dependent phagocytosis – spreading from microadhesion to new concepts. *J. Cell Sci.* **121,** 1773–1783 (2008).

146. Granucci, F. *et al.* The scavenger receptor MARCO mediates cytoskeleton rearrangements in dendritic cells and microglia. *Blood* **102,** 2940–7 (2003).

147. Acton, S. *et al.* The collagenous domains of macrophage scavenger receptors and complement component C1q mediate their similar, but not identical, binding specificities for polyanionic ligands. *J. Biol. Chem.* **268,** 3530–7 (1993).

148. Yan, N. *et al.* Therapeutic upregulation of Class A scavenger receptor member 5 inhibits tumor growth and metastasis. *Cancer Sci.* **103,** 1631–9 (2012).

149. Post, S. R. Class A scavenger receptors mediate cell adhesion via activation of Gi/o and formation of focal adhesion complexes. *J. Lipid Res.* **43,** 1829–1836 (2002).

150. Todt, J. C., Hu, B. & Curtis, J. L. The scavenger receptor SR-A I/II (CD204) signals via the receptor tyrosine kinase Mertk during apoptotic cell uptake by murine macrophages. *J. Leukoc. Biol.* **84,** 510–518 (2008).

151. van der Laan, L. J. *et al.* Regulation and functional involvement of macrophage scavenger receptor MARCO in clearance of bacteria in vivo. *J. Immunol.* **162,** 939–47 (1999).

152. Shoulders, M. D. & Raines, R. T. Collagen Structure and Stability. *Annu. Rev. Biochem.* **78,** 929–958 (2009).

153. Monera, O. D., Sereda, T. J., Zhou, N. E., Kay, C. M. & Hodgesis, T. S. Relationship of Sidechain Hydrophobicity and a-Helical Propensity on the Stability of the Single-stranded Amphipathic a-Helix. *J. Pept. Sci.* **1,** 319–329

(1995).

154. Anjana, R. *et al.* Aromatic-aromatic interactions in structures of proteins and protein-DNA complexes : a study based on orientation and distance. *Bioinformatician* **8,** 1220–1224 (2012).

155. Brooks, M. N. *et al.* NOD2 controls the nature of the inflammatory response and subsequent fate of Mycobacterium tuberculosis and M. bovis BCG in human macrophages. *Cell. Microbiol.* **13,** 402–418 (2012).

156. Bafica, A. *et al.* TLR9 regulates Th1 responses and cooperates with TLR2 in mediating optimal resistance to Mycobacterium tuberculosis. *J. Exp. Med.* **202,** 1715–1724 (2005).

157. Hossain, M. & Norazmi, M. Pattern Recognition Receptors and Cytokines in Mycobacterium tuberculosis Infection — The Double-Edged Sword ? *Biomed Res. Int.* **2013,** 1–18 (2013).

158. Jedrzejas, M. J. Pneumococcal Virulence Factors : Structure and Function. **65,** 187–207 (2001).

159. Ünal, C. M. & Steinert, M. Microbial Peptidyl-Prolyl cis/trans Isomerases (PPIases): Virulence Factors and Potential Alternative Drug Targets. *Microbiol. Mol. Biol. Rev.* **78,** 544–571 (2014).

160. Triantafilou, M. *et al.* Membrane sorting of toll-like receptor (TLR)-2/6 and TLR2/1 heterodimers at the cell surface determines heterotypic associations

with CD36 and intracellular targeting. *J. Biol. Chem.* **281,** 31002–31011 (2006).

A

```
                          Cytoplasmic (Domain I)          Transmem-
MARCO     1   MRNKKILKEDELLSETQQAAFHQIAMEPFEINVPKPKRRNGVNFSLAVVVIYLILLTAGA  60
MARCOII   1   MRNKKILKEDELLSETQQAAFHQIAMEPFEINVPKPKRRNGVNFSLAVVVIYLILLTAGA  60
              ************************************************************

              -brane(Domain II)      Spacer (Domain III)
MARCO    61   GLLVVQVLNLQARLRVLEMYFLNDTLAAEDSPSFSLLQSAHPGEHLAQGASRLQVLQAQL  120
MARCOII  61   GLLVVQVLNLQARLRVLEMYFLNDTLAAEDSPSFSLLQSAHPGEHLAQGASRLQVLQAQL  120
              ************************************************************

MARCO    121  TWVRVSHEHLLQRVDNFTQNPGMFRIKGEQGAPGLQGHKGAMGMPGAPGPPGPPAEKGAK  180
MARCOII  121  TWVRVSHEHLLQRVDNFTQNPGMFRIKGEQGAPGLQGHKGAMGMPGAPGPPGPPAEKGAK  180
              ************************************************************

MARCO    181  GAMGRDGATGPSGPQGPPGVKGEAGLQGPQGAPGKQGATGTPGPQGEKGSKGDGGLIGPK  240
MARCOII  181  GAMGRDGATGPSGPQGPPGVKGEAGLQGPQGAPGKQGATGTPGPQGEKGSKGDGGLIGPK  240
              ************************************************************

                                Collagenous (Domain IV)
MARCO    241  GETGTKGEKGDLGLPGSKGDRGMKGDAGVMGPPGAQGSKGDFGRPGPPGLAGFPGAKGDQ  300
MARCOII  241  GETGTKGEKGDLGLPGSKGDRGMKGDAGVMGPPGAQGSKGDFGRPGPPGLAGFPGAKGDQ  300
              ************************************************************

MARCO    301  GQPGLQGVPGPPGAVGHPGAKGEPGSAGSPGRAGLPGSPGSPGATGLKGSKGDTGLQGQQ  360
MARCOII  301  GQPGLQGVPGPPGAVGHPGAKGEPGSAGSPGRAGLPGSPGSPGATGLKGSKGDTGLQGQQ  360
              ************************************************************

MARCO    361  GRKGESGVPGPAGVKGEQGSPGLAGPKGAPGQAGQKGDQGVKGSSGEQGVKGEKGERGEN  420
MARCOII  361  GRKGESGVPGPAGVKGEQGSPGLAGPKGAPGQAGQKGDQGVKGSSGEQGVKGEKGERGEN  420
              ************************************************************

                                SRCR (Domain V)
MARCO    421  SVSVRIVGSSNRGRAEVYYSGTWGTICDDEWQNSDAIVFCRMLGYSKGRALYKVGAGTGQ  480
MARCOII  421  SVSVRIVPGGQFS---VSGHGEYPVELHQE----------------------------- (447)
              ******* ..: .   *   * : .  .:*

MARCO    481  IWLDNVQCRGTESTLWSCTKNSWGHHDCSHEEDAGVECSV              520
MARCOII      -------------------------------------
```

B

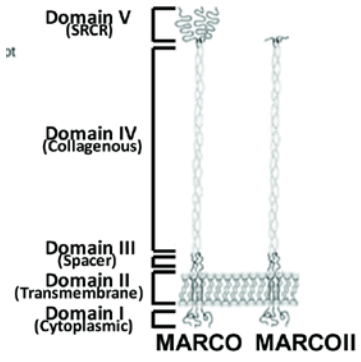

C

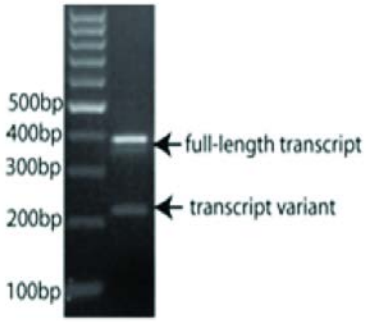

Figure 1: Amino acid alignment and comparative structures of MARCO and MARCOII.

The MARCOII transcript variant is truncated, resulting in a loss of almost the entire SRCR domain. (**A**) Alignment of amino acid sequences of MARCO and MARCOII illustrating a near total loss of the SRCR domain. MARCOII contains 8 residues

within the SRCR domain that are homologous to MARCO and 20 residues that are non-homologous. (**B**) Hypothesized structures of MARCO and MARCOII. (**C**) PCR amplification of reverse-transcribed PBMC transcripts from 4 human donors. Primers surrounded MARCO exons 16/17. A full-length transcript is highlighted at 380 bp and a truncated variant is highlighted at 218 bp.

A

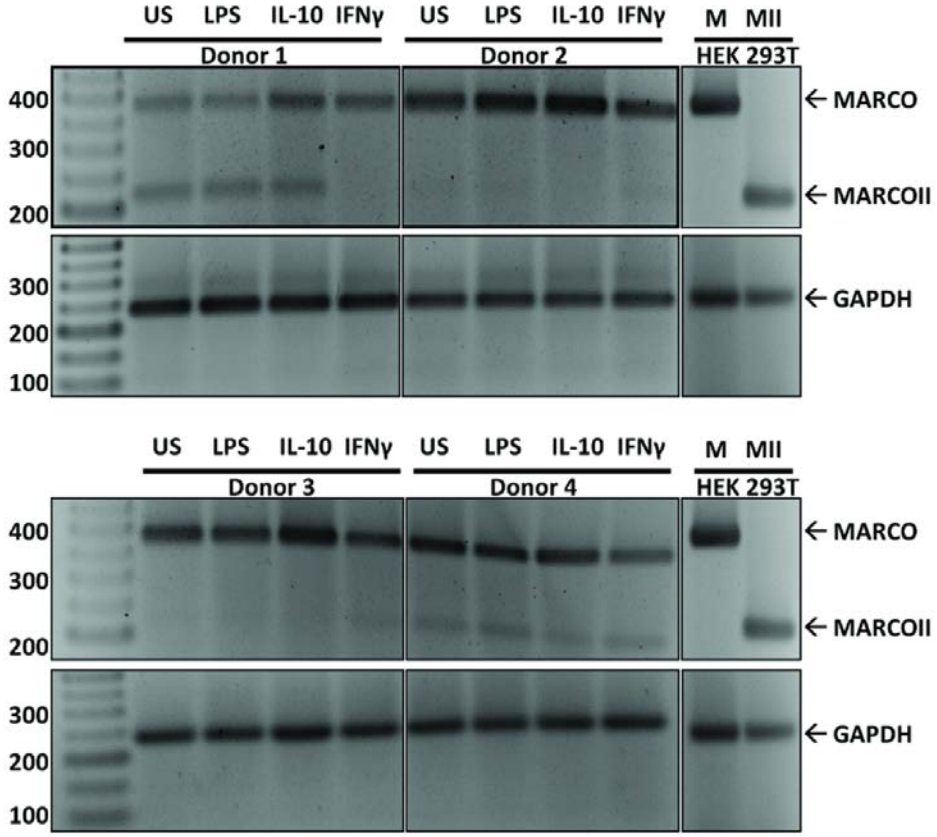

Figure 2: Differential regulation and expression of MARCOII in human leukocytes

The MARCOII transcript variant is not expressed in all donors and does not follow the induction pattern of MARCO. (**A**) PBMCs from four human donors were stimulated with PBS (US), lipopolysaccharide (LPS), interleukin-10 (IL-10) or interferon-gamma (IFN-γ) for 48 h. Transcripts were reverse transcribed and PCR was performed to detect MARCO and MARCOII transcripts. MARCOII transcript was not detected in 2 of 4 donors. MARCO transcript is induced by IL-10 stimulation in 3 of 4 donors, whereas MARCOII transcript is not induced with any treatment. Reference bands were generated from transcripts from HEK 293T cells transiently transfected to express MARCO (M) or MARCOII (MII).

A

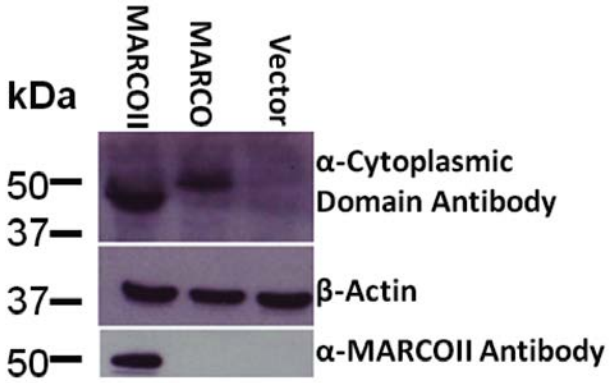
MARCOII
MARCO
Vector
kDa
50
37
37
50
α-Cytoplasmic Domain Antibody
β-Actin
α-MARCOII Antibody

B

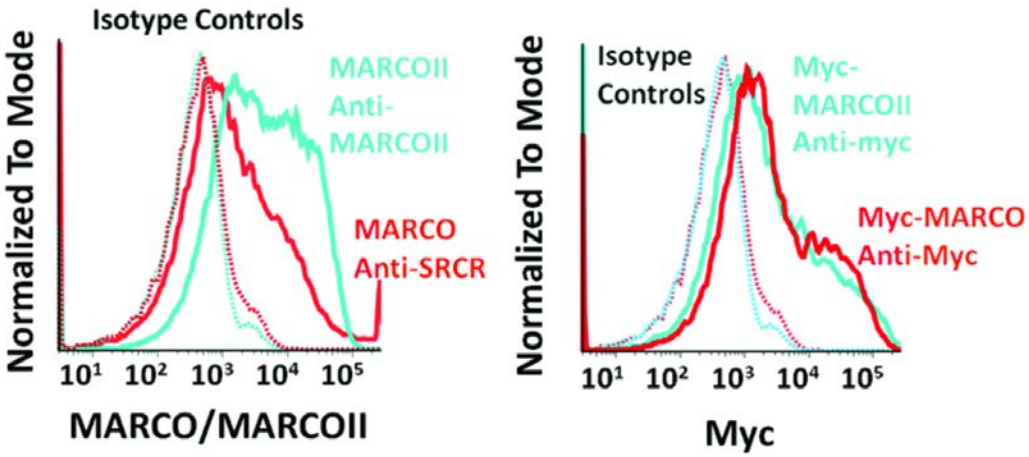
Isotype Controls
MARCOII Anti-MARCOII
MARCO Anti-SRCR
Normalized To Mode
10¹ 10² 10³ 10⁴ 10⁵
MARCO/MARCOII
Isotype Controls
Myc-MARCOII Anti-myc
Myc-MARCO Anti-Myc
Normalized To Mode
10¹ 10² 10³ 10⁴ 10⁵
Myc

C-J

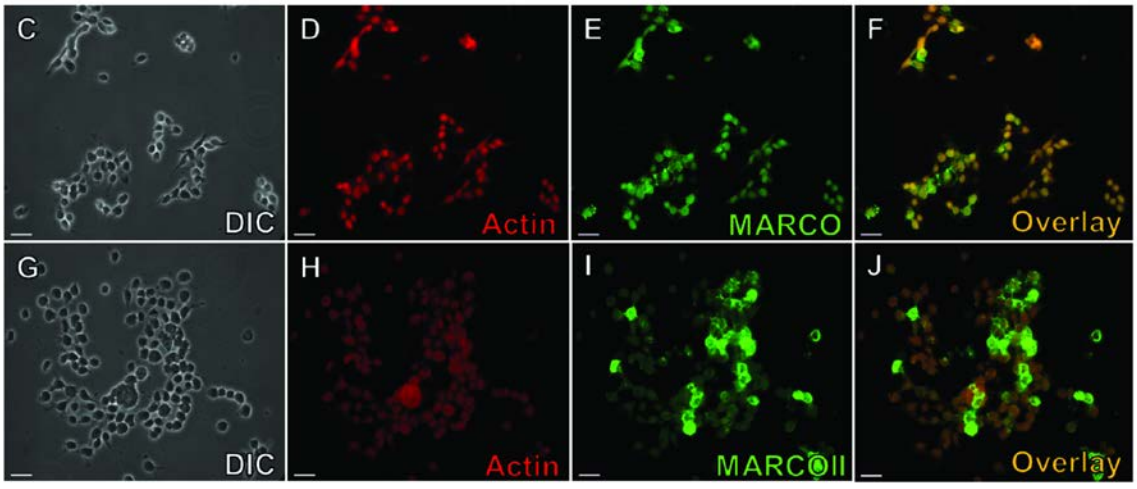
C
DIC
D
Actin
E
MARCO
F
Overlay
G
DIC
H
Actin
I
MARCOII
J
Overlay

Figure 3: Expression of MARCO and MARCOII in transiently transfected HEK 293T cells

MARCO and MARCOII are expressed at similar levels in transiently transfected HEK 293T cells. Cells were transfected to express MARCO, MARCOII or with an empty vector and protein expression was quantified after 48 h by multiple techniques. (**A**) Western blot analysis of MARCO/MARCOII-expressing HEK 293T cell lysates suggests MARCOII can be expressed as a protein. (**B**) Myc-tagged MARCO and MARCOII show similar levels of surface expression when analyzed by flow cytometry. (**C-J**) Immunofluorescence microscopy was performed on myc-MARCO (C-F) and myc-MARCOII (G-J) transfected cells. DIC = differential interference contrast; red = Phalloidin; green = myc. Scale bars represent 25 µm.

A-H

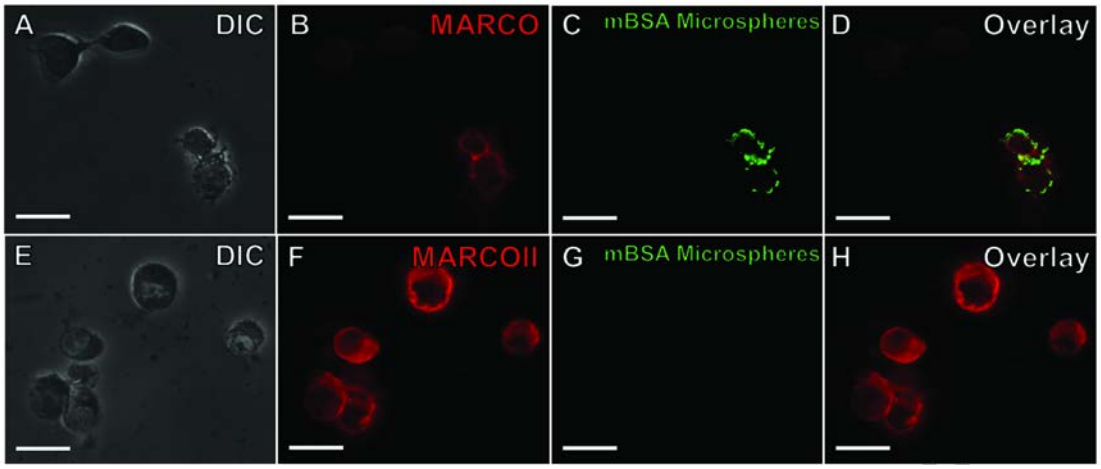
A
DIC
B
MARCO
C
mBSA Microspheres
D
Overlay
E
DIC
F
MARCOII
G
mBSA Microspheres
H
Overlay

I

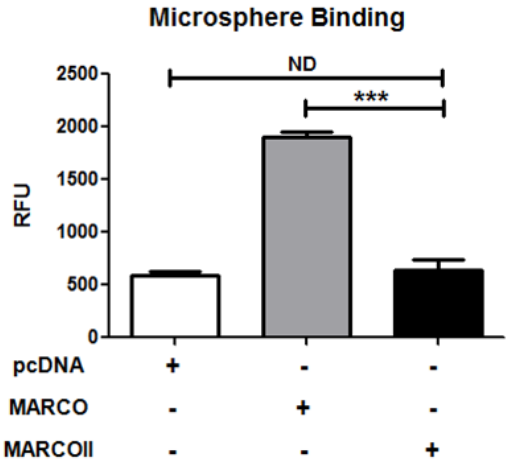
Microsphere Binding
ND
***
2500
2000
1500
1000
500
0
RFU
pcDNA + - -
MARCO - + -
MARCOII - - +

J

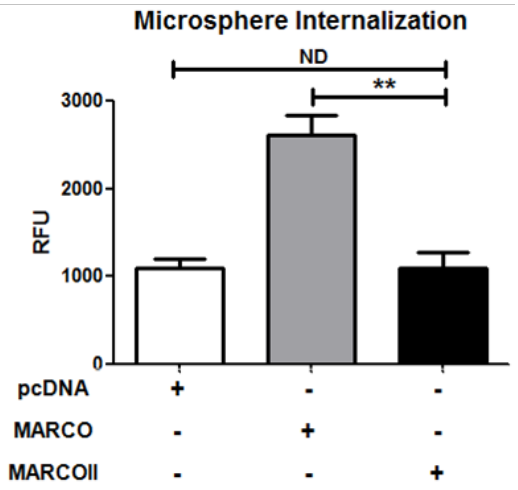
Microsphere Internalization
ND
**
3000
2000
1000
0
RFU
pcDNA + - -
MARCO - + -
MARCOII - - +

K

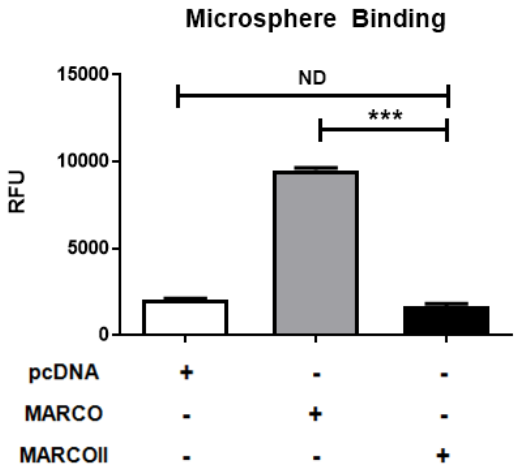
Microsphere Binding
15000
10000
5000
0
RFU
ND
***
pcDNA + - -
MARCO - + -
MARCOII - - +

L

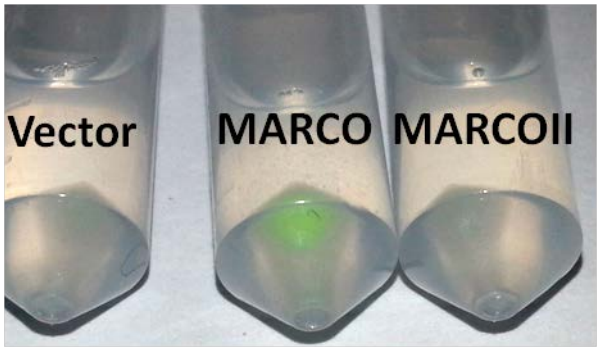
Vector
MARCO
MARCOII

M

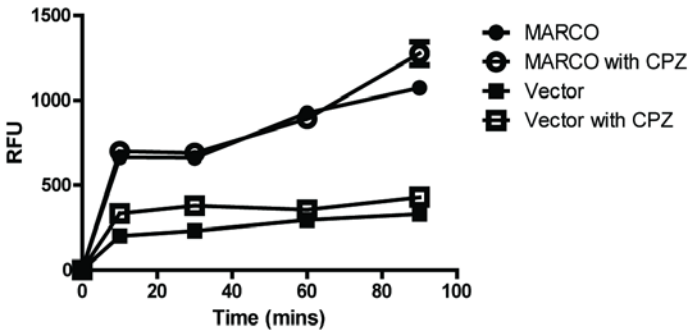
1500
1000
500
0
RFU
0
20
40
60
80
100
Time (mins)
MARCO
MARCO with CPZ
Vector
Vector with CPZ

N

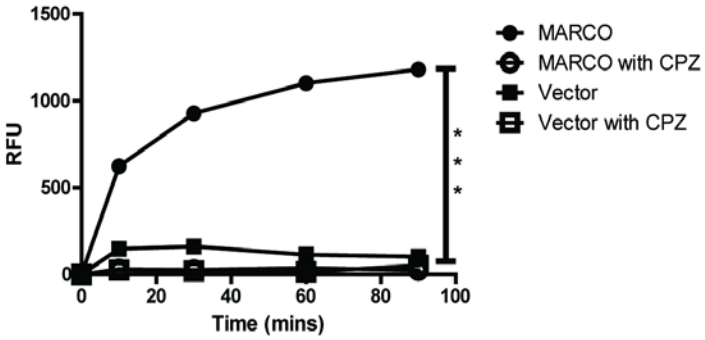

Figure 4: MARCOII-expressing cells show decreased binding and internalization of Mal-BSA-coated microspheres

HEK 293T cells were transfected with empty vector, MARCO or MARCOII, incubated with 500 nm Mal-BSA-coated fluorescent microspheres at 37 °C, and analyzed for microsphere binding and internalization. (**A-H**) myc-MARCOII-transfected cells (E-H) show abrogated ligand binding and uptake when compared with myc-MARCO (A–D). DIC = Differential interference contrast; Red = Myc; Green = Mal-BSA microspheres. Scale bars represent 15 μm. (**I-J**) Quantification of microsphere binding (I) and internalization (J). (**K**) Addition of a c-terminal myc tag to the SRCR domain does not affect microsphere binding. (**L**) Enhanced microsphere binding by MARCO-transfected cells is visible to the unaided eye. (**M-N**) Microsphere binding is not inhibited by treatment with chlorpromazine (CPZ), but internalization is abolished[1]. Statistical significance was calculated by Student's t-test. Error bars indicate mean±S.E.M. **p*<0.05, ***p*<0.01, ****p* <0.001.

A

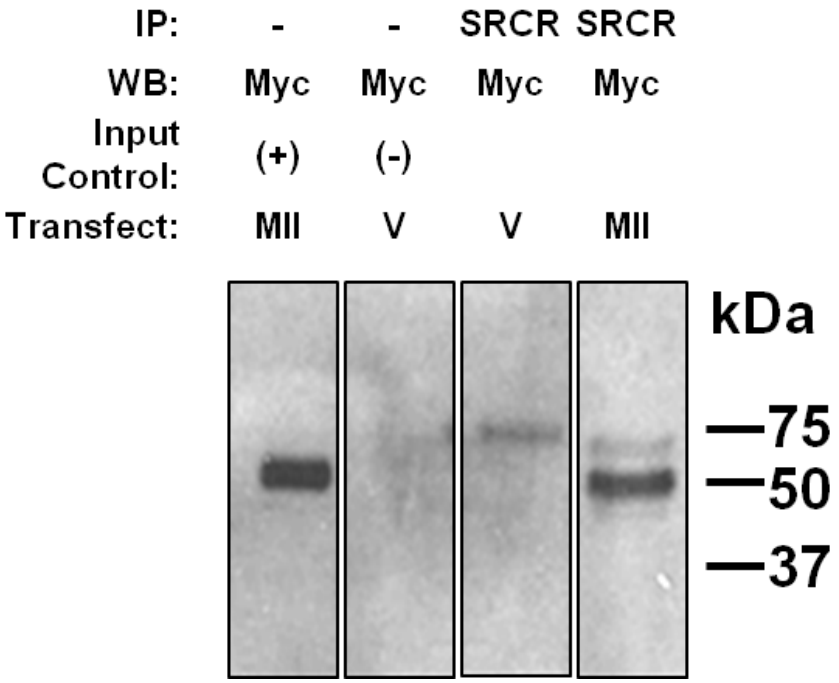

Figure 5: MARCO and MARCOII can form heteromeric complexes

(**A**) Co-immunoprecipitation of myc-MARCOII from stably expressing MARCO HEK 293 T cells. Cells were transfected with either myc-MARCOII (MII) or an empty vector negative control (V). MARCO was immunoprecipitated (IP) with an anti-SRCR antibody, followed by an immunoblot (WB) for myc-MARCOII using anti-myc antibodies. Positive (+) and negative (-) input controls were loaded at 10% of IP samples.

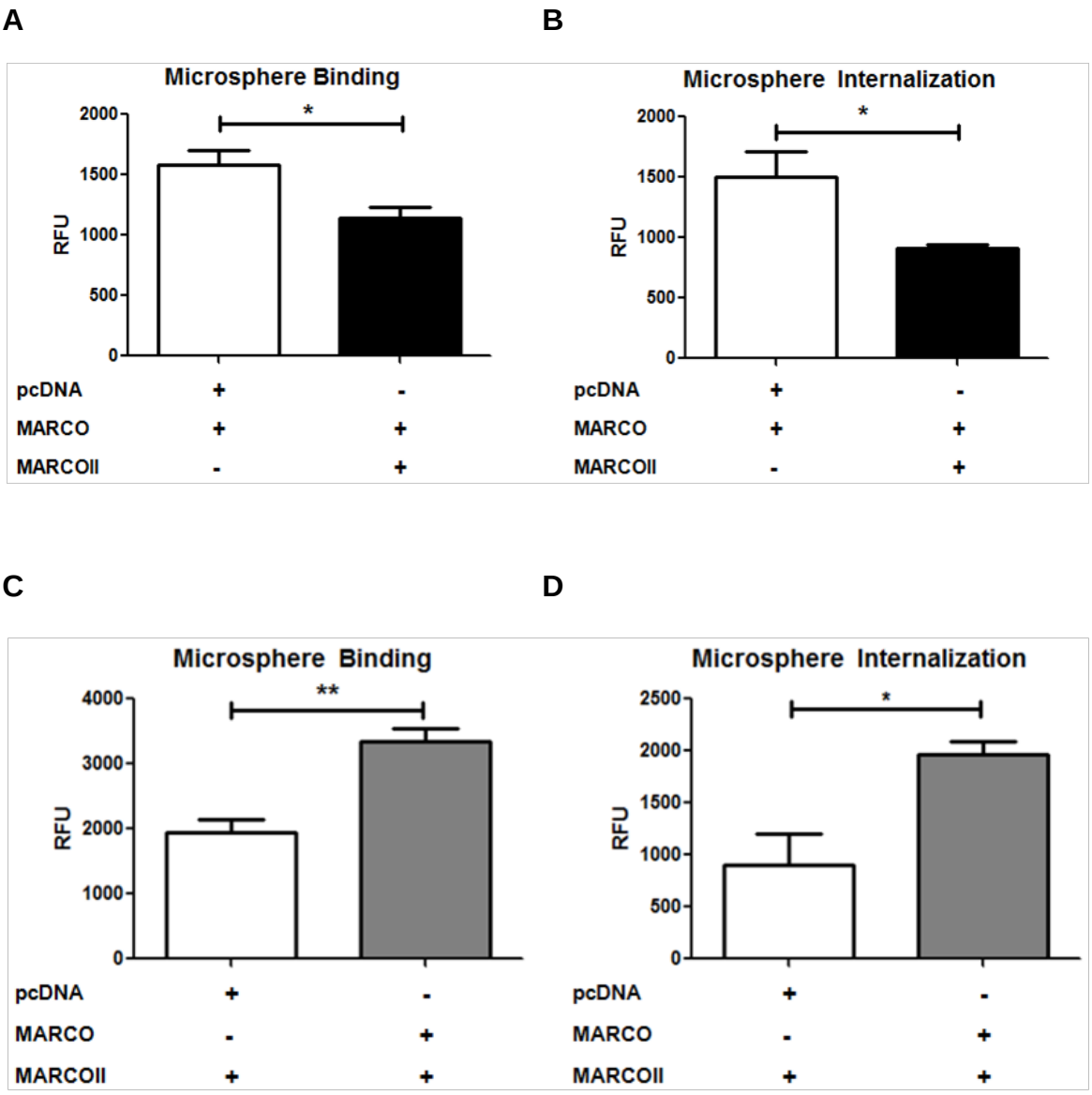

Figure 6: Receptor function can be rescued or knocked down by co-expressing MARCO and MARCOII

Microsphere binding and internalization assays were performed using stably-transfected hM 293T or hMII 293T cells. Knockdown of endogenous ligand binding (**A**) and internalization (**B**) by transfecting hM 293T with MARCOII. Rescue of ligand binding (**C**) and internalization (**D**) by transfecting hMII 293T with MARCO. Statistical significance was calculated by Student's t-test. Error bars indicate mean±S.E.M. *p<0.05, **p<0.01.

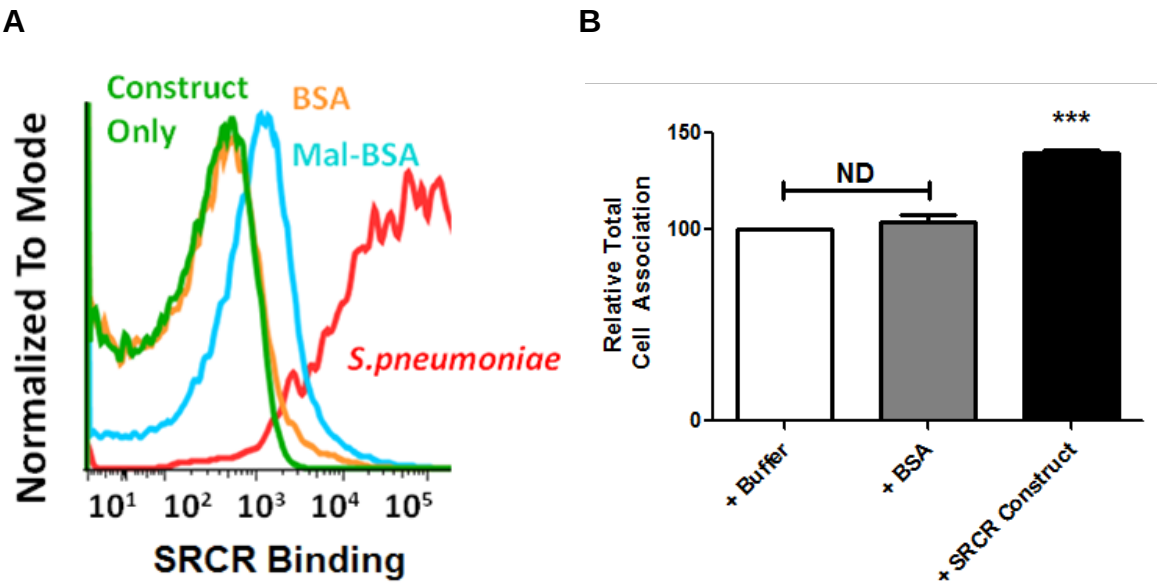

Figure 7: The SRCR domain of MARCO directly binds *S. pneumoniae* and can enhance cell association with bacteria

(**A**) A soluble SRCR construct was incubated with BSA or Mal-BSA-coated microspheres and *S. pneumoniae*. Construct binding was quantified by staining with an anti-SRCR antibody followed by flow cytometry. Enhanced binding of Mal-BSA and *S. pneumoniae* was observed. (**B**) *S. pneumoniae* was pre-incubated with folding buffer, BSA or SRCR construct for 2 h. Bacteria were then incubated with peritoneal macrophages at a multiplicity of infection (MOI) of 25 for 30 min. Percent bacterial association was calculated as the bacteria recovered at 30 min. The relative total cell association was normalized to buffer pre-treated *S. pneumoniae*. Statistical significance was calculated by one-way analysis of variance (ANOVA) with Tukey's post-hoc test. Error bars indicate mean±S.E.M. ***p<0.001.

A

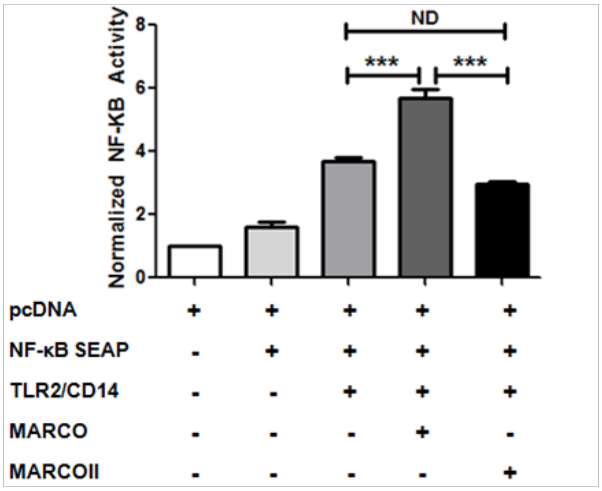

Figure 8: The SRCR domain of MARCO enhances TLR2/CD14-mediated NF-κB activity in response to *S. pneumoniae*

(**A**) HEK 293 T cells were transfected with combinations of NF-κB secreted embryonic alkaline phosphatase (SEAP) reporter plasmid, TLR2/CD14, and MARCO or MARCOII. Cells were then stimulated *with* HKLD *S. pneumoniae* for 48 h followed by quantification of NF-κB activity. MARCOII-transfected cells show no significant enhancement of NF-κB activity when compared with MARCO.

A-H

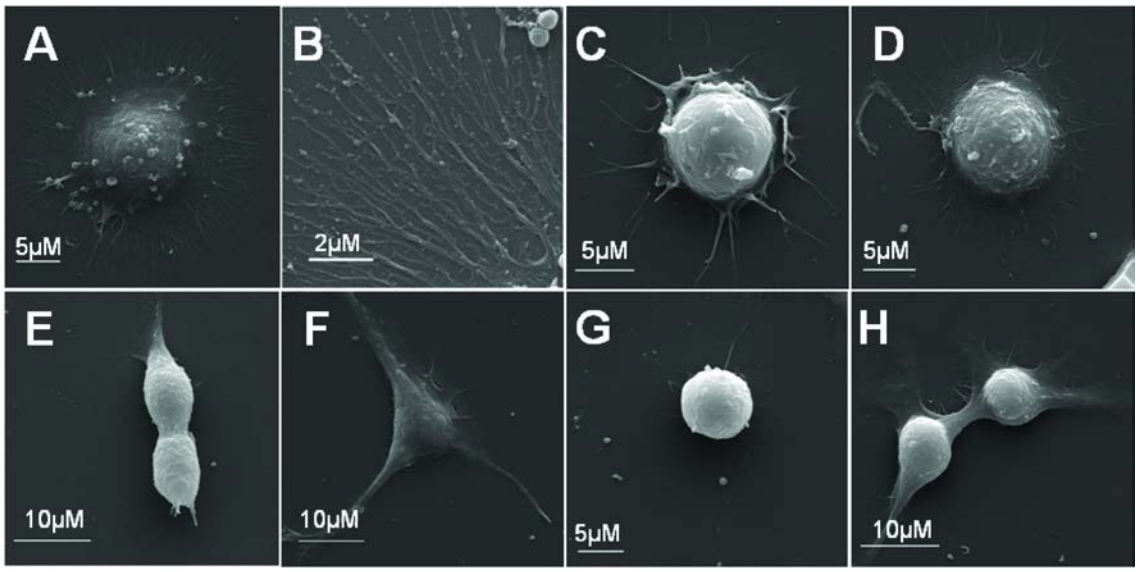
A
5μM
B
2μM
C
5μM
D
5μM
E
10μM
F
10μM
G
5μM
H
10μM

I

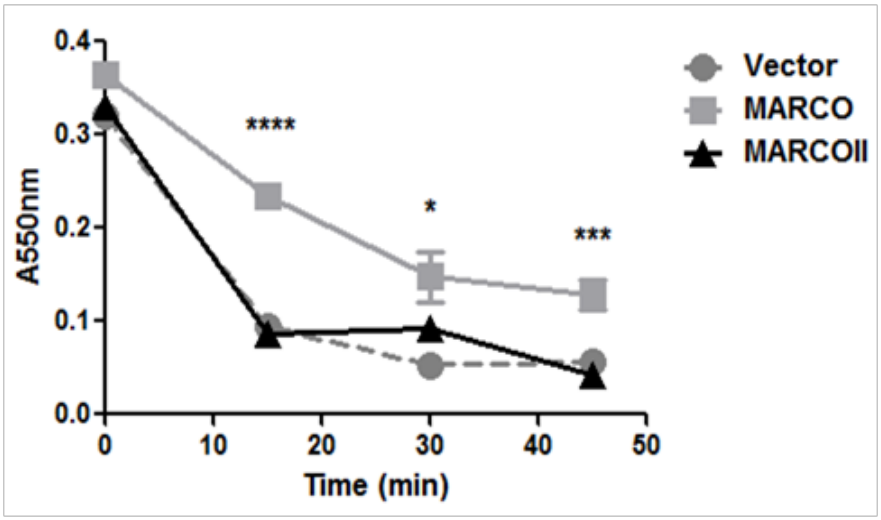
A550nm
0.4
0.3
0.2
0.1
0.0
0
10
20
30
40
50
Time (min)
****
*
***
Vector
MARCO
MARCOII

J

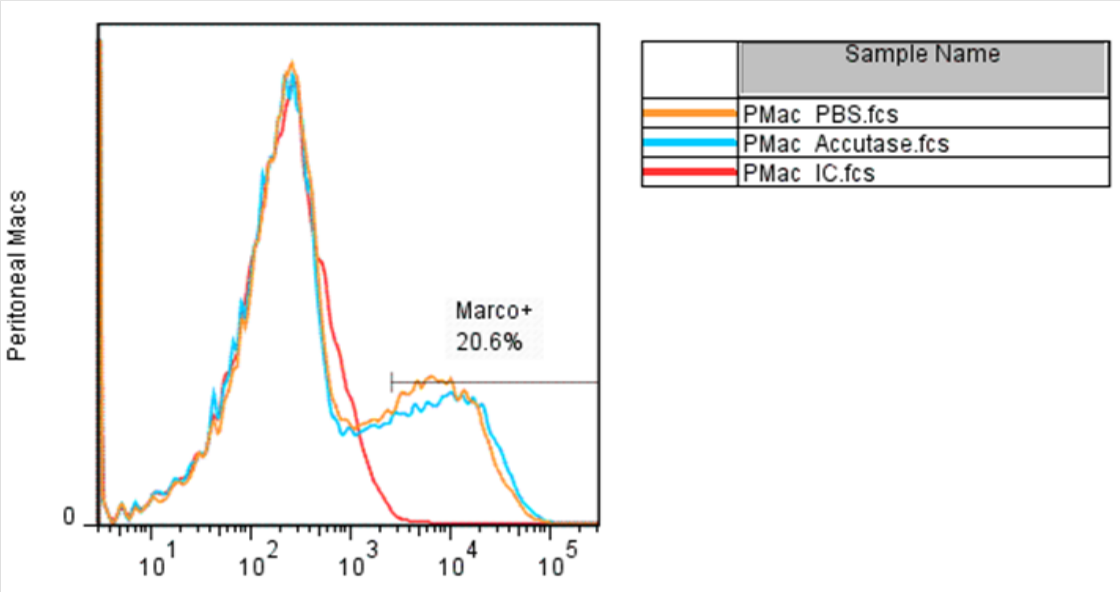

Figure 9: The SRCR domain of MARCO alters cellular morphology and enhances adhesion

The SRCR domain is required for MARCO-mediated cellular adhesion. HEK 293 T cells were transfected with MARCO (**A-D**) or MARCOII (**E-H**) and morphology was examined by scanning electron microscopy. (**I**) MARCO-expressing cells were significantly more adherent after 15, 30 and 45 min of Accutase incubation when compared with MARCOII-transfected cells. (**J**) Accutase treatment did not affect MARCO expression at the cell surface. Statistical significance was calculated by two-way analysis of variance (ANOVA) with Tukey's post-hoc test. Error bars indicate mean±S.E.M. Stars indicate comparisons between MARCO and MARCOII where *p<0.05, ***p<0.01, ****p<0.001.

A

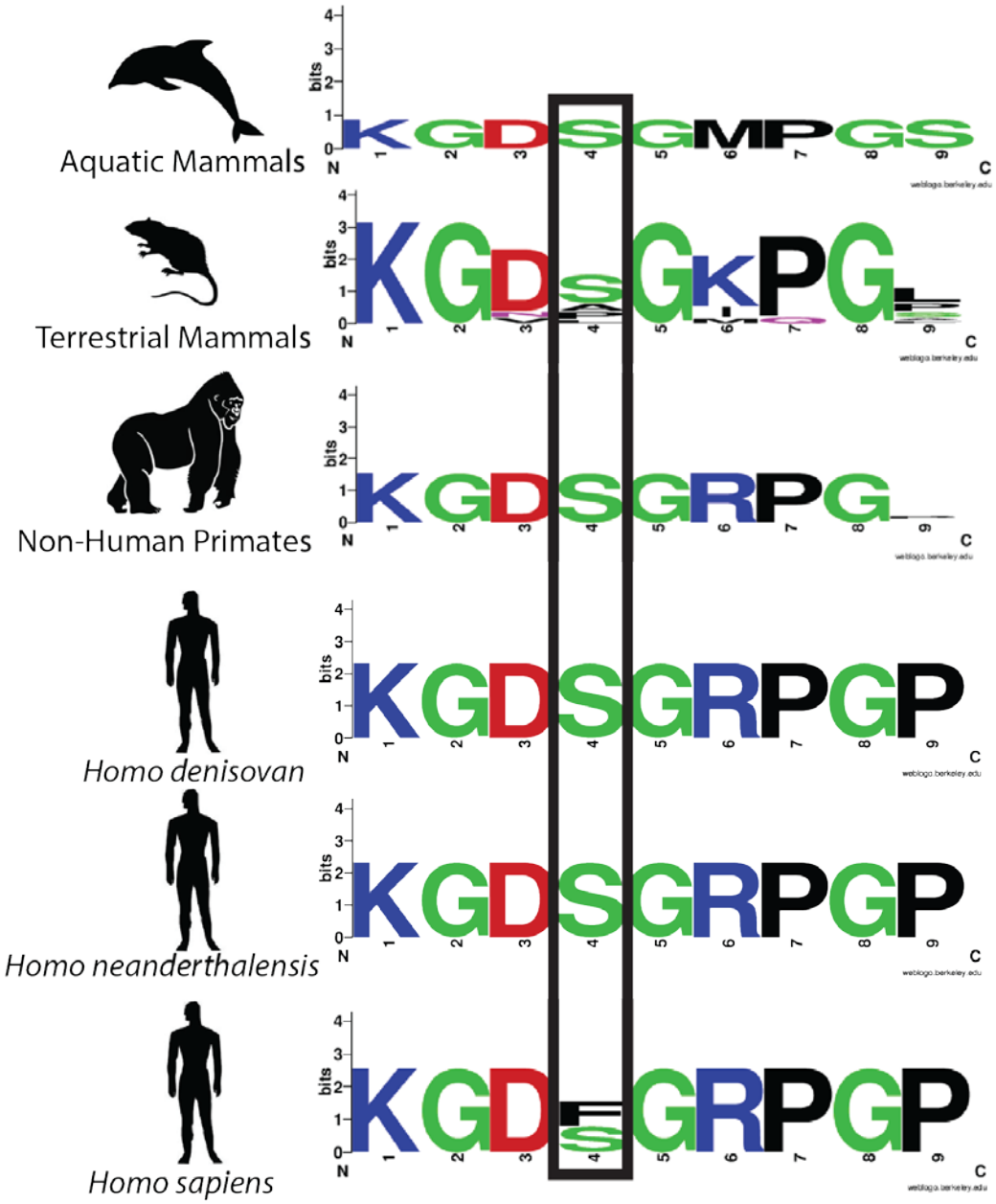

Figure 10: Partial alignment of the collagenous domain of MARCO highlighting residue 282

(**A**) Humans possess a unique phenylalanine residue at residue 282, except those with the rs6761637 polymorphism, who possess the ancestral serine residue. For a list of species included in each group, see Table 6.

A

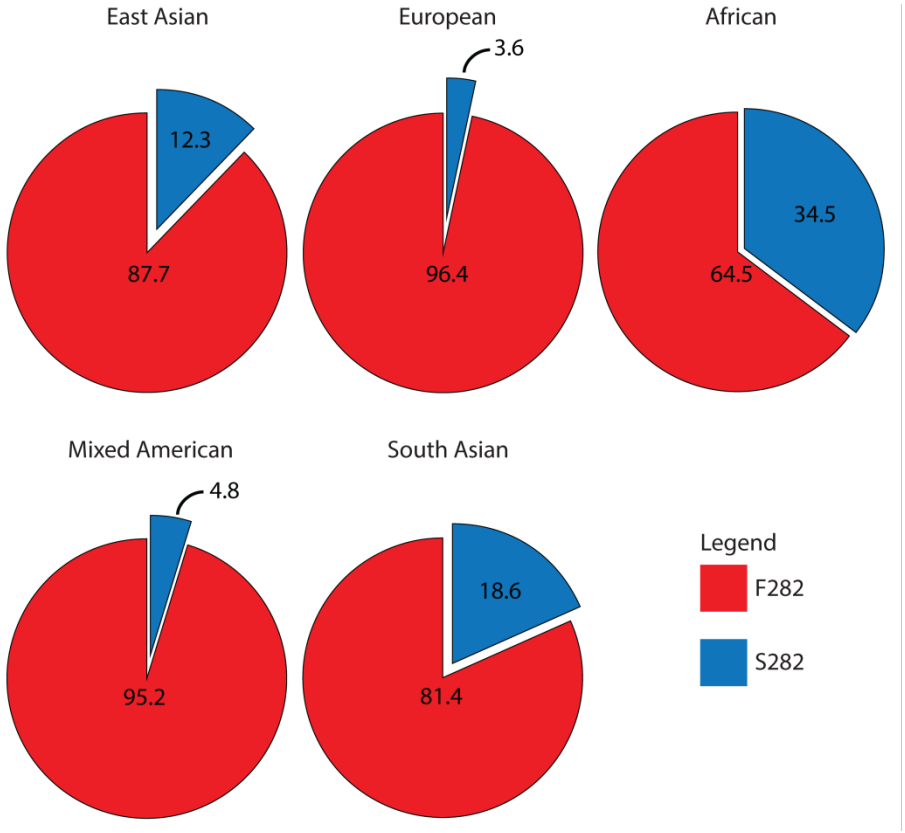
East Asian
European
African
12.3
87.7
3.6
96.4
34.5
64.5
Mixed American
South Asian
4.8
95.2
18.6
81.4
Legend
F282
S282

B

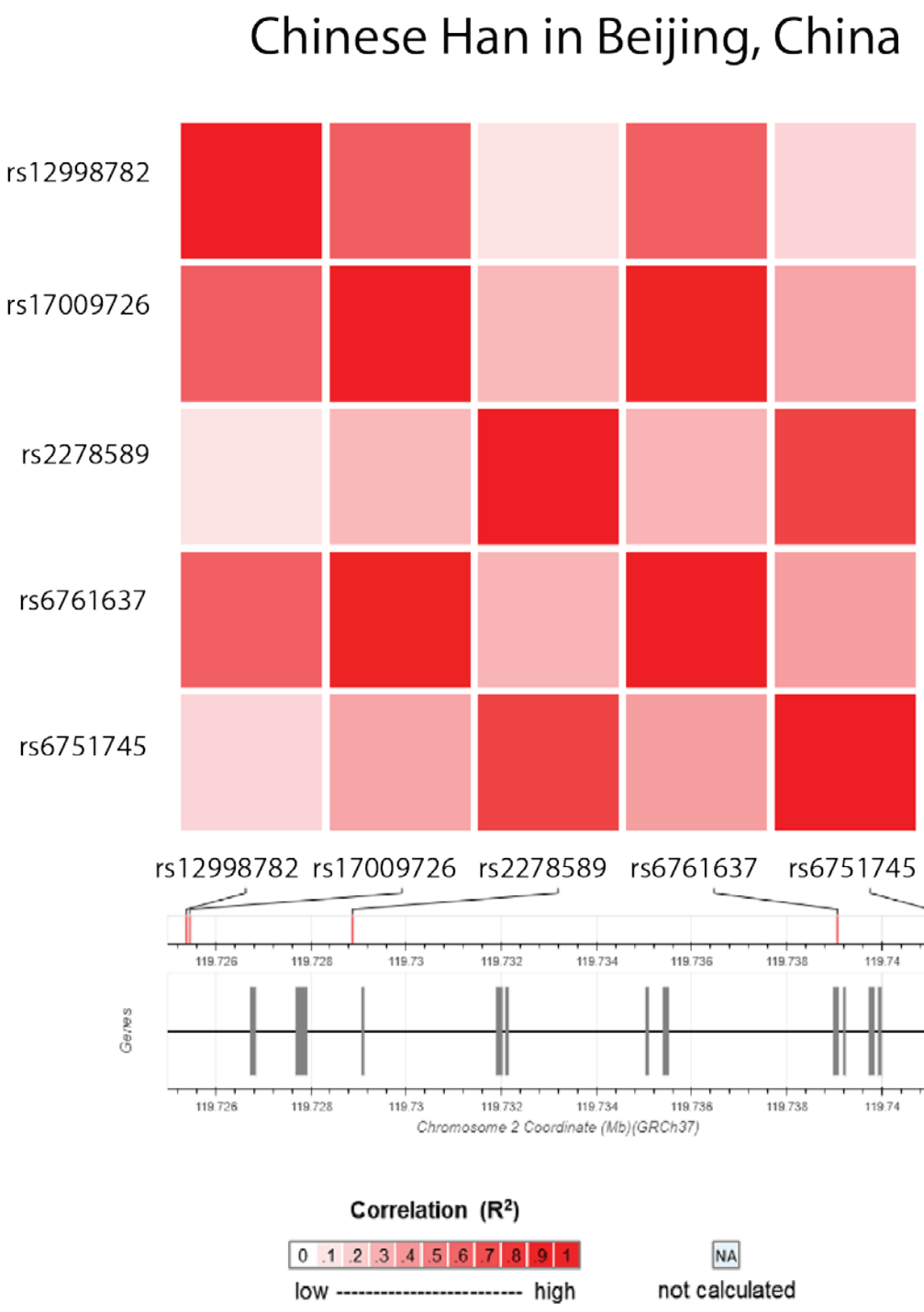
Chinese Han in Beijing, China
rs12998782
rs17009726
rs2278589
rs6761637
rs6751745
rs12998782 rs17009726 rs2278589 rs6761637 rs6751745
119.726
119.728
119.73
119.732
119.734
119.736
119.738
119.74
Genes
Chromosome 2 Coordinate (Mb)(GRCh37)
Correlation (R²)
0 .1 .2 .3 .4 .5 .6 .7 .8 .9 1
low ---------- high
NA
not calculated

c

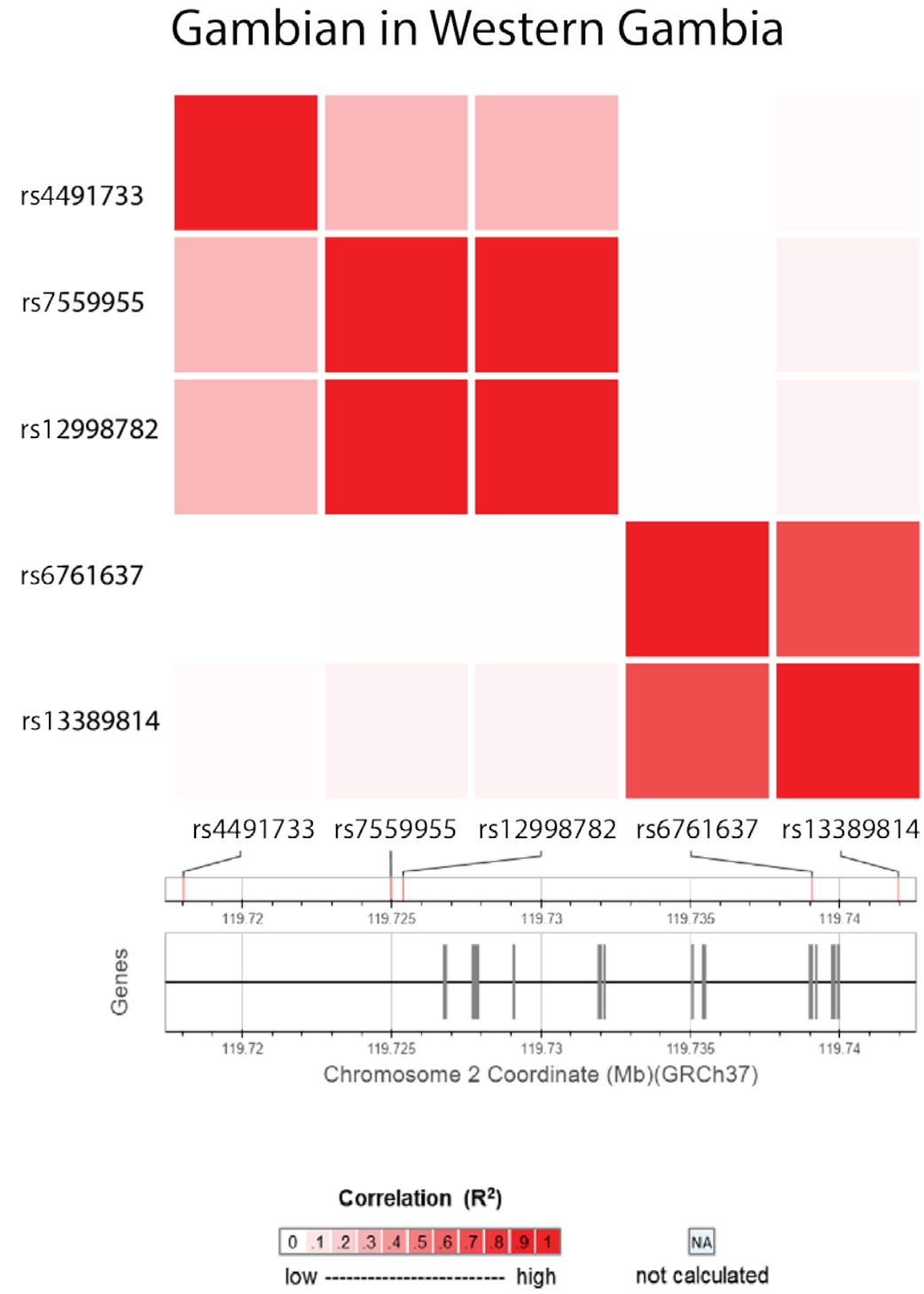
Gambian in Western Gambia
rs4491733
rs7559955
rs12998782
rs6761637
rs13389814
rs4491733 rs7559955 rs12998782 rs6761637 rs13389814
119.72
119.725
119.73
119.735
119.74
Genes
Chromosome 2 Coordinate (Mb)(GRCh37)
Correlation (R²)
0 .1 .2 .3 .4 .5 .6 .7 .8 .9 1
low ---------- high
NA
not calculated

D

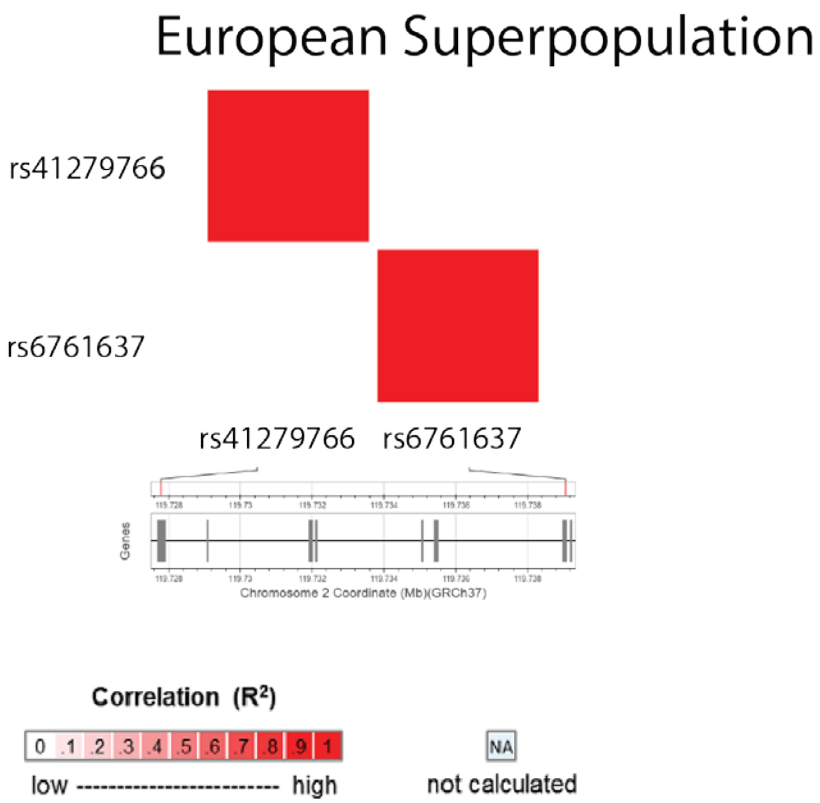

Figure 11: F282 is undergoing positive selection, is polymorphic in humans and in linkage disequilibrium with other MARCO polymorphisms associated with disease

Tests for positive selection at site 282 were performed using Tajima's D statistic and Fay and Wu's H statistic. The results can be seen in chapter 3.2.2. (**A**) The F282S polymorphism is found at higher frequencies in East Asian (12.3%, n=629), South Asian (18.6%, n=657) and African (34.5%, n=902) populations, relative to European (3.6%, n=535) and Mixed American (4.8%, n=468) populations. Each population is composed of multiple subpopulations (i.e. the Mixed American population is composed of Mexican Ancestry from Los Angeles USA, Puerto Ricans from Puerto Rico, Colombians from Medellin, Colombia and Peruvians from Lima, Peru). Complete descriptions of each population are available in the 1000 genomes project. The rs6761637 SNP is in linkage disequilibrium (LD) with other MARCO SNPs that are associated with disease. The rs6761637 SNP is in LD with four SNPs in the Chinese Han population (**B**); rs2278589, rs67517405, rs12998782 and rs17009726, n=163, one in the Gambian population (**C**); rs13389814, n=179 and none in European population; n=535 (**D**). All analyses were considered significant if $p < 0.05$. *p* values are available in Table 4.

Table 4: The rs6761637 SNP is in LD with other polymorphisms associated with infection

SNP	R^2	χ^2	*p*-value	Source	Region	Pheno
rs2278589	0.2914	60.0213	**<0.0001**	CHB	Intron 1	*Mtb*+
rs6751745	0.3729	76.9289	**<0.0001**	CHB	Intron 13	*Mtb*+
rs17009726	0.932	191.9832	**<0.0001**	CHB	Intron 1	*Mtb*+
rs12998782	0.6245	128.6414	**<0.0001**	CHB	Intron 1	*Mtb*+
rs13389814	0.7092	160.2789	**<0.0001**	GWD	Intron16	*Mtb*+
rs12998782	0.0141	3.1829	0.0744	GWD	Intron1	*Mtb*+
rs4491733	0.0051	1.144	0.2848	GWD	Intron1	*Mtb*+
rs7559955	0.0141	3.1829	0.0744	GWD	Intron1	*Mtb*-
rs41279766	0.0001	0.0744	0.7851	EUR	Exon3 (Spacer)	Sepsis

Abbreviations: CHB = Han Chinese in Beijing (n=120), GWD = Gambian in Western Africa (n=179), EUR = European (n=535), *Mtb*+ = Pulmonary Tuberculosis Susceptibility, *Mtb*- = Pulmonary Tuberculosis Resistance.

Footnotes: rs2278589, and rs6751745 were linked to *Mtb* susceptibility by Thuong *et al* (2016). rs17009726 was linked to *Mtb* susceptibility by Ma *et al* (2011). rs12998782 was linked to *Mtb* susceptibility by Lao *et al* (2017). rs13389814, rs12998782, rs4491733, and rs7559955 were linked to *Mtb* susceptibility and resistance by Bowdish *et al* (2013). rs41279766 was linked to sepsis in COPD patients by Thomsen *et al* (2012).

A

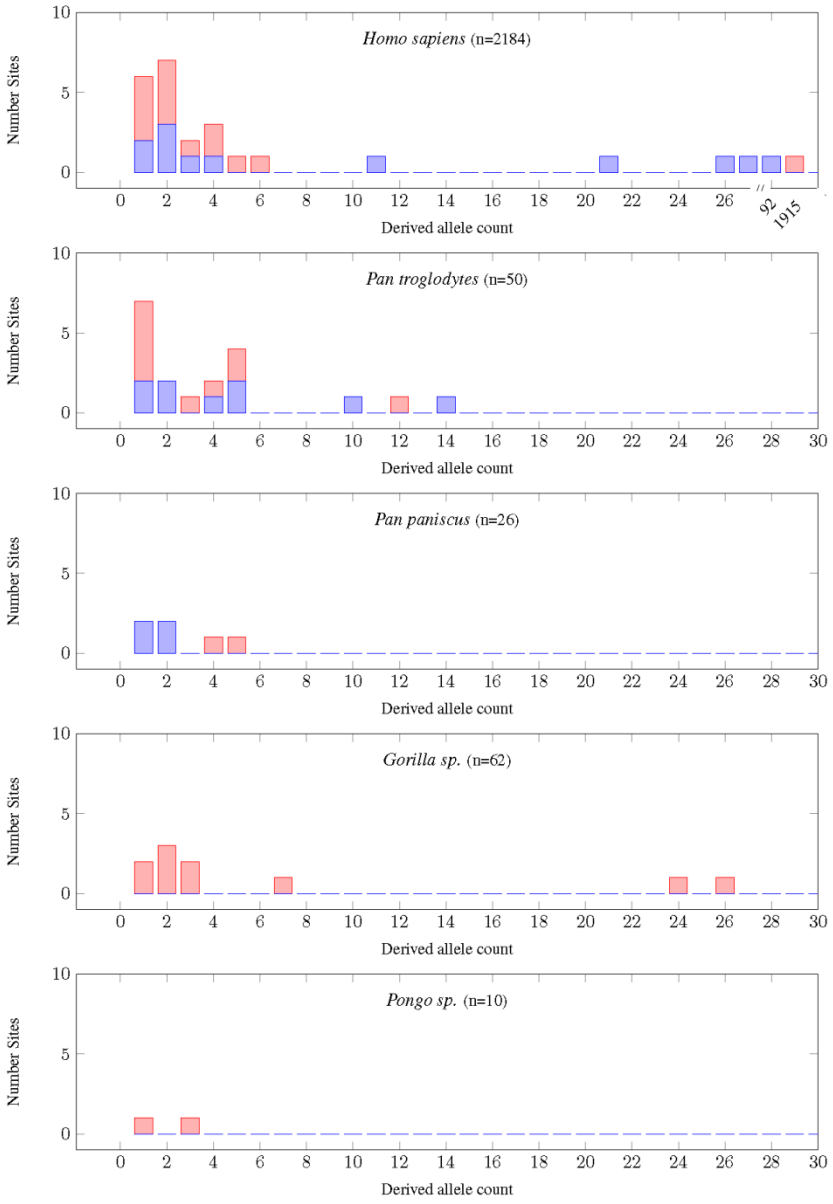

Figure 12: Site frequency spectra for MARCO for each of the primate species

(**A**) The site frequency spectra for MARCO are shown for each of the primate species. Red squares indicate non-synonymous changes while the blue squares indicate synonymous changes. The largest number of derived alleles in humans is at residue 282, with 1915 derived alleles. Note that the species have not been randomly sampled and hence these cannot be considered proper spectra. The y-axes each indicate the count of the number of observed sites with the observed number of variant alleles. The sample sizes are shown in parentheses. The human spectrum has a discontinuous x-axis.

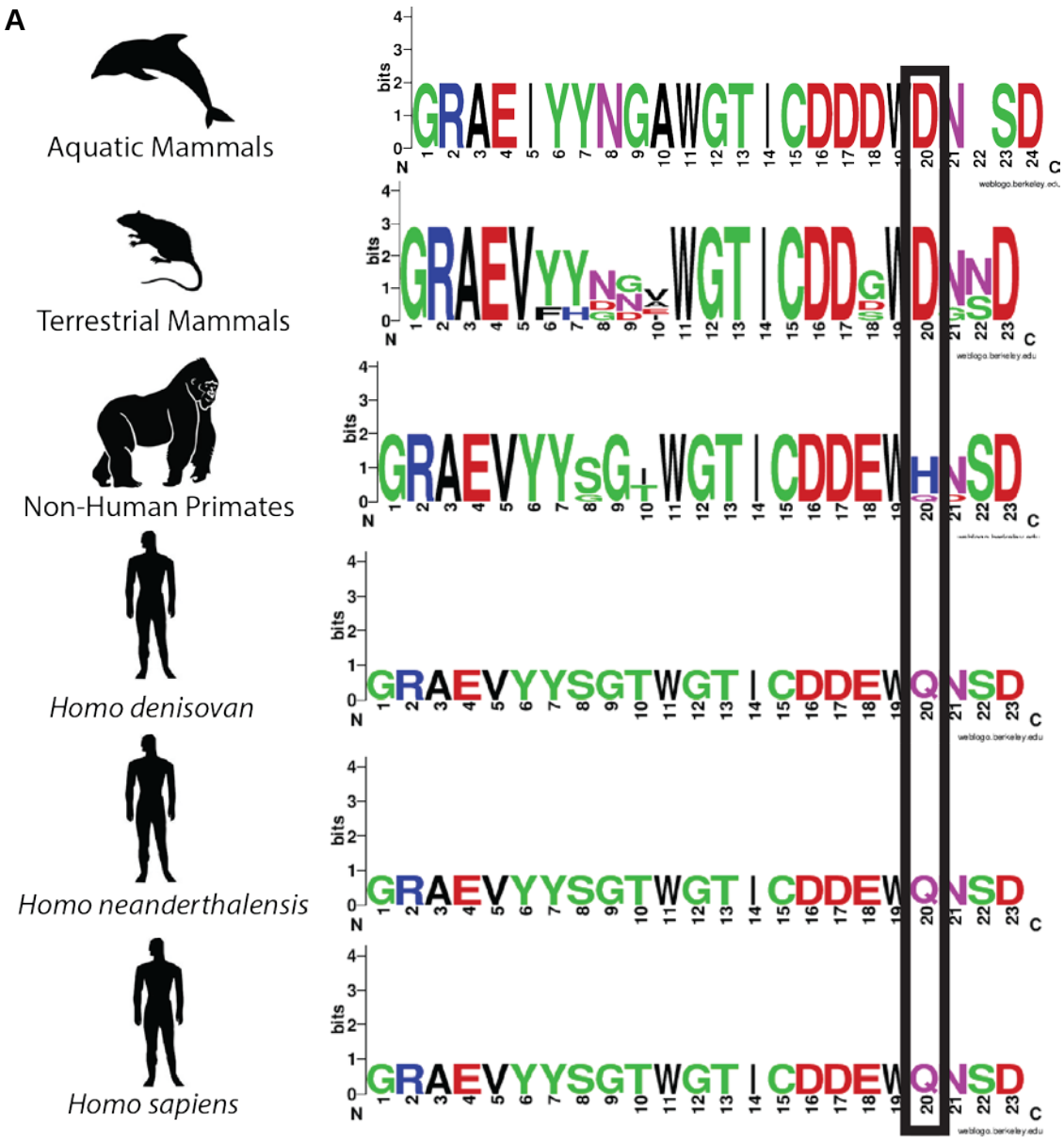

Figure 13: Partial alignment of the SRCR domain of MARCO highlighting a residue that is undergoing positive selection at position 452

We included sequences from Neanderthals and Denisovans to further strengthen our previous findings[2,3]. (**A**) Aquatic (n=2) and terrestrial (n=15) mammals possess a conserved aspartic acid residue at position 452, non-human primates (n=5) vary. Neanderthals (n=1), Denisovans (n=1), and humans (n=1) possess a glutamine residue. For a list of species included in each group, see Table 6.

Table 5: SNPs mapped from non-human primates, *H. neanderthalensis* and Denisovan to the SRCR domain of human MARCO

Genomic Position	Amino Acid Position	Ape Allele	Neander-thal/ Denisovan Allele	Human Allele	Ape Amino Acid	Neander-thal/ Denisovan Amino Acid	Human Amino Acid
119467242	442	T/C	C	C	I/T	T	T
119467252	445	C	A	A	T	T	T
119467273	**452**	**C/A**	**A**	**A**	**H/Q**	**Q**	**Q**
119467287	457	C	T	T	T	I	I
119468482	493	C	T	T	S	S	S
119468516	505	T	C	C	H	H	H
119468533	510	T	C	C	H	H	H

Footnotes: Based on data from the Great Apes Project, common SNPs from *Pan troglodytes, Gorilla gorilla,* and *Pan paniscus* to the SRCR domain are shown. *Pongo pygmaeus* was incomplete and only contained SNPs mapped to the first half of the MARCO gene. For position 452, *Nomascus leucogenys* was also included, as it was found to have a glutamine residue. Human genome build 18 was used.

Table 6: Organisms included in phylogenetic analyses

Non-Human Primates	Terrestrial Mammals	Aquatic Mammals	Other
Gorilla gorilla	*Dasypus novemcinctus*	*Tursiops truncatus*	*Homo sapiens*
Macaca mulatta	*Cavia porcellus*	*Orcinus orca*	*Homo neanderthalensis*
Pan paniscus	*Cricetulus griseus*		*Homo sapiens ssp. Denisova*
Pan troglodytes	*Canis lupus familiaris*		
Pongo abelii	*Loxodonta africana*		
	Mesocricetus auratus		
	Mus musculus		
	Oryctolagus cuniculus		
	Sus scrofa		
	Rattus norvegicus		
	Ovis aries		
	Bos taurus		

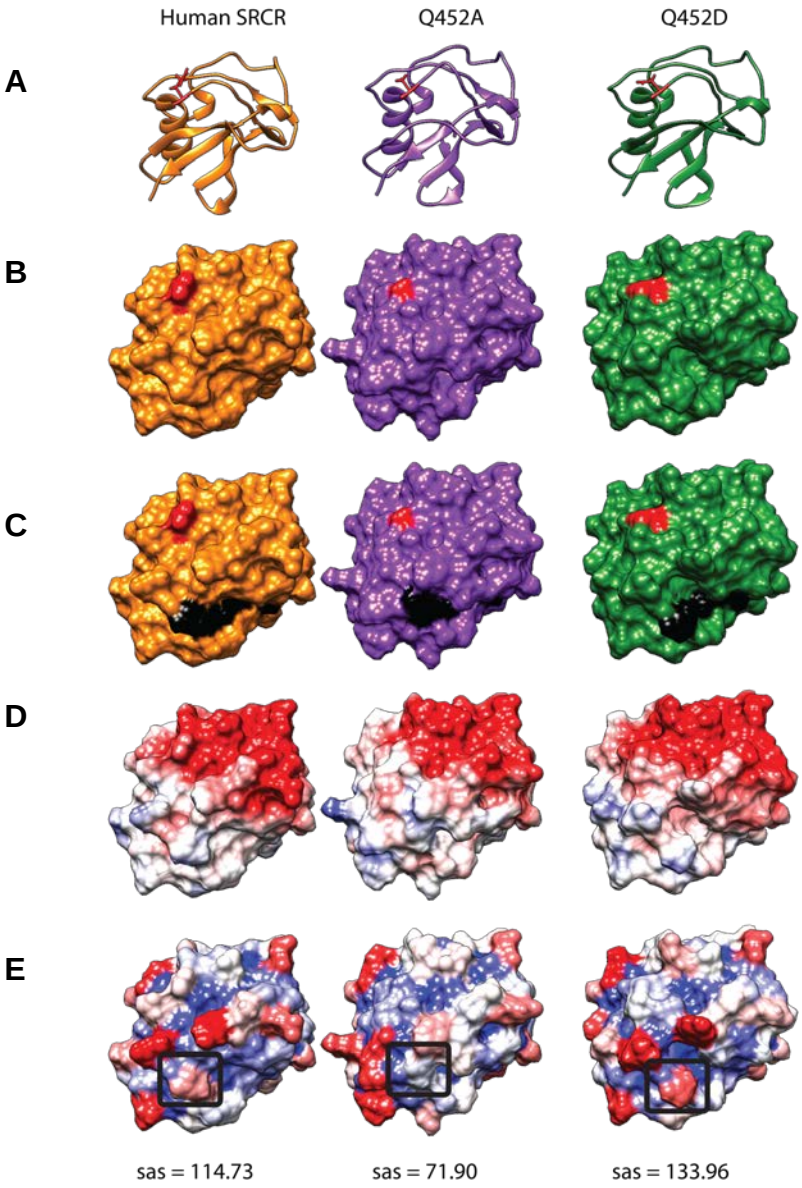

Figure 14: Structural comparisons of WT, Q452A and Q452D SRCR domain constructs

Mutation of residue 452 alters the exposure of a ligand-binding motif in the SRCR domain. (**A**) Ribbon diagrams of the respective SRCR variants with residue 452 highlighted in red. (**B**) Molecular surface model of the respecive SRCR variants with residue 452 highlighted in red. (**C**) Molecular surface model highlighting the RGRAEVYY motif in black and residue 452 in red. (**D**) Coulombic surface charge modelling applied. Red = -10, white = 0, blue = +10 in kcal/(mol·e) at 298K. (**E**) Solvent accessible surface area (sas) modelling applied. Red = 160 Å, white = 80 Å, blue = 0 Å. Raw sas values of arginine 13, of the SRCR domain **R**GRAEVYY, circled in black, are shown below each model in $Å^2$.

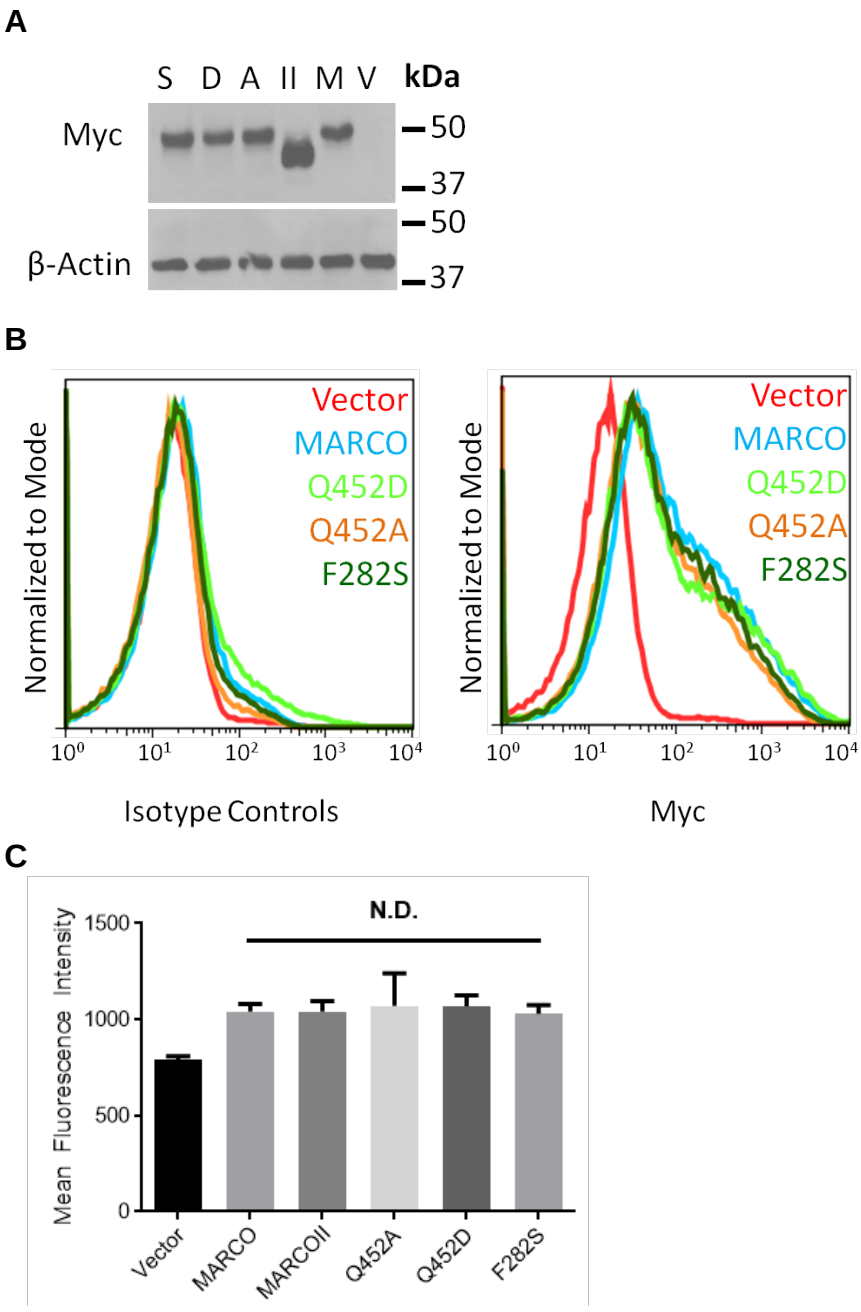

Figure 15: Mutation of sites Q452 and F282 do not affect expression of MARCO

HEK 293T cells transfected with empty vector, MARCO, MARCOII, Q452A, Q452D, or F282S were examined for total protein expression by western blot (**A**) and surface expression by flow cytometry (**B**). Abbreviations: V = vector, M = MARCO, II = MARCOII, A = Q452A, D = Q452D, S = F282S. (**C**) RAW 264.7 showed no difference in expression between MARCO constructs when analyzed by manually tracing the cell membrane and quantification of pixel intensity in ImageJ.

A

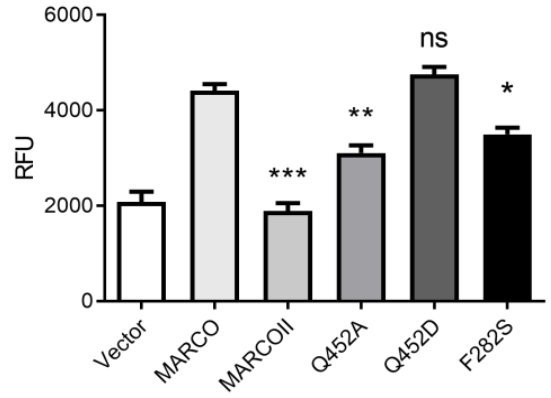
6000
4000
2000
0
RFU
ns
**
***
*
Vector
MARCO
MARCOII
Q452A
Q452D
F282S

B

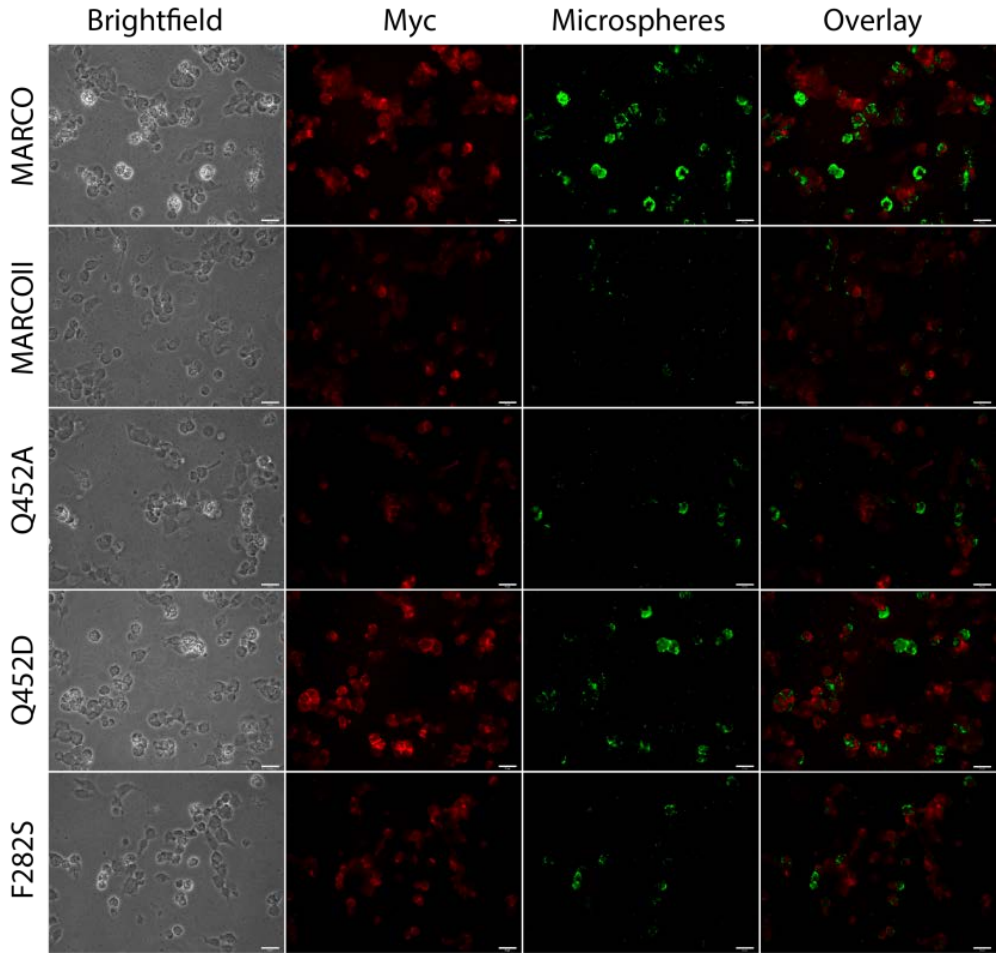
Brightfield
Myc
Microspheres
Overlay
MARCO
MARCOII
Q452A
Q452D
F282S

C

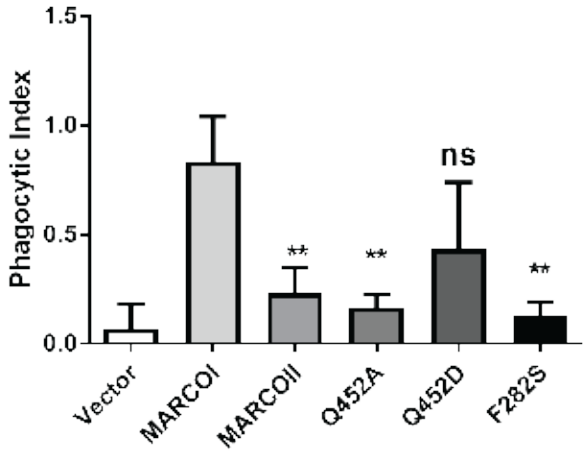
Phagocytic Index
1.5
1.0
0.5
0.0
ns
**
**
**
Vector
MARCOI
MARCOII
Q452A
Q452D
F282S

D

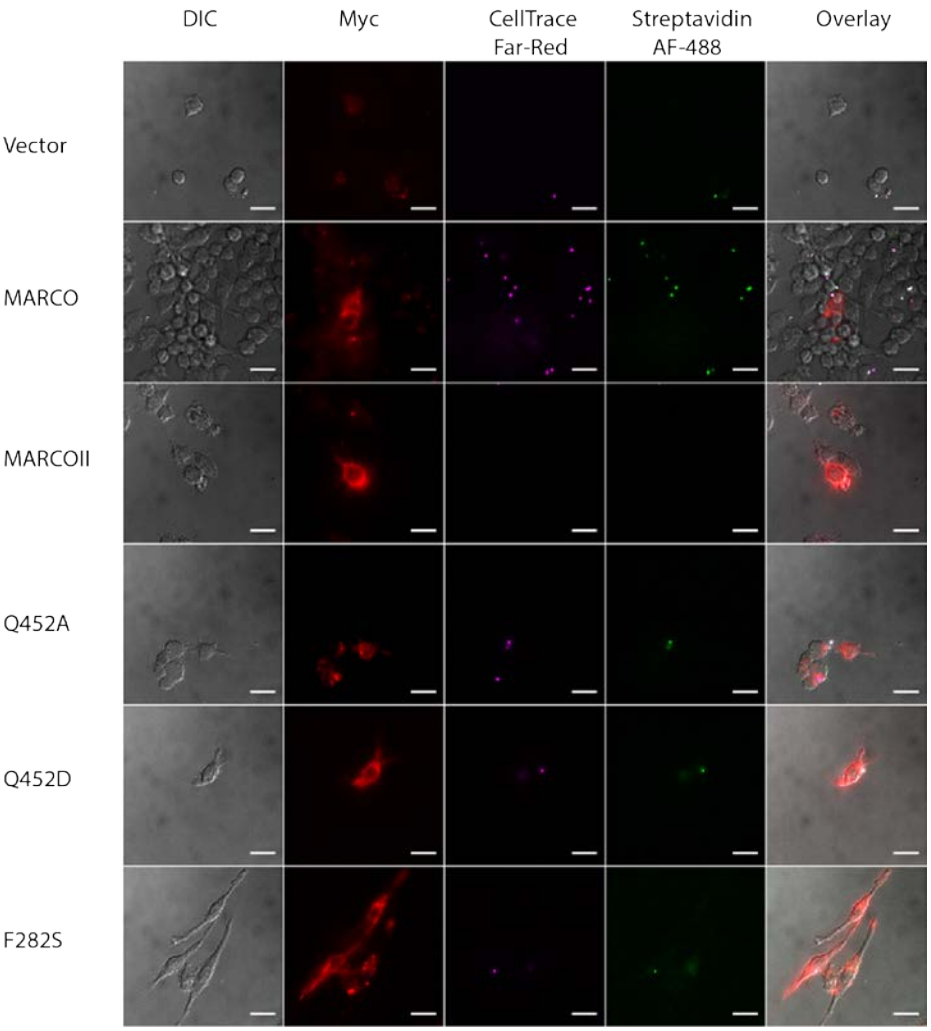
DIC
Myc
CellTrace Far-Red
Streptavidin AF-488
Overlay
Vector
MARCO
MARCOII
Q452A
Q452D
F282S

Figure 16: Residues at positions 452 and 282 of MARCO influence ligand association and bacterial internalization

(**A**) Mutation of glutamine residue 452 to alanine (Q452A) reduces ligand-coated microsphere association in HEK 293T cells, whereas mutation to the ancestral aspartic acid (Q452D) does not. Mutation of residue phenylalanine 282 to the ancestral serine (F282S) also reduces microsphere association. Statistical comparisons relative to MARCO were made using 1-way ANOVA with Tukey's post-hoc test. Error bars indicate mean±S.E.M. *$p < 0.05$, **$p < 0.01$, ***$p < 0.001$. (**B**) Immunofluorescence microscopy of microsphere association in HEK 293T transfected with empty vector, MARCO, MARCOII, or variants Q452A, Q452D, and F282S. Green = Mal-BSA Microspheres, Red = Myc. Scale bars represent 25 µm. (**C**) Mutation of residue 452 to alanine (Q452A) or aspartic acid (Q452D) or residue 282 to serine (F282S) greatly reduced the phagocytic index of RAW 264.7 macrophages. Phagocytic index was calculated as number of internalized bacteria divided by the number of RAW 264.7 macrophages counted. Statistical comparisons relative to MARCO were made using 1-way ANOVA with Tukey's post-hoc test. Error bars indicate mean±S.E.M. **$p < 0.01$ (**D**) Representative images of RAW 264.7 cells used to quantify phagocytic index. Only cells that stained brightly for anti-myc were analyzed in MARCO, MARCOII, Q452A, Q452D and F282S samples. Bacteria were counted as phagocytosed were positively stained for CellTrace Far Red and streptavidin Alexa Fluor-488 was negative.

APPENDIX I: BACTERIAL BINDING, PHAGOCYTOSIS AND KILLING: MEASUREMENTS USING COLONY FORMING UNITS

Published in *Methods in Molecular Biology*. 1519, 297-309 (2017).

Declaration of Academic Achievement:

This methodology book chapter was prepared by myself, with the editorial assistance of Dessi Loukov and Dr. Dawn M.E. Bowdish. Vikash Chawla provided the data that was used in this publication.

Chapter 20

Bacterial Binding, Phagocytosis, and Killing: Measurements Using Colony Forming Units

Kyle E. Novakowski, Dessi Loukov, Vikash Chawla, and Dawn M.E. Bowdish

Abstract

Herein we provide a colony forming unit (CFU)-based counting method for quantitating the bacterial binding, phagocytosis, and killing capacity of phagocytes. Although these functions can be measured by immunofluorescence and dye-based assays, quantitating CFUs is comparatively inexpensive and easy to perform. The protocol described below is easily modified for use with different phagocytes (e.g., macrophages, neutrophils, cell lines), types of bacteria or opsonic conditions.

Key words Phagocytosis, Bacterial killing, Particle binding, Macrophage, Gentamicin protection, Phagocyte

1 Introduction

Essential functions of the innate immune system include the detection, engulfment, and destruction of bacteria, which is primarily performed by neutrophils and macrophages. Profiling the functions of professional phagocytes provides valuable insight into innate immune function and can be used in a wide range of biological applications. These include testing the effect of a chemical compound, or characterizing the phenotype of a genetic knockout. Methods to quantify cellular association, phagocytosis, and killing by enumeration of viable microbial units were first described in the 1930s and 1940s [1]. Since then assays have diversified to include quantification of bacterial binding, uptake, and killing of fluorescently labeled bacteria by flow cytometry or fluorescence microscopy. However viability-based assays remain the most cost-effective and versatile.

To better understand the principles of this assay, a distinction must be made between binding and total cell association. Total cell association refers to bacteria that have been internalized by a phagocyte, *in addition to* bacteria that are bound, but remain

outside the cell. This distinction is important, because not all bound bacteria are phagocytosed. If, for example, the bacteria produce anti-phagocytic factors, or the presence of specific chemical inhibitors or gene deletions interfere with receptor expression, bacterial binding may occur without internalization [2–5]. One method to distinguish between bound and internalized bacteria is to differentially label internal and external bacteria using two different fluorescent dyes, or to use a pH-sensitive dye which only fluoresces in the low pH-environment of phagosome [6]. Unfortunately these methods require expensive reagents and analysis equipment (e.g., flow cytometers, fluorescence microscopes). Furthermore, examination of samples by microscopy can be time consuming and is relatively low-throughput.

An alternative approach is the use of viability-based assays. These assays are simpler and more affordable alternatives that can be used with a wide range of bacteria, some of which may not be amenable to fluorescent labeling by dyes or fluorescent proteins. Bacterial binding can be quantified by incubating phagocytes and bacteria at cold temperatures, which allows for phagocyte–bacteria interaction, but prevents internalization because processes such as actin polymerization and membrane trafficking do not occur at sub-physiological temperatures [7]. Total cell association can be quantified by incubating phagocytes and bacteria at physiologic temperatures (i.e. 37 °C), which allows for both bacterial binding and internalization. In order to distinguish between bound and internalized bacteria, extracellular bacteria can be killed through the addition of antibiotics. In order to determine the rate at which phagocytosed bacteria are killed, one can measure bacterial numbers over time. We have successfully used this assay to characterize the role of a macrophage receptor in anti-pneumococcal immunity, to study the effects of age on macrophage killing capacity using human and mouse macrophages and to discover drugs that increased macrophage phagocytosis [8–11]. Herein, we describe methods to characterize three distinct phagocyte functions: binding of particles/bacteria, phagocytosis/internalization of bacteria, and killing of bacteria.

2 Materials

Reagents used in this assay are specific to assays performed using *Streptococcus pneumoniae*. When performing this assay with other bacteria, reagents such as liquid culture media and agar growth plates can be substituted for appropriate growth media. This protocol can also be adapted for use with inert particles (*see* Subheading 3.1, **step 1**).

2.1 Bacteria and Microbiology Components

1. Early-to-mid-log phase bacteria (*see* **Notes** 1 and 2).
2. Appropriate liquid culture media (e.g., Luria–Bertani broth or tryptic soy broth). Follow manufacturer's instructions for broth preparation. Autoclave to sterilize. Store at 4 °C. Only open under sterile conditions (*see* **Note** 3).
3. Sterile water.
4. Hank's Balanced Salt Solution (HBSS).
5. Gentamicin solution: Dissolve gentamicin sulfate salt to a final concentration of 50 mg/mL in sterile water. Store at −20 °C in aliquots (*see* **Note** 2).
6. Tryptic soy agar (TSA)/Sheep's blood plates: dissolve 15 g of TSA in 500 mL deionized water. Autoclave to sterilize. Cool for 1.5 h in a 60 °C water bath. Under sterile conditions, add 25 mL sterile, defibrinated sheep's blood, and swirl gently to mix (*see* **Note** 3).
7. Spectrophotometer.
8. 15 mL polystyrene culture centrifuge tubes.
9. Incubator. The incubation conditions of plates for quantification of bacteria will vary depending on the bacteria being used.

2.2 Macrophage Components

1. Macrophages: any source of macrophages can be used, including bone marrow-derived, alveolar, resident or recruited peritoneal, blood monocyte-derived (*see* **Note** 4).
2. Phosphate buffered saline (PBS): Warm PBS to 37 °C prior to use.
3. Accutase cell detachment solution: Store at −20 °C in 10 mL aliquots. Warm to 37 °C prior to use (*see* **Note** 5).
4. Cell lifters (*see* **Note** 6).
5. Trypan blue, 0.4%.
6. Hemocytometer.
7. Light microscope with a minimum objective magnification of 20×.
8. 50 mL conical tubes.

2.3 General Assay Components

1. 2 mL microcentrifuge tubes.
2. Vortex.
3. Microcentrifuge.
4. Serological pipettes (5, 10, and 25 mL).
5. Micropipettes and micropipette tips.
6. Appropriate disposal reagents and equipment for liquid biological waste. Please follow institutional requirements.
7. Nutating Mixer.

8. Black 96-well plate.
9. Spectrophotometer capable of reading fluorescence.
10. *If performing assays for particle uptake:* Fluorescent polystyrene microspheres, 0.5–2 μM (Polysciences, Warrington, PA, USA).

3 Methods

3.1 Bacterial Binding Assay

Carry out all procedures under sterile conditions in a biological safety cabinet. For the experiments using *S. pneumoniae* in Figs. 1, 2, and 3, TSB/Sheep's blood plates were used.

1. Grow liquid cultures to early or mid-log phase (*see* **Notes 1** and 7). While waiting, prepare and label tubes containing 900 μL sterile water and appropriate media plates for the experiments.
2. When the liquid bacterial culture reaches early to mid-log growth (measured using OD_{600}, *see* **Note 1**) remove 1 mL into a 2 mL microcentrifuge tube and centrifuge at 12,000 × *g* for 1 min.
3. Carefully remove the supernatant and resuspend the pellet in 1 mL HBSS. Keep on ice to prevent additional bacterial growth.
4. Visually inspect macrophage culture under a light microscope to ensure high cell viability and that the culture is free of contamination. Viable macrophages typically have a dendritic-like

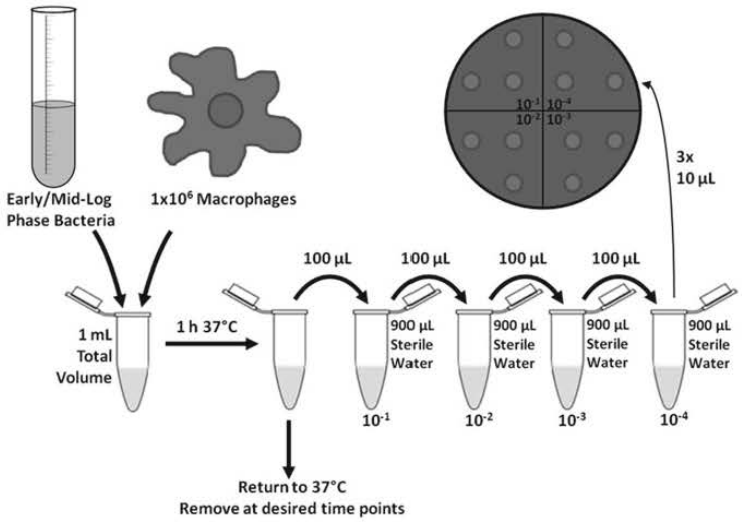

Fig. 1 A schematic outlining the major steps to perform a CFU-based bacterial killing assay

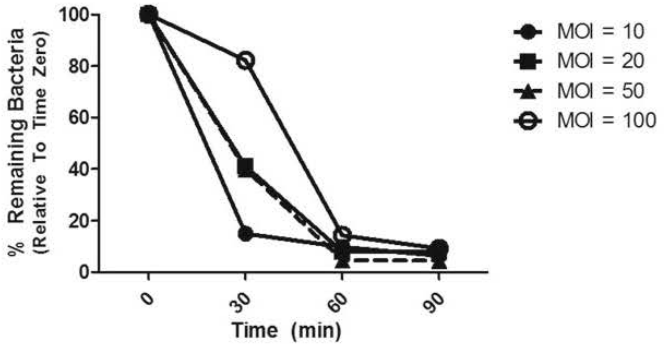

Fig. 2 A representative killing assay highlighting differences in kill curves with varying multiplicities of infection (MOI) using bone marrow-derived macrophages

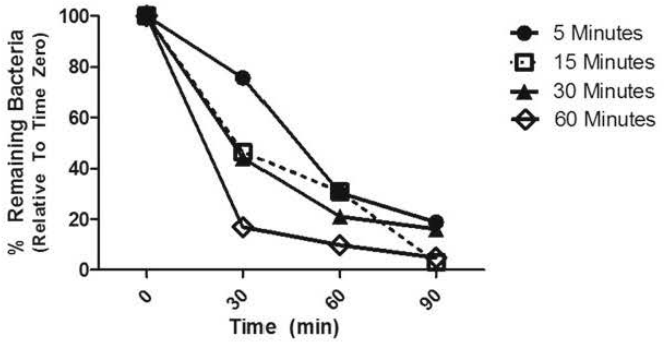

Fig. 3 A representative killing assay highlighting differences in kill curves with varying pre-incubation times before assaying bacterial killing using bone marrow-derived macrophages

morphology and should be strongly adherent. Floating or rounded cells generally indicate a loss of viability, which can be confirmed by trypan blue staining.

5. Remove macrophage culture media and gently wash with warm PBS.
6. Remove PBS and add 10 mL of warm Accutase cell detachment solution. Cover the plate and place in a 37 °C incubator for 10 min. Visually inspect the plate under a light microscope to determine cell detachment. Some cells should be completely detached and remaining adherent cells should be round in morphology. If cells still remain adherent, incubate for an additional 5–10 min.
7. Gently scrape the plate with a cell lifter, to remove any remaining attached cells (*see* **Note 6**). Pipette Accutase solution containing macrophages into a 50 mL conical tube. To maximize

macrophage recovery, wash the plate with 10 mL warm PBS and add to the 50 mL conical tube.

8. Centrifuge for 10 min at 500 ×*g*.
9. Carefully remove all supernatant and gently resuspend the pellet in 1 mL warm PBS. Do not vortex.
10. Determine the cells/mL by diluting cells 1:1 with trypan blue and pipette 10 µL into a hemocytometer. Count viable cells following standard usage of a hemocytometer.
11. Add up to 1×10^6 viable macrophages into a 2 mL microcentrifuge tube. Bring the volume of solution up to 900 µL by adding PBS. Repeat for each desired time point. For example, if performing time points of 0, 30, 60, and 90 min, you will require 4 tubes containing equal numbers of macrophages (*see* **Note 8**).
12. Briefly vortex bacteria and add the desired multiplicity of infection (MOI) to each tube. The MOI will vary depending on the bacteria used in the assay and number/type of macrophages, but generally ranges from 10 to 100 (*see* **Note 9**, Fig. 2). In the case of *Streptococcus pneumoniae*, an MOI of 20 is optimal. The final volume of the macrophage/bacteria solution should be brought to 1 mL with PBS.
13. Incubate with gentle mixing at 4 °C for 1 h. This incubation allows for cell to cell association. At time points 0, 20, 40, and 60 min, remove the tube and centrifuge at 500 ×*g* for 5 min. At low speeds, macrophages (and bound bacteria) will form a pellet whereas unbound bacteria will remain in the supernatant.
14. Carefully remove the supernatant to remove unbound bacteria and gently resuspend in 1 mL cold PBS. Centrifuge at 500 ×*g*, 4 °C for 5 min. Repeat wash two times.
15. Resuspend in 1 mL of PBS and lyse macrophages by pipetting 100 µL of the macrophage solution into 900 µL sterile water (prepared in **step 1**) (*see* **Note 10**). Briefly vortex. This tube is now a 10^{-1} dilution.
16. Perform a serial dilution by repeating **step 14** using 100 µL of the 10^{-1} dilution into 900 µL sterile water. Briefly vortex. This tube is now a 10^{-2} dilution. Repeat for 10^{-3} and 10^{-4} dilutions.
17. Working from the most dilute to the most concentrated dilution, briefly vortex and pipette three separate 10 µL drops onto the agar plate. Repeat for all other dilutions (*see* Fig. 1).
18. Allow the plate to dry at room temperature for approximately 20 min or until the droplets are no longer visible on the agar plate.
19. Incubate plates inverted in a 37 °C incubator overnight.

20. Count colonies for each dilution. This will quantitate all cell-associated bacteria. To determine CFU/mL or total number of internalized bacteria, multiply the number of colonies by the inverse of the dilution factor and by 10^2, to account for the 10 µL plating volume. For example, 17 colonies counted on a 10^{-3} droplet would be calculated as:

17×10^3 (dilution factor) $\times 10^2$ (plating volume) $= 1.7 \times 10^6$ CFU/mL (*see* Fig. 1).

3.2 Gentamicin Protection Assay for Bacterial Phagocytosis

Carry out all procedures under sterile conditions in a biological safety cabinet. This protocol has been optimized for use with *Streptococcus pneumoniae*, but can be performed with other bacteria. Ensure that the bacteria are susceptible to this concentration of gentamicin prior to beginning the experiment (*see* **Note 2**).

1. Grow bacteria to early or mid-log phase in liquid culture (*see* **Note 1**). While waiting, prepare and label tubes containing 900 µL sterile water and TSB/Sheep's blood plates to be used in **steps 16** and **18**.
2. When the liquid bacterial culture reaches early to mid-log growth (as measured by OD_{600}) remove 1 mL into a 2 mL microcentrifuge tube and centrifuge at 12,000 × *g* for 1 min. For *S. pneumoniae*, early log phase ($OD_{600} = 0.5$) is generally obtained from 1 to 4 h when prepared from a 1 mL freezer stock. Carefully remove the supernatant and resuspend the pellet in 1 mL HBSS. Keep on ice until use.
3. Visually inspect macrophage culture under a light microscope to ensure high cell viability and the culture is free of contamination. Macrophages typically have a dendritic-like morphology and should be strongly adherent.
4. Remove macrophage culture media and gently wash with warm PBS.
5. Remove PBS and add 10 mL of warm Accutase cell detachment solution. Cover the plate and place in a 37 °C incubator for 10 min. Visually inspect the plate under a light microscope to determine whether cells have detached. If cells still remain adherent, incubate for an additional 5–10 min.
6. Gently scrape the plate with a cell lifter to remove any loosely adherent cells (*see* **Note 6**). Pipette Accutase solution containing macrophages into a 50 mL conical tube. To maximize macrophage recovery, wash the plate with 10 mL warm PBS and add to the 50 mL conical tube.
7. Centrifuge for 10 min at 500 × *g*.
8. Carefully remove all supernatant and gently resuspend the pellet in 1 mL of warm PBS. Do not vortex.

9. Determine the CFU/mL by diluting cells 1:1 with trypan blue and pipette 10 µL into a hemocytometer. Count viable cells following standard usage of a hemocytometer.
10. Add up to 1×10^6 viable macrophages into a 2 mL microcentrifuge tube. Bring the volume of solution up to 900 µL by adding PBS. Repeat for each desired time point. For example, if performing time points of 0, 30, 60, and 90 min, you will require four tubes containing equal numbers of macrophages (*see* **Note** 8).
11. Briefly vortex bacteria and add the desired multiplicity of infection (MOI) to each tube (*see* Fig. 2). The MOI will vary depending on the bacteria used in the assay and number/type of macrophages. In the examples in Figs. 2 and 3, *Streptococcus pneumoniae* was added at an MOI of 20. The final volume of the macrophage/bacteria solution should be brought to 1 mL with PBS.
12. Incubate with gentle mixing at 37 °C for 30 min to allow for bacterial binding and internalization (*see* Fig. 3). After this preincubation, at time points +0, +20, +40, and +60 min, remove the tube and centrifuge at 500 × *g* for 5 min.
13. Carefully remove the supernatant to remove unbound bacteria and gently resuspend in 1 mL HBSS + 50 µg/mL gentamicin. Incubate with gentle mixing at 37 °C for 40 min (*see* **Note** 2).
14. Add 1 mL HBSS and centrifuge at 500 × *g* for 5 min. Wash cells two additional times with 1 mL HBSS to completely remove gentamicin.
15. Following the final wash, resuspend in 1 mL HBSS and lyse macrophages by pipetting 100 µL of the macrophage solution into 900 µL sterile water (prepared in **step 1**) (*see* **Note** 9). Briefly vortex. This tube is now a 10^{-1} dilution.
16. Perform a serial dilution by repeating **step 16** using 100 µL of the 10^{-1} dilution into 900 µL sterile water. Briefly vortex. This tube is now a 10^{-2} dilution. Repeat for 10^{-3} and 10^{-4} dilutions.
17. Working from the most dilute to the most concentrated dilution, briefly vortex and pipette three separate 10 µL drops onto the agar plate. Repeat for all other dilutions.
18. Allow the plate to dry at room temperature for approximately 20 min or until the droplets are no longer visible on the agar plate.
19. Incubate plates inverted in a 37 °C incubator overnight.
20. Count colonies for each dilution. To determine CFU/mL or total number of internalized bacteria, multiply the number of colonies by the inverse of the dilution factor and by 10^2, to

account for plating volume. For example, 17 colonies counted on a 10^{-5} droplet would be calculated as:

17×10^5 (dilution factor) $\times 10^2$ (plating volume) $= 1.7 \times 10^6$ CFU/mL (*see* Fig. 1).

3.3 Particle Binding Assay 12

This adapted protocol uses inert fluorescent particles such as polystyrene microspheres in place of bacteria. When using inert particles, attention should be given to particle size since some cell lines and phagocytes cannot internalize particles larger than 1–2 μm. In general, particles greater than 0.5 μm are internalized by phagocytosis and those smaller than 0.5 μm are internalized by endocytosis [13]. Particles may be coated with ligands, such as bacterial cell wall components or antibodies either by passive adsorption or covalent coupling. Finally, it is advisable to perform a dose-response experiment to determine optimal particle–phagocyte ratios.

1. Visually inspect macrophage culture under a light microscope to ensure high cell viability and the culture is free of contamination. Macrophages typically have a dendritic-like morphology and should be strongly adherent.
2. Remove macrophage culture media and gently wash with warm PBS.
3. Remove PBS and add 10 mL of warm Accutase cell detachment solution. Cover the plate and place in a 37 °C incubator for 10 min. Visually inspect the plate under a light microscope to determine whether cells have detached. If cells still remain adherent, incubate for an additional 5–10 min.
4. Gently scrape the plate with a cell lifter to remove any loosely adherent cells (*see* **Note 6**). Pipette Accutase solution containing macrophages into a 50 mL conical tube. To maximize macrophage recovery, wash the plate with 10 mL warm PBS and add to the 50 mL conical tube.
5. Centrifuge for 10 min at 500 × *g*.
6. Carefully remove all supernatant and gently resuspend the pellet in 1 mL of warm PBS. Do not vortex.
7. Determine the CFU/mL by diluting cells 1:1 with trypan blue and pipette 10 μL into a hemocytometer. Count viable cells following standard usage of a hemocytometer.
8. Add up to 1×10^6 viable macrophages into a 2 mL microcentrifuge tube. Bring the volume of solution up to 900 μL by adding PBS. Repeat for each desired time point. For example, if performing time points of 0, 30, 60 and 90 min, you will require four tubes containing equal numbers of macrophages (*see* **Note 8**).
9. Vortex particles and add at the desired particle–macrophage ratio and bring the total volume up to 1 mL with either PBS or cell culture media

10. Incubate on with gentle agitation at 4 °C for 1 h. At time points 0, 20, 40, and 60 min, remove the tube and centrifuge at 500 ×*g* for 5 min.
11. Carefully remove the supernatant to remove unbound particles and gently resuspend in 1 mL PBS or media. Centrifuge at 500 ×*g* for 5 min. Repeat wash twice more.
12. Resuspend in 200 μL PBS or media.
13. Add suspension to one well of a black 96-well plate. Read at the excitation and emission recommended by the particle manufacturer.

3.4 Bacterial Killing Assay

Carry out all procedures under sterile conditions in a biological safety cabinet. This protocol has been optimized for use with *Streptococcus pneumoniae*, but can be performed with other bacteria. Please see additional notes for assay modifications.

1. Grow bacteria to early or mid-log phase in liquid culture (*see* **Note** 1). While waiting, prepare and label tubes containing 900 μL sterile water and TSB/Sheep's blood plates to be used in **steps 16** and **18** (*see* Fig. 1 for experimental schematic).
2. When the liquid bacterial culture reaches the desired OD_{600}, remove 1 mL into a 2 mL microcentrifuge tube and centrifuge at 12,000 ×*g* for 1 min.
3. Carefully remove the supernatant and resuspend the pellet in 1 mL HBSS. Keep on ice to prevent additional bacterial growth.
4. Visually inspect the macrophage culture under a light microscope to ensure high cell viability and that the culture is free of contamination. Macrophages typically have a dendritic-like morphology and should be strongly adherent.
5. Remove macrophage culture media and gently wash with warm PBS.
6. Remove PBS and add 10 mL of warm Accutase cell detachment solution. Cover the plate and place in a 37 °C incubator for 10 min. Visually inspect the plate under a light microscope to determine cell detachment. Some cells should be completely detached and remaining adherent cells should be round in morphology. If cells still remain adherent, incubate for an additional 5–10 min.
7. Gently scrape the plate with a cell lifter, covering all surface area (*see* **Note** 6). Pipette Accutase solution containing macrophages into a 50 mL conical tube. To maximize macrophage recovery, wash the plate with 10 mL warm PBS and add to the 50 mL conical tube.
8. Centrifuge for 10 min at 500 ×*g*.
9. Carefully remove all supernatant and gently resuspend the pellet in 1 mL warm PBS. Do not vortex.

10. Determine the CFU/mL by diluting cells 1:1 with trypan blue and pipette 10 µL into a hemocytometer. Count viable cells following standard usage of a hemocytometer.
11. Add up to 1×10^6 viable macrophages into a 2 mL microcentrifuge tube. Bring the volume of solution to 900 µL by adding PBS.
12. Briefly vortex bacteria and add the desired multiplicity of infection (MOI) to each tube (*see* Fig. 2). The MOI will vary depending on the bacteria used in the assay and number/type of macrophages. In the examples in Figs. 2 and 3, *Streptococcus pneumoniae* was added at an MOI of 20. The final volume of the macrophage/bacteria solution should be brought to 1 mL with PBS.
13. Incubate with gentle mixing at 37 °C for 30 min to allow for bacterial binding and internalization (*see* Fig. 3). After this preincubation, remove the tube and centrifuge at 500 ×*g* for 5 min.
14. Carefully remove the supernatant to remove unbound bacteria and gently resuspend in 1 mL HBSS.
15. Wash cells 1 additional time with 1 mL HBSS to completely remove unbound bacteria.
16. Following the final wash, resuspend in 1 mL HBSS.
17. Lyse macrophages by pipetting 100 µL of the macrophage solution into 900 µL sterile water (prepared in **step 1**) (*see* **Note 9**). Briefly vortex. This tube is now a 10^{-1} dilution at time point +0 min. Return the original tube containing macrophages and bound/internalized bacteria to the mixer at 37 °C for time points of +30, +60, and +90 min, +120 and +180 min.
18. Perform a serial dilution using 100 µL of the 10^{-1} dilution into 900 µL sterile water for each time point. Briefly vortex. This tube is now a 10^{-2} dilution. Repeat for 10^{-3} and 10^{-4} dilutions.
19. Working from the most dilute to the most concentrated dilution, briefly vortex and pipette three separate 10 µL drops onto the agar plate. Repeat for all other dilutions.
20. Allow the plate to dry at room temperature for approximately 20 min or until the droplets are no longer visible on the agar plate.
21. Repeat **steps 17–20** for time points of +30, +60, and +90, +120, and +180 min.
22. Incubate plates inverted in a 37 °C incubator overnight.
23. Count colonies for each dilution. To determine CFU/mL or total number of internalized bacteria, multiply the number of colonies by the inverse of the dilution factor and by 10^2, to account for plating volume. For example, 17 colonies counted on a 10^{-3} droplet would be calculated as:

    17×10^3 (dilution factor) $\times 10^2$ (plating volume) $= 1.7 \times 10^6$ CFU/mL (*see* Fig. 1).

4 Notes

1. Accurate quantitation of the MOI is essential to ensure reproducibility. Therefore, it is critical to perform a growth curve for the strain of bacteria to be used in the assay in order to prepare the assay with an accurate MOI. Determine the CFU/mL when the culture is analyzed via a spectrophotometer at OD_{600}.
2. The sensitivity of a given strain of bacteria to gentamicin should be titrated by performing a standard kill curve procedure in the presence of varying doses of gentamicin at 10 min time points for approximately 1 h.
3. The type of liquid culture media, agar plate and incubation conditions can be modified depending on the strain of bacteria being used for the assay.
4. Permeability of the phagocytic cells should be given consideration when performing a gentamicin protection assay, as gentamicin can penetrate permeabilized membranes and kill internalized bacteria. This can occur, for example, when cells are forcefully washed or stored at incorrect temperatures.
5. Accutase is preferred over trypsin, as trypsin has been shown to cleave some phagocytic receptors. If assaying the relevance of specific receptors, it is advisable to treat cells with Accutase and check receptor expression via FACS or IF microscopy. Include a saline or untreated control.
6. Cell viability can be significantly enhanced by using cell lifters in place of cell scrapers.
7. Before using this assay to quantify bacterial binding, ensure that the bacteria will survive at this temperature for the desired time course. To do so, grow bacteria to early or mid-log phase, perform a serial dilution and plate droplets to determine CFU/mL. Then incubate bacteria at 4 °C. At desired the time point(s), remove bacteria, perform serial dilutions and plate. Following overnight incubation at optimal growth conditions for the desired bacteria, compare initial CFU/mL to CFU/mL at each time point.
8. A minimum of 1×10^5 macrophages are required to perform this assay. In our experience 1×10^6 macrophages per condition increases reproducibility.
9. Bacteria should be titrated using serial dilutions in PBS, plated on appropriate solid agar medium to count CFUs.
10. Lysis of macrophages ensures that bacterial killing is immediately halted; however plating should be performed immediately to ensure that bacterial viability doesn't decrease.

References

1. Cohn ZA, Morse SI (1959) Interactions between rabbit polymorphonuclear leucocytes and staphylococci. J Exp Med 110:419–443
2. Fox EN (1974) M proteins of group A Streptococci. Bacteriol Rev 38:57–86
3. Cho K, Arimoto T, Igarashi T, Yamamoto M (2013) Involvement of lipoprotein PpiA of Streptococcus gordonii in evasion of phagocytosis by macrophages. Mol Oral Microbiol 28:379–391. doi:10.1111/omi.12031
4. Mukouhara T, Arimoto T, Cho K et al (2011) Surface lipoprotein PpiA of Streptococcus mutans suppresses scavenger receptor MARCO-dependent phagocytosis by macrophages. Infect Immun 79:4933–4940. doi:10.1128/IAI.05693-11
5. Dilworth JA, Hendley JO, Mandell GL (1975) Attachment and ingestion of gonococci by human neutrophils. Infect Immun 11:512–516
6. Campbell PA, Canono BP, Drevets DA (2001) Measurement of bacterial ingestion and killing by macrophages. Curr Protoc Immunol Chapter 14: Unit 14.6. doi: 10.1002/0471142735.im1406s12
7. Underhill DM, Ozinsky A (2002) Phagocytosis of microbes: complexity in action. Annu Rev Immunol 20:825–852. doi:10.1146/annurev.immunol.20.103001.114744
8. Dorrington MG, Roche AM, Chauvin SE et al (2013) MARCO Is required for TLR2- and Nod2-mediated responses to Streptococcus pneumoniae and clearance of pneumococcal colonization in the murine nasopharynx. J Immunol 190:250–258. doi:10.4049/jimmunol.1202113
9. Puchta A, Naidoo A, Verschoor CP et al (2016) TNF drives monocyte dysfunction with age and results in impaired anti-pneumococcal immunity. PLoS Pathog 12, e1005368. doi:10.1371/journal.ppat.1005368
10. Verschoor CP, Johnstone J, Loeb M et al (2014) Anti-pneumococcal deficits of monocyte-derived macrophages from the advanced-age, frail elderly and related impairments in PI3K-AKT signaling. Hum Immunol 75:1192–1196. doi:10.1016/j.humimm.2014.10.004
11. Perry JA, Koteva K, Verschoor CP et al (2015) A macrophage-stimulating compound from a screen of microbial natural products. J Antibiot 68:40–46. doi:10.1038/ja.2014.83
12. Novakowski KE, Huynh A, Han S, Dorrington MG, Yin C, Tu Z, Pelka P, Whyte P, Guarné A, Sakamoto K, Bowdish DM (2016) A naturally occurring transcript variant of MARCO reveals the SRCR domain is critical for function. Immunol Cell Biol 94(7):646–55. doi:10.1038/icb.2016.20
13. Mellman I (1996) Endocytosis and molecular sorting. Annu Rev Cell Dev Biol 12:575–625. doi:10.1146/annurev.cellbio.12.1.575

APPENDIX II: ARTICLE AND BOOK REUSE AND REPRINT PERMISSIONS

The following documents contain copyright permissions to reuse the manuscripts and book chapter that I have authored within this thesis.

SPRINGER LICENSE
TERMS AND CONDITIONS

Sep 05, 2017

This Agreement between McMaster University -- Kyle Novakowski ("You") and Springer ("Springer") consists of your license details and the terms and conditions provided by Springer and Copyright Clearance Center.

License Number	4182530576581
License date	Sep 05, 2017
Licensed Content Publisher	Springer
Licensed Content Publication	Springer eBook
Licensed Content Title	Bacterial Binding, Phagocytosis, and Killing: Measurements Using Colony Forming Units
Licensed Content Author	Kyle E. Novakowski
Licensed Content Date	Jan 1, 2017
Type of Use	Thesis/Dissertation
Portion	Full text
Number of copies	5
Author of this Springer article	Yes and you are a contributor of the new work
Order reference number	
Title of your thesis / dissertation	IDENTIFICATION AND FUNCTIONAL CHARACTERIZATION OF CONSERVED RESIDUES AND DOMAINS IN THE MACROPHAGE SCAVENGER RECEPTOR MARCO
Expected completion date	Dec 2017
Estimated size(pages)	180
Requestor Location	McMaster University 1280 Main St W MDCL 4020 Hamilton, ON L8S4L8 Canada Attn: McMaster University
Billing Type	Invoice
Billing Address	McMaster University 1280 Main St W MDCL 4020 Hamilton, ON L8S4L8 Canada Attn: Kyle Novakowski
Total	0.00 CAD
Terms and Conditions	

Introduction

The publisher for this copyrighted material is Springer. By clicking "accept" in connection with completing this licensing transaction, you agree that the following terms and conditions

apply to this transaction (along with the Billing and Payment terms and conditions established by Copyright Clearance Center, Inc. ("CCC"), at the time that you opened your Rightslink account and that are available at any time at http://myaccount.copyright.com).

Limited License

With reference to your request to reuse material on which Springer controls the copyright, permission is granted for the use indicated in your enquiry under the following conditions:

- Licenses are for one-time use only with a maximum distribution equal to the number stated in your request.
- Springer material represents original material which does not carry references to other sources. If the material in question appears with a credit to another source, this permission is not valid and authorization has to be obtained from the original copyright holder.
- This permission
• is non-exclusive
• is only valid if no personal rights, trademarks, or competitive products are infringed.
• explicitly excludes the right for derivatives.
- Springer does not supply original artwork or content.
- According to the format which you have selected, the following conditions apply accordingly:
• **Print and Electronic:** This License include use in electronic form provided it is password protected, on intranet, or CD-Rom/DVD or E-book/E-journal. It may not be republished in electronic open access.
• **Print:** This License excludes use in electronic form.
• **Electronic:** This License only pertains to use in electronic form provided it is password protected, on intranet, or CD-Rom/DVD or E-book/E-journal. It may not be republished in electronic open access.

For any electronic use not mentioned, please contact Springer at permissions.springer@spi-global.com.

- Although Springer controls the copyright to the material and is entitled to negotiate on rights, this license is only valid subject to courtesy information to the author (address is given in the article/chapter).
- If you are an STM Signatory or your work will be published by an STM Signatory and you are requesting to reuse figures/tables/illustrations or single text extracts, permission is granted according to STM Permissions Guidelines: http://www.stm-assoc.org/permissions-guidelines/

For any electronic use not mentioned in the Guidelines, please contact Springer at permissions.springer@spi-global.com. If you request to reuse more content than stipulated in the STM Permissions Guidelines, you will be charged a permission fee for the excess content.

Permission is valid upon payment of the fee as indicated in the licensing process. If permission is granted free of charge on this occasion, that does not prejudice any rights we might have to charge for reproduction of our copyrighted material in the future.

-If your request is for reuse in a Thesis, permission is granted free of charge under the following conditions:

This license is valid for one-time use only for the purpose of defending your thesis and with a maximum of 100 extra copies in paper. If the thesis is going to be published, permission needs to be reobtained.

- includes use in an electronic form, provided it is an author-created version of the thesis on his/her own website and his/her university's repository, including UMI (according to the definition on the Sherpa website: http://www.sherpa.ac.uk/romeo/);
- is subject to courtesy information to the co-author or corresponding author.

Geographic Rights: Scope

Licenses may be exercised anywhere in the world.

Altering/Modifying Material: Not Permitted

Figures, tables, and illustrations may be altered minimally to serve your work. You may not

alter or modify text in any manner. Abbreviations, additions, deletions and/or any other alterations shall be made only with prior written authorization of the author(s).
Reservation of Rights
Springer reserves all rights not specifically granted in the combination of (i) the license details provided by you and accepted in the course of this licensing transaction and (ii) these terms and conditions and (iii) CCC's Billing and Payment terms and conditions.
License Contingent on Payment
While you may exercise the rights licensed immediately upon issuance of the license at the end of the licensing process for the transaction, provided that you have disclosed complete and accurate details of your proposed use, no license is finally effective unless and until full payment is received from you (either by Springer or by CCC) as provided in CCC's Billing and Payment terms and conditions. If full payment is not received by the date due, then any license preliminarily granted shall be deemed automatically revoked and shall be void as if never granted. Further, in the event that you breach any of these terms and conditions or any of CCC's Billing and Payment terms and conditions, the license is automatically revoked and shall be void as if never granted. Use of materials as described in a revoked license, as well as any use of the materials beyond the scope of an unrevoked license, may constitute copyright infringement and Springer reserves the right to take any and all action to protect its copyright in the materials.
Copyright Notice: Disclaimer
You must include the following copyright and permission notice in connection with any reproduction of the licensed material:
"Springer book/journal title, chapter/article title, volume, year of publication, page, name(s) of author(s), (original copyright notice as given in the publication in which the material was originally published) "With permission of Springer"
In case of use of a graph or illustration, the caption of the graph or illustration must be included, as it is indicated in the original publication.
Warranties: None
Springer makes no representations or warranties with respect to the licensed material and adopts on its own behalf the limitations and disclaimers established by CCC on its behalf in its Billing and Payment terms and conditions for this licensing transaction.
Indemnity
You hereby indemnify and agree to hold harmless Springer and CCC, and their respective officers, directors, employees and agents, from and against any and all claims arising out of your use of the licensed material other than as specifically authorized pursuant to this license.
No Transfer of License
This license is personal to you and may not be sublicensed, assigned, or transferred by you without Springer's written permission.
No Amendment Except in Writing
This license may not be amended except in a writing signed by both parties (or, in the case of Springer, by CCC on Springer's behalf).
Objection to Contrary Terms
Springer hereby objects to any terms contained in any purchase order, acknowledgment, check endorsement or other writing prepared by you, which terms are inconsistent with these terms and conditions or CCC's Billing and Payment terms and conditions. These terms and conditions, together with CCC's Billing and Payment terms and conditions (which are incorporated herein), comprise the entire agreement between you and Springer (and CCC) concerning this licensing transaction. In the event of any conflict between your obligations established by these terms and conditions and those established by CCC's Billing and Payment terms and conditions, these terms and conditions shall control.
Jurisdiction
All disputes that may arise in connection with this present License, or the breach thereof,

shall be settled exclusively by arbitration, to be held in the Federal Republic of Germany, in accordance with German law.

Other conditions:

V 12AUG2015

OXFORD UNIVERSITY PRESS LICENSE
TERMS AND CONDITIONS

Dec 03, 2017

This Agreement between McMaster University -- Kyle Novakowski ("You") and Oxford University Press ("Oxford University Press") consists of your license details and the terms and conditions provided by Oxford University Press and Copyright Clearance Center.

License Number	4241501376274
License date	Dec 03, 2017
Licensed content publisher	Oxford University Press
Licensed content publication	Molecular Biology and Evolution
Licensed content title	Human-specific mutations and positively-selected sites in MARCO confer functional changes
Licensed content author	Novakowski, Kyle E; Yap, Nicholas V L
Licensed content date	Nov 20, 2017
Type of Use	Thesis/Dissertation
Institution name	
Title of your work	IDENTIFICATION AND FUNCTIONAL CHARACTERIZATION OF CONSERVED RESIDUES AND DOMAINS IN THE MACROPHAGE SCAVENGER RECEPTOR MARCO
Publisher of your work	n/a
Expected publication date	Dec 2017
Permissions cost	0.00 CAD
Value added tax	0.00 CAD
Total	0.00 CAD
Requestor Location	McMaster University 1280 Main St W MDCL 4020 Hamilton, ON L8S4L8 Canada Attn: McMaster University
Publisher Tax ID	GB125506730
Billing Type	Invoice
Billing Address	McMaster University 1280 Main St W MDCL 4020 Hamilton, ON L8S4L8 Canada Attn: Kyle Novakowski
Total	0.00 CAD
Terms and Conditions	

STANDARD TERMS AND CONDITIONS FOR REPRODUCTION OF MATERIAL FROM AN OXFORD UNIVERSITY PRESS JOURNAL

1. Use of the material is restricted to the type of use specified in your order details.

2. This permission covers the use of the material in the English language in the following territory: world. If you have requested additional permission to translate this material, the terms and conditions of this reuse will be set out in clause 12.
3. This permission is limited to the particular use authorized in (1) above and does not allow you to sanction its use elsewhere in any other format other than specified above, nor does it apply to quotations, images, artistic works etc that have been reproduced from other sources which may be part of the material to be used.
4. No alteration, omission or addition is made to the material without our written consent. Permission must be re-cleared with Oxford University Press if/when you decide to reprint.
5. The following credit line appears wherever the material is used: author, title, journal, year, volume, issue number, pagination, by permission of Oxford University Press or the sponsoring society if the journal is a society journal. Where a journal is being published on behalf of a learned society, the details of that society must be included in the credit line.
6. For the reproduction of a full article from an Oxford University Press journal for whatever purpose, the corresponding author of the material concerned should be informed of the proposed use. Contact details for the corresponding authors of all Oxford University Press journal contact can be found alongside either the abstract or full text of the article concerned, accessible from www.oxfordjournals.org Should there be a problem clearing these rights, please contact journals.permissions@oup.com
7. If the credit line or acknowledgement in our publication indicates that any of the figures, images or photos was reproduced, drawn or modified from an earlier source it will be necessary for you to clear this permission with the original publisher as well. If this permission has not been obtained, please note that this material cannot be included in your publication/photocopies.
8. While you may exercise the rights licensed immediately upon issuance of the license at the end of the licensing process for the transaction, provided that you have disclosed complete and accurate details of your proposed use, no license is finally effective unless and until full payment is received from you (either by Oxford University Press or by Copyright Clearance Center (CCC)) as provided in CCC's Billing and Payment terms and conditions. If full payment is not received on a timely basis, then any license preliminarily granted shall be deemed automatically revoked and shall be void as if never granted. Further, in the event that you breach any of these terms and conditions or any of CCC's Billing and Payment terms and conditions, the license is automatically revoked and shall be void as if never granted. Use of materials as described in a revoked license, as well as any use of the materials beyond the scope of an unrevoked license, may constitute copyright infringement and Oxford University Press reserves the right to take any and all action to protect its copyright in the materials.
9. This license is personal to you and may not be sublicensed, assigned or transferred by you to any other person without Oxford University Press's written permission.
10. Oxford University Press reserves all rights not specifically granted in the combination of (i) the license details provided by you and accepted in the course of this licensing transaction, (ii) these terms and conditions and (iii) CCC's Billing and Payment terms and conditions.
11. You hereby indemnify and agree to hold harmless Oxford University Press and CCC, and their respective officers, directors, employs and agents, from and against any and all claims arising out of your use of the licensed material other than as specifically authorized pursuant to this license.
12. Other Terms and Conditions:
v1.4

Questions? customercare@copyright.com or +1-855-239-3415 (toll free in the US) or +1-978-646-2777.

OXFORD UNIVERSITY PRESS LICENSE
TERMS AND CONDITIONS

Dec 03, 2017

This Agreement between McMaster University -- Kyle Novakowski ("You") and Oxford University Press ("Oxford University Press") consists of your license details and the terms and conditions provided by Oxford University Press and Copyright Clearance Center.

License Number	4241501146492
License date	Dec 03, 2017
Licensed content publisher	Oxford University Press
Licensed content publication	Molecular Biology and Evolution
Licensed content title	Human-specific mutations and positively-selected sites in MARCO confer functional changes
Licensed content author	Novakowski, Kyle E; Yap, Nicholas V L
Licensed content date	Nov 20, 2017
Type of Use	Thesis/Dissertation
Institution name	
Title of your work	IDENTIFICATION AND FUNCTIONAL CHARACTERIZATION OF CONSERVED RESIDUES AND DOMAINS IN THE MACROPHAGE SCAVENGER RECEPTOR MARCO
Publisher of your work	n/a
Expected publication date	Dec 2017
Permissions cost	0.00 CAD
Value added tax	0.00 CAD
Total	0.00 CAD
Requestor Location	McMaster University 1280 Main St W MDCL 4020 Hamilton, ON L8S4L8 Canada Attn: McMaster University
Publisher Tax ID	GB125506730
Billing Type	Invoice
Billing Address	McMaster University 1280 Main St W MDCL 4020 Hamilton, ON L8S4L8 Canada Attn: Kyle Novakowski
Total	0.00 CAD
Terms and Conditions	

STANDARD TERMS AND CONDITIONS FOR REPRODUCTION OF MATERIAL FROM AN OXFORD UNIVERSITY PRESS JOURNAL

1. Use of the material is restricted to the type of use specified in your order details.

2. This permission covers the use of the material in the English language in the following territory: world. If you have requested additional permission to translate this material, the terms and conditions of this reuse will be set out in clause 12.
3. This permission is limited to the particular use authorized in (1) above and does not allow you to sanction its use elsewhere in any other format other than specified above, nor does it apply to quotations, images, artistic works etc that have been reproduced from other sources which may be part of the material to be used.
4. No alteration, omission or addition is made to the material without our written consent. Permission must be re-cleared with Oxford University Press if/when you decide to reprint.
5. The following credit line appears wherever the material is used: author, title, journal, year, volume, issue number, pagination, by permission of Oxford University Press or the sponsoring society if the journal is a society journal. Where a journal is being published on behalf of a learned society, the details of that society must be included in the credit line.
6. For the reproduction of a full article from an Oxford University Press journal for whatever purpose, the corresponding author of the material concerned should be informed of the proposed use. Contact details for the corresponding authors of all Oxford University Press journal contact can be found alongside either the abstract or full text of the article concerned, accessible from www.oxfordjournals.org Should there be a problem clearing these rights, please contact journals.permissions@oup.com
7. If the credit line or acknowledgement in our publication indicates that any of the figures, images or photos was reproduced, drawn or modified from an earlier source it will be necessary for you to clear this permission with the original publisher as well. If this permission has not been obtained, please note that this material cannot be included in your publication/photocopies.
8. While you may exercise the rights licensed immediately upon issuance of the license at the end of the licensing process for the transaction, provided that you have disclosed complete and accurate details of your proposed use, no license is finally effective unless and until full payment is received from you (either by Oxford University Press or by Copyright Clearance Center (CCC)) as provided in CCC's Billing and Payment terms and conditions. If full payment is not received on a timely basis, then any license preliminarily granted shall be deemed automatically revoked and shall be void as if never granted. Further, in the event that you breach any of these terms and conditions or any of CCC's Billing and Payment terms and conditions, the license is automatically revoked and shall be void as if never granted. Use of materials as described in a revoked license, as well as any use of the materials beyond the scope of an unrevoked license, may constitute copyright infringement and Oxford University Press reserves the right to take any and all action to protect its copyright in the materials.
9. This license is personal to you and may not be sublicensed, assigned or transferred by you to any other person without Oxford University Press's written permission.
10. Oxford University Press reserves all rights not specifically granted in the combination of (i) the license details provided by you and accepted in the course of this licensing transaction, (ii) these terms and conditions and (iii) CCC's Billing and Payment terms and conditions.
11. You hereby indemnify and agree to hold harmless Oxford University Press and CCC, and their respective officers, directors, employs and agents, from and against any and all claims arising out of your use of the licensed material other than as specifically authorized pursuant to this license.
12. Other Terms and Conditions:
v1.4

Questions? customercare@copyright.com or +1-855-239-3415 (toll free in the US) or +1-978-646-2777.